ACTA PHARMACEUTICA SCIENCIA

International Journal in Pharmaceutical Sciences, Published Quarterly

ISSN: 2636-8552
e-ISSN: 1307-2080,
Volume: 57, No: 4, 2019
Formerly: Eczacılık Bülteni / Acta Pharmaceutica Turcica
Founded in 1953 by Kasım Cemal GÜVEN

ACTA PHARMACEUTICA SCIENCIA

International Journal in Pharmaceutical Sciences
is Published Quarterly
ISSN: 2636-8552
e-ISSN: 1307-2080,
Volume: 57, No: 4, 2019
Formerly: Eczacılık Bülteni/Acta Pharmaceutica Turcica
Founded in 1953 by Kasım Cemal Güven

Address
İstanbul Medipol Üniversitesi
Kavacık Güney Kampüsü
Göztepe Mah. Atatürk Cad.
No: 40 34810 Beykoz/İSTANBUL
Tel: 0216 681 51 00

E-mail
editor@actapharmsci.com
secretary@actapharmsci.com

Web site
http://www.actapharmsci.com

Printing Office
Has Kopyalama Baskı ve Kırtasiye A.Ş
Kavacık Mah. Ekinciler Cad. No:19
Medipol Üniversitesi Kuzey Yerleşkesi
Tel: 0216 681 53 72

Contents

Aims and Scope of Acta Pharmaceutica Sciencia

Acta Pharmaceutica Sciencia is a continuation of the former "Eczacılık Bülteni" which was first published in 1953 by Prof. Dr. Kasım Cemal GÜVEN's editorship. At that time, "Eczacılık Bülteni" hosted scientific papers from the School of Medicine-Pharmacy at Istanbul University, Turkey.

In 1984, the name of the journal was changed to "Acta Pharmaceutica Turcica" and it became a journal for national and international manuscripts, in all fields of pharmaceutical sciences in both English and Turkish. (1984-1995, edited by Prof. Dr. Kasım Cemal GÜVEN, 1995-2001, edited by Prof. Dr. Erden GÜLER, 2002-2011, edited by Prof. Dr. Kasım Cemal GÜVEN)

Since 2006, the journal has been published only in English with the name, "Acta Pharmaceutica Sciencia" which represents internationally accepted high-level scientific standards. The journal has been published quarterly except for an interval from 2002 to 2009 in which its issues were released at intervals of four months. The publication was also temporarily discontinued at the end of 2011 but since 2016, Acta Pharmaceutica Sciencia has continued publication with the reestablished Editorial Board and also with the support of you as precious scientists.

Yours Faithfully

Prof. Dr. Şeref DEMİRAYAK

Editor

INSTRUCTIONS FOR AUTHORS

1. Scope and Editorial Policy

1.1. Scope of the Journal

Acta Pharmaceutica Sciencia (Acta Pharm. Sci.), formerly known as Bulletin of Pharmacy and Acta Pharmaceutica Turcica is a peer-reviewed scientific journal publishing current research and reviews covering all fields of pharmaceutical sciences since 1953.

The original studies accepted for publication must be unpublished work and should contain data that have not been published elsewhere as a whole or a part. The reviews must provide critical evaluation of the state of knowledge related with the subject.

All manuscripts has to be written in clear and concise English. Starting from 2016, the journal will be issued quarterly both in paper and online formates also publish special issues for national or international scientific meetings and activities in the coverage field.

1.2 Manuscript Categories

Manuscripts can be submitted as Research Articles and Reviews.

1.2.1 Research Articles are definitive accounts of significant, original studies. They are expected to present important new data or provide a fresh approach to an established subject.

1.2.2 Reviews integrate, correlate, and evaluate results from published literature on a particular subject. They expected to report new and up to date experimental findings. They have to have a well-defined theme, are usually critical, and may present novel theoretical interpretations. Up to date experimental procedures may be included. Reviews are usually submitted at the invitation of the Editors. However, experts are welcome to contact the Editors to ensure that a topic is suitable. Approval is recommended prior to submission.

1.3 Prior Publication

Authors should submit only original work that has not been previously published and is not under consideration for publication elsewhere. Academic theses, including those on the Web or at a college Web site, are not considered to be prior publication.

1.4 Patents and Intellectual Property

Authors need to resolve all patent and intellectual property issues. Acceptance

and publication will not be delayed for pending or unresolved issues of this type. Note that Accepted manuscripts and online manuscripts are considered as published documents.

1.5 Professional Ethics

Editors, reviewers, and authors are expected to adhere to internationally accepted criteria's for scientific publishing.

1.5.1 Author Consent. Submitting authors are reminded that consent of all coauthors must be obtained prior to submission of manuscripts. If an author is removed after submission, the submitting author must have the removed author consent to the change by e-mail or faxed letter to the assigned Editor.

1.5.2. Plagiarism. Manuscripts must be original with respect to concept, content, and writing. It is not appropriate for an author to reuse wording from other publications, including one›s own previous publications, whether or not that publication is cited. Suspected plagiarism should be reported immediately to the editorial office. Report should specifically indicate the plagiarized material within the manuscripts. Acta Pharmaceutica Sciencia uses iThenticate or Turnitin software to screen submitted manuscripts for similarity to published material. Note that your manuscript may be screened during the submission process.

1.5.3. Use of Human or Animal Subjects. For research involving biological samples obtained from animals or human subjects, editors reserve the right to request additional information from authors. Studies submitted for publication approval must present evidence that the described experimental activities have undergone local institutional review assessing safety and humane usage of study subject animals. In the case of human subjects authors must also provide a statement that study samples were obtained through the informed consent of the donors, or in lieu of that evidence, by the authority of the institutional board that licensed the use of such material. Authors are requested to declare the identification or case number of institution approval as well as the name of the licensing committee in a statement placed in the section describing the studies' Material and Methods.

1.6 Issue Frequency

The Journal publishes 4 issues per year.

2. Preparing the Manuscript

2.1 General Considerations

Manuscripts should be kept to a minimum length. Authors should write in clear,

concise English, employing an editing service if necessary. For professional assistance with improving the English, figures, or formatting in the manuscript before submission please contact to editorial office by e-mail for suggestions.

The responsibility for all aspects of manuscript preparation rests with the authors. Extensive changes or rewriting of the manuscript will not be undertaken by the Editors. A standard list of Abbreviations, Acronyms and Symbols is in section 5.

It is best to use the fonts "Times" and "Symbol." Other fonts, particularly those that do not come bundled with the system software, may not translate properly. Ensure that all special characters (e.g., Greek characters, math symbols) are present in the body of the text as characters and not as graphic representations. Be sure that all characters are correctly represented throughout the manuscript—e.g., 1 (one) and l (letter l), 0 (zero) and O (letter o).

All text (including the title page, abstract, all sections of the body of the paper, figure captions, scheme or chart titles, and footnotes and references) and tables should be in one file. Graphics may be included with the text or uploaded as separate files. Manuscripts that do not adhere to the guidelines may be returned to authors for correction.

2.1.1 Articles of all kind. Use page size A4. Vertically orient all pages. Articles of all kind must be double-spaced including text, references, tables, and legends. This applies to figures, schemes, and tables as well as text. They do not have page limitations but should be kept to a minimum length. The experimental procedures for all of experimental steps must be clearly and fully included in the experimental section of the manuscripts.

2.1.2 Nomenclature. It is the responsibility of the authors to provide correct nomenclature. It is acceptable to use semisynthetic or generic names for certain specialized classes of compounds, such as steroids, peptides, carbohydrates, etc. In such a case, the name should conform to the generally accepted nomenclature conventions for the compound class. Chemical names for drugs are preferred. If these are not practical, generic names, or names approved by the World Health Organization, may be used.

Authors may find the following sources useful for recommended nomenclature:

· The ACS Style Guide; Coghill, A. M., Garson, L. R., Eds.; American Chemical Society: Washington DC, 2006.

· Enzyme Nomenclature; Webb, E. C., Ed.; Academic Press: Orlando, 1992.

· IUPHAR database of receptors and ion channels (http://www.guidetopharmacology.org/).

2.1.3 Compound Code Numbers. Code numbers (including peptides) assigned to a compound may be used as follows:

· Once in the manuscript title, when placed in parentheses AFTER the chemical or descriptive name.

· Once in the abstract.

· Once in the text (includes legends) and once to label a structure. Code numbers in the text must correspond to structures or, if used only once, the chemical name must be provided before the parenthesized code number, e.g., "chemical name (JEM-398)." If appearing a second time in the text, a bold Arabic number must be assigned on first usage, followed by the parenthesized code number, e.g., "1 (JEM-398)." Subsequently, only the bold Arabic number may be used. All code numbers in the text must have a citation to a publication or a patent on first appearance.

Compounds widely employed as research tools and recognized primarily by code numbers may be designated in the manuscript by code numbers without the above restrictions. Their chemical name or structure should be provided as above. Editors have the discretion of determining which code numbers are considered widely employed.

2.1.4 Trademark Names. Trademark names for reagents or drugs must be used only in the experimental section. Do not use trademark or service mark symbols.

2.1.5 Interference Compounds. Active compounds from any source must be examined for known classes of assay interference compounds and this analysis must be provided in the General Experimental section. Many of these compounds have been classified as Pan Assay Interference Compounds (PAINS; see Baell & Holloway, J. Med. Chem. 2010, 53, 2719-2740). These compounds shown to display misleading assay readouts by a variety of mechanisms by forming reactive compounds. Provide firm experimental evidence in at least two different assays that reported compounds with potential PAINS liability are specifically active and their apparent activity is not an artifact.

2.2 Manuscript Organization

2.2.1 Title Page. Title: The title of the manuscript should reflect the purposes and findings of the work in order to provide maximum information in a

computerized title search. Minimal use of nonfunctional words is encouraged. Only commonly employed abbreviations (e.g., DNA, RNA, ATP) are acceptable. Code numbers for compounds may be used in a manuscript title when placed in parentheses AFTER the chemical or descriptive name.

Authors' Names and Affiliations: The authors' full first names, middle initials, last names, and affiliations with addresses at time of work completion should be listed below the title. The name of the corresponding author should be marked with an asterisk (*).

2.2.2 Abstract and keywords. Articles of all types must have an abstract following the title page. The maximum length of the Abstract should be 150 words, organized in a findings-oriented format in which the most important results and conclusions are summarized. Code numbers may be used once in the abstract.

After the abstract, a section of Keywords not more than five has to be given. Be aware that the keywords, chosen according to the general concept, are very significant during searching and indexing of the manuscripts.

2.2.3 Introduction. The rationale and objectives of the research should be discussed in this section. The background material should be brief and relevant to the research described.

2.2.4. Methodology. Materials, synthetic, biological, demographic, statistical or experimental methods of the research should be given detailed in this section. The authors are free to subdivide this section in the logical flow of the study. For the experimental sections, authors should be as concise as possible in experimental descriptions. General reaction, isolation, preparation conditions should be given only once. The title of an experiment should include the chemical name and a bold Arabic identifier number; subsequently, only the bold Arabic number should be used. Experiments should be listed in numerical order. Molar equivalents of all reactants and percentage yields of products should be included. A general introductory section should include general procedures, standard techniques, and instruments employed (e.g., determination of purity, chromatography, NMR spectra, mass spectra, names of equipment) in the synthesis and characterization of compounds, isolates and preparations described subsequently in this section. Special attention should be called to hazardous reactions or toxic compounds. Provide analysis for known classes of assay interference compounds.

The preferred forms for some of the more commonly used abbrevations are mp, bp, ^{o}C, K, min, h, mL, μL, g, mg, μg, cm, mm, nm, mol, mmol, μmol, ppm,

TLC, GC, NMR, UV, and IR. Units are abbreviated in table column heads and when used with numbers, not otherwise. (See section 4 for more abbreviations)

2.2.5 Results and Discussion. This section could include preparation, isolation, synthetic schemes and tables of biological and statistical data. The discussions should be descriptive. Authors should discuss the analysis of the data together with the significance of results and conclusions. An optional conclusions section is not required.

2.2.6 Ancillary Information. Include pertinent information in the order listed immediately before the references.

PDB ID Codes: Include the PDB ID codes with assigned compound Arabic number. Include the statement "Authors will release the atomic coordinates and experimental data upon article publication."

Homology Models: Include the PDB ID codes with assigned compound Arabic number. Include the statement "Authors will release the atomic coordinates upon article publication."

Corresponding Author Information: Provide telephone numbers and email addresses for each of the designated corresponding authors.

Present/Current Author Addresses: Provide information for authors whose affiliations or addresses have changed.

Author Contributions: Include statement such as "These authors contributed equally."

Acknowledgment: Authors may acknowledge people, organizations, and financial supporters in this section.

Abbreviations Used: Provide a list of nonstandard abbreviations and acronyms used in the paper, e.g., YFP, yellow fluorescent protein. Do not include compound code numbers in this list. It is not necessary to include abbreviations and acronyms from the Standard Abbreviations and Acronyms listed in section 4.

2.2.7 References and Notes. Number literature references and notes in one consecutive series by order of mention in the text. Numbers in the text are nonparenthesized superscripts. The accuracy of the references is the responsibility of the author. List all authors; do not use et al. Provide inclusive page numbers. Titles may have capitalization of first word only (excluding, for example, acronyms and trade names) or standard capitalization as shown below. The chosen style should be used consistently throughout the references. Double-space the references using the following format.

· For journals: Rich, D. H.; Green, J.; Toth, M. V.; Marshall, G. R.; Kent, S. B. H. Hydroxyethylamine Analogues of the p17/p24 Substrate Cleavage Site Are Tight Binding Inhibitors of HIV Protease. *J. Med. Chem.* **1990**, *33*, 1285-1288.

· For online early access: Rubner, G.; Bensdorf, K.; Wellner, A.; Kircher, B.; Bergemann, S.; Ott, I.; Gust, R. Synthesis and Biological Activities of Transition Metal Complexes Based on Acetylsalicylic Acid as Neo-Anticancer Agents. *J. Med. Chem.* [Online early access]. DOI: 10.1021/jm101019j. Published Online: September 21, 2010.

· For periodicals published in electronic format only: Author 1; Author 2; Author 3; etc. Title of Article. *Journal Abbreviation* [Online] **Year**, *Volume*, Article Number or other identifying information.

· For monographs: Casy, A. F.; Parfitt, R. T. *Opioid Analgesics*; Plenum: New York, 1986.

· For edited books: Rall, T. W.; Schleifer, L. S. Drugs Effective in the Therapy of the Epilepsies. In *The Pharmacological Basis of Therapeutics*, 7th ed.; Gilman, A. G., Goodman, L. S., Rall, T. W., Murad, F., Eds.; Macmillan: New York, 1985; pp 446-472

List submitted manuscripts as "in press" only if formally accepted for publication. Manuscripts available on the Web with a DOI number are considered published. For manuscripts not accepted, use "unpublished results" after the names of authors. Incorporate notes in the correct numerical sequence with the references. Footnotes are not used.

2.2.8 Tables. Tabulation of experimental results is encouraged when this leads to more effective presentation or to more economical use of space. Tables should be numbered consecutively in order of citation in the text with Arabic numerals. Footnotes in tables should be given italic lowercase letter designations and cited in the tables as superscripts. The sequence of letters should proceed by row rather than by column. If a reference is cited in both table and text, insert a lettered footnote in the table to refer to the numbered reference in the text. Each table must be provided with a descriptive title that, together with column headings, should make the table self-explanatory. Titles and footnotes should be on the same page as the table. Tables may be created using a word processor's text mode or table format feature. The table format feature is preferred. Ensure each data entry is in its own table cell. If the text mode is used, separate columns with a single tab and use a return at the end of each row. Tables may be inserted in the text where first mentioned or may be grouped after the references.

2.2.9 Figures, Schemes/Structures, and Charts. The use of illustrations to convey or clarify information is encouraged. Structures should be produced with the use of a drawing program such as ChemDraw. Authors using other drawing packages should, in as far as possible, modify their program's parameters so that they conform to ChemDraw preferences. Remove all color from illustrations, except for those you would like published in color. Illustrations may be inserted into the text where mentioned or may be consolidated at the end of the manuscript. If consolidated, legends should be grouped on a separate page(s). Include as part of the manuscript file.

To facilitate the publication process, please submit manuscript graphics using the following guidelines:

1. The preferred submission procedure is to embed graphic files in a Word document. It may help to print the manuscript on a laser printer to ensure all artwork is clear and legible.

2. Additional acceptable file formats are: TIFF, PDF, EPS (vector artwork) or CDX (ChemDraw file). If submitting individual graphic files in addition to them being embedded in a Word document, ensure the files are named based on graphic function (i.e. Scheme 1, Figure 2, Chart 3), not the scientific name. Labeling of all figure parts should be present and the parts should be assembled into a single graphic.

EPS files: Ensure that all fonts are converted to outlines or embedded in the graphic file. The document settings should be in RGB mode. **NOTE:** While EPS files are accepted, the vector-based graphics will be rasterized for production. Please see below for TIFF file production resolutions.

3. TIFF files (either embedded in a Word doc or submitted as individual files) should have the following resolution requirements:

- Black & White line art: 1200 dpi

- Grayscale art (a monochromatic image containing shades of gray): 600 dpi

- Color art (RGB color mode): 300 dpi

· The RGB and resolution requirements are essential for producing high-quality graphics within the published manuscript. Graphics submitted in CMYK or at lower resolutions may be used; however, the colors may not be consistent and graphics of poor quality may not be able to be improved.

· Most graphic programs provide an option for changing the resolution when you are saving the image. Best practice is to save the graphic file at the final resolution and size using the program used to create the graphic.

4. Graphics should be sized at the final production size when possible. Single column graphics are preferred and can be sized up to 240 points wide (8.38 cm.). Double column graphics must be sized between 300 and 504 points (10.584 and 17.78 cm's). All graphics have a maximum depth of 660 points (23.28 cm.) including the caption (please allow 12 points for each line of caption text).

Consistently sizing letters and labels in graphics throughout your manuscript will help ensure consistent graphic presentation for publication.

2.2.10 Image Manipulation. Images should be free from misleading manipulation. Images included in an account of research performed or in the data collection as part of the research require an accurate description of how the images were generated and produced. Apply digital processing uniformly to images, with both samples and controls. Cropping must be reported in the figure legend. For gels and blots, use of positive and negative controls is highly recommended. Avoid high contrast settings to avoid overexposure of gels and blots. For microscopy, apply color adjustment to entire image and note in the legend. When necessary, authors should include a section on equipment and settings to describe all image acquisition tools, techniques and settings, and software used. All final images must have resolutions of 300 dpi or higher. Authors should retain unprocessed data in the event that the Editors request them.

2.3 Specialized Data

2.3.1 Biological Data. Quantitative biological data are required for all tested compounds. Biological test methods must be referenced or described in sufficient detail to permit the experiments to be repeated by others. Detailed descriptions of biological methods should be placed in the experimental section. Standard compounds or established drugs should be tested in the same system for comparison. Data may be presented as numerical expressions or in graphical form; biological data for extensive series of compounds should be presented in tabular form.

Active compounds obtained from combinatorial syntheses should be resynthesized and retested to verify that the biology conforms to the initial observation. Statistical limits (statistical significance) for the biological data are usually required. If statistical limits cannot be provided, the number of determinations and some indication of the variability and reliability of the results should be given. References to statistical methods of calculation should be included.

Doses and concentrations should be expressed as molar quantities (e.g., mol/kg, μmol/kg, M, mM). The routes of administration of test compounds and vehicles used should be indicated, and any salt forms used (hydrochlorides, sulfates, etc.) should be noted. The physical state of the compound dosed (crystalline, amorphous; solution, suspension) and the formulation for dosing (micronized, jet-milled, nanoparticles) should be indicated. For those compounds found to be inactive, the highest concentration (in vitro) or dose level (in vivo) tested should be indicated.

If human cell lines are used, authors are strongly encouraged to include the following information in their manuscript:

· the cell line source, including when and from where it was obtained;

· whether the cell line has recently been authenticated and by what method;

· whether the cell line has recently been tested for mycoplasma contamination.

2.3.2 Purity of Tested Compounds.

Methods: All scientifically established methods of establishing purity are acceptable. If the target compounds are solvated, the quantity of solvent should be included in the compound formulas. No documentation is required unless asked by the editors.

Purity Percentage: All tested compounds, whether synthesized or purchased, should possess a purity of at least 95%. Target compounds must have a purity of at least 95%. In exceptional cases, authors can request a waiver when compounds are less than 95% pure. For solids, the melting point or melting point range should be reported as an indicator of purity.

Elemental analysis: Found values for carbon, hydrogen, and nitrogen (if present) should be within 0.4% of the calculated values for the proposed formula.

2.3.3 Confirmation of Structure. Adequate evidence to establish structural identity must accompany all new compounds that appear in the experimental section. Sufficient spectral data should be presented in the experimental section to allow for the identification of the same compound by comparison. Generally, a listing of 1H or 13C NMR peaks is sufficient. However, when the NMR data are used as a basis of structural identification, the peaks must be assigned.

List only infrared absorptions that are diagnostic for key functional groups. If a series contains very closely related compounds, it may be appropriate merely to list the spectral data for a single representative member when they share a common major structural component that has identical or very similar spectral features.

3. Submitting the Manuscript

3.1 Communication and log in to Author's Module All submissions to Acta Pharmaceutica Sciencia should be made by using e-Collittera (Online Article Acceptance and Evaluation) system on the journal main page (www.actapharmsci.com)

3.2 Registration to System It is required to register into the e-Collittera system for the first time while entering by clicking "Create Account" button on the registration screen and the fill the opening form with real information. Some of the information required in form is absolutely necessary and the registration will not work if these fields are not completely filled.

After the registration, a "Welcome" mail is sent to the user by the system automatically reminding user name and password. Authors are expected to return to the entry screen and log on with their user name and password for the submission. Please use only English characters while determining your username and password.

If you already registered into the e-Collittera system and forget your password, you should click on "Forgot My Password" button and your user name and password will be mailed to your e-mail in a short while.

3.3 Submitting A New Article The main page of author module consists of various parts showing the situation of manuscripts in process. By clicking the New Manuscript button, authors create the beginning of new submission, a process with a total of 9 consecutive levels. In first 7 levels, information such as the article's kind, institutions, authors, title, summary, keywords etc. are asked respectively as entered. Authors can move back and forth while the information is saved automatically. If the is transaction is discontinued, the system move the new submission to "Partially Submitted Manuscripts" part and the transaction can be continued from here.

3.1.1 Sort of Article Authors should first select the type of article from the dropdown menu.

Warning. If "Return to Main Page" button is clicked after this level, the article automatically assined as "Partially Submitted Manuscripts".

3.2.2 Institutions Authors should give their institutional information during submission.

3.2.3 Authors The authors' surnames, names, institutional information appear as entered order in the previous page. Filling all e-mail adresses are re-

quired. Institutional information is available in **Manuscript Details** table at the top of the screen. After filling all required fields, you may click the **Continue** button.

3.2.4 Title should be English, explaining the significance of the study. If the title includes some special characters such as alpha, beta, pi or gamma, they can easily be added by using the **Title** window. You may add the character by clicking the relevant button and the system will automatically add the required character to the text.

Warning. No additions to cornered parenthesis are allowed. Otherwise the system will not be able to show the special characters.

3.2.5 Abstract The summary of the article should be entered to **Abstract** window at this level. There must be an English summary for all articles and the quantity of words must be not more than 150. If special characters such as alpha, beta, pi or gamma are used in summary, they can be added by **Abstract** window. You may add the character by clicking the relevant button and the system will automatically add the required character to the text. The abstract of the articles are accessible for arbitrators; so you should not add any information related to the institutions and authors in this summary part. Otherwise the article will returned without evaluation. Authors will be required to comply with the rules.

Warning. No additions to cornered parenthesis are allowed. Otherwise the system will not be able to show the special characters.

3.2.6 Keywords There must be five words to define the article at the keywords window, which will diverged with commas. Authors should pay attention to use words, which are appropriate for "*Medical Subjects Headings*" list by National Library of Medicine (NLM).

3.2.7 Cover Letter If the submitting article was published as thesis and/or presented in a congress or elsewhere, all information of thesis, presented congress or elsewhere should be delivered to the editor and must be mentioned by the "Cover Letter" field.

3.3.1 Adding Article This process consists four different steps beginning with the loading of the article in to system. **Browse** button is used to reach the article file, under the **Choose a file to upload** tab. After finding the article you may click to **Choose File** and file will be attached.

Second step is to select the file category. Options are: Main Document, Black and White Figure, Color Figure and Video.

The explanation of the files (E.g.. Figure 1, Full Text Word File, supplements etc.) should be added on third step and the last step is submitting the prepared article into the system. Therefore, **Download** button under the **Send your file by clicking on download button** tab is clicked.

Reminder If the prepared article includes more than one file (such as main document, black and white figure, video), the transaction will be continued by starting from the first step. The image files must be in previously defined format. After all required files were added, **Continue** button should be clicked. All details and features of the article might be reached from the **Article Information** page.

This page is the last step of the transaction which ensures that entered information is controlled.

3.3.2 Your Files After adding the article you may find all information related to article under **Your Files** window.

File Information This window includes file names, sizes, forming dates, categories, order numbers and explanations of files. The details about the files can be reached by clicking on **Information** button.

If you click on **Name of File**, the file download window will be opened to reach the copy of the file in system.

File Download This window submits two alternatives, one of them is to ensure the file to be opened in valid site and the second one is to ensure to download submitted file into the computer.

Opening the Category part on fourth column can change the category of the file.

Opening the Order column on fifth column can change the order of file.

The file can be deleted by clicking on **Delete** button on the last column. Before deleting, system will ask the user again if it's appropriate or not.

3.3.3 Sending Article Last level is submitting the article and the files into the system. Before continuing the transaction, **Article Information** window must be controlled where it is possible to return back; by using **Previous** button and required corrections can be made. If not, clicking the **Send the Article** button completes transaction.

3.3.4 Page to Follow The Article The Main Page of Author ensures possibility to follow the article. This page consists three different parts; some infor-

mation and bridges related to the sent articles, revision required articles and the articles that are not completed to be sent.

3.3.4.1 Articles Not Completed to be Sent After the sending transaction was started, if article is not able to continue until the ninth step or could not be sent due to technical problems shown at this part. Here you can find the information such as the article's number which is assigned by system, title and formation date. You may delete the articles by using **Delete** button on the right column, if the article is not considered to send into the system.

3.3.4.2 Articles That Require Revision Articles, which were evaluated by the referee and accepted by the editor with revision, continues to **Waiting for Revision** table.

The required revisions can be seen in "**Notes**" part by clicking the articles title.

In order to send any revision, **Submit Revision** button on the last column should be clicked. This connection will take the author to the first level of **Adding Article** and the author can complete the revision transaction by carrying out the steps one by one. All changes must be made in the registered file and this changed file must be resent. Author's most efficacious replies relating to the changes must be typed in "Cover Letter" part.

If the is transaction is discontinued, the system move the revised article to **Submitted Manuscripts** part and the transaction can be continued from here.

After the transaction was completed, the system moves the revised article to "Submitted Manuscripts" part.

3.3.5 Submitted Manuscripts Information related to articles can be followed through the **Submitted Manuscripts** line. Here you can find the information such as the article's number assigned by system, title, sending date and transaction situation. The **Manuscript Details** and summary files can be reached by clicking the title of the article and the **Processing Status** part makes it possible to follow the evaluation process of the article.

ORIGINAL ARTICLES

Acta Pharm. Sci. Vol 57 No: 4. 2019
DOI: 10.23893/1307-2080.APS.05722

Material, Compressional and Tableting Properties of Ipomea Batatas (Sweet Potato) Starch Co-Processed with Silicon Dioxide

Lateef Bakre[1*], Damola Osibajo[1], Gbenga Koiki[1], Oluyemisi Bamiro[1]

1 Department of Pharmaceutics and Pharmaceutical Technology, Faculty of Pharmacy, Olabisi Onabanjo University, Nigeria

ABSTRACT

This study aims to co-process native *Ipomea batatas* starch (NPS) with colloidal silicon dioxide and evaluate the properties of the co-processed excipient (CPS). The powder morphology was determined by scanning electron microscopy (SEM), differential scanning calorimetry (DSC) and X-Ray Diffraction (XRD) measurements. The compressional, mechanical and release properties of metronidazole tablet formulations were evaluated. NPS was predominantly oval in shape while CPS had more large truncated ellipsoidal granules. Both NPS and CPS exhibited spectra typical of a Type A XRD pattern, but CPS has a sharp peak with strong intensity at 27° 2θ which was absent in NPS. Although NPS had a faster onset of plastic deformation, the overall amount of plastic deformation was higher in CPS. Tablets formulated with CPS had faster dissolution than those containing similar concentration of NPS. The co-processing of *Ipomea batatas* starch with colloidal silicon dioxide resulted in modification of its powder and tableting properties.

Keywords: Co-processing, *Ipomea batatas* starch, powder and compressional characteristics, tableting properties.

INTRODUCTION

Excipients play an important role in drug delivery and in the formulation of a stable and safe dosage form. International Pharmaceutical Excipients Council (IPEC) defines excipients as "substances, other than the API, in finished dosage form, which have been appropriately evaluated for safety and are included

*Corresponding Author: Lateef Bakre, e-mail: lateef.bakre@oouagoiwoye.edu.ng
Lateef Bakre ORCID Number: https://orcid.org/0000-0003-1222-1057
Damola Osibajo ORCID Number: https://orcid.org/0000-0001-7557-7654
Gbenga Koiki ORCID Number: https://orcid.org/0000-0001-6774-0597
Oluyemisi Bamiro ORCID Number: https://orcid.org/0000-0002-6032-6075
(Received 12 March 2019, accepted 05 June 2019)

in a drug delivery system to either aid the processing or to aid manufacture, protect, support, enhance stability, bioavailability or patient acceptability, assist in product identification, or enhance any other attributes of the overall safety and effectiveness of the drug delivery system during storage or use" [1]. In recent years, scientists have directed their studies at developing novel excipients with multifunctional applications which helps to lower production cost because some stages in production and excipients are eliminated [2,3]. To achieve this, a particle engineering technique called co processing was introduced and this has gained wide acceptance over the years. Co-processing involves combining two or more existing excipients through interaction at the sub-particle level and does not result in the formation of covalent bonding. It brings about a functional synergy and masks the undesirable qualities of the individual components. The co-processed excipients have new functionalities that cannot be achieved by simple physical mixture of individual components [4,5].

A survey of the literature reveals that a number of excipients have been co-processed with resultant enhanced functionalities [6,7,8,9]. However, there appears to be no information on co processing of potato starch with silicon dioxide. Starch has been widely used as excipients (disintegrants, binders, glidants, fillers, thickeners and bulking agents) in the food and pharmaceutical industries [10]. As a result of this versatile application of starch in drug formulations, it is necessary to continuously develop new starch excipients with improved functionalities with a view to meeting specific needs of drug formulators. Colloidal silicon dioxide is employed as a glidant in formulations to enhance powder flow. It has the ability to coat materials and thereby reduces forces of attraction (van der Waals) within particles. In addition, it absorbs water molecules present on hygroscopic powders and thus minimizes clumping and caking. These two properties prevent the development of "bridges" within the powder and thus improve flow through hoppers during tableting. The purpose of this investigation was to co-process potato starch with silicon dioxide and evaluate the powder, compressional and tableting properties of the co-processed excipient.

METHODOLOGY

Materials

The following materials were used: Metronidazole (DMV, Veghel, Netherlands), colloidal silicon dioxide (CAB-O-SIL®, CABOT GmbH, Germany), corn starch and magnesium stearate (BDH Chemical, Poole, UK). The potato starch was prepared in the laboratory and analytical grade chemicals were used in the study.

Preparation of potato starch

Starch was obtained by the method of Alebiowu [11] with slight modification. The fresh sweet potato tubers were washed, peeled, cut into small pieces, soaked in distilled water for 24 hrs and thereafter homogenized in a blender to obtain a slurry. This was filtered using a muslin cloth and the filtrate was allowed to stand for 5 hours to allow for the starch to settle. The sediment was centrifuged, the supernatant discarded, and the crude starch cake was washed repeatedly with distilled water to further remove impurity. The purified starch cake was air dried, pulverized into fine powder and kept in air tight container for further use.

Preparation of co-processed starch

The co-processed starch was prepared by the method of Mshelia et.al. [7] A 100 g of a suspension containing 40% w/w of potato starch was prepared in a 500 mL capacity beaker by adding 250 mL of distilled water. 2.04 g of silicon dioxide was then dispersed in the suspension and constantly stirred for 10 min before heating in a water bath at 50±2 ^{o}C for 20 mins. The co-processed starch was washed with 99 % ethanol, passed through a 0.8 mm sieve size, air dried and then kept in an air-tight container until ready for use.

Fourier transmission infrared spectra (FT-IR) spectroscopy.

The samples were dried and kept in a desiccator before the FTIR analysis. Spectra were obtained by using potassium bromide discs obtained from a mixture of the starch and dry potassium bromide on a FT-IR spectrophotometer (BX 273, Perkin-Elmer, USA).

Differential scanning calorimetry (DSC)

DSC thermograms of the sample were determined on a Mettler instrument (DSC1, Toledo, USA). A 4-10 mg weight of sample were compressed into pellets in an aluminium pan and heated from 30 to 430 ^{o}C at a rate of 20 ^{o}C/min under inert nitrogen atmosphere with a flow rate of 20 mLmin^{-1}. The reference used was an empty aluminum pan.

Scanning electron microscopy (SEM)

A Scanning electron microscope ZEISS EVO18 (Germany) was used for the test. Dried starch powders were mounted in a double sided adhesive conductive carbon tape with aluminum stub and coated with gold in a sputter coater with 7 mA current for 90 s.

X-Ray Diffraction Measurements:

The XRD spectra were obtained by exposing the samples to X - ray beam at 40mA and 45KV in an X-ray diffractometer (Empyrean, PAN analytical, Netherlands). The 2θ range of 10 °–90 ° was recorded with 0.1° resolution.

Determination of Swelling Capacity

Three grams of the starch powders was added to 20mL of water in a 50mL ground-glass stoppered graduated cylinder and the volume noted (V_o). The suspension was shaken every 10 minutes for 1 hr, allowed to stand for 5 hrs and the volume occupied by the sample (V) was recorded. The swelling index was calculated as the ratio of V to V_o. The procedure was repeated thrice, and the result obtained was recorded as mean ± standard deviation.

Determination of particle, tapped and bulk densities

The liquid immersion technique (pycnometer method) was used to determine the particle density with xylene as the displacement liquid according to the method of Bakre and Ajala [12]. The bulk density was determined by pouring a 10 g weight of powder into a measuring cylinder and the volume occupied noted. The bulk density was obtained as the ratio of weight (10 g) to the volume occupied. The procedure was carried out in triplicate and the mean ± standard deviation calculated. The tapped density was obtained by tapping the sample 300 times at the rate of 38 taps in a minute [13]. This procedure was redone with 700 taps.

Determination of porosity and flow properties

The porosity was calculated using bulk (ρb) and true densities (ρs) data according to Equation 1

$$e=1-{}^{\rho b}/_{\rho s} \quad (1)$$

The static angle of repose was determined by the funnel method. A 10 g quantity of powder sample was weighed and allowed to flow via a glass funnel fixed 10 cm above a flat surface. The radius and the height of the resultant conical heap were measured. The tangent of the ratio of the height to the radius of the conical heap was taken as the angle of repose. The values obtained from the ratio of the tapped and bulk density was taken as the Hausner ratio while the Carr's index was obtained using Equation 2

$$\text{Carr's Index} = \left[\frac{PT-PB}{PT}\right] \times 100 \quad (2)$$

Where PT and PB are tapped and bulk densities respectively

Preparation of sweet potato starch compacts

Powder starch (500 mg) were compressed into compacts using 28N, 56.5N, 84N, 113N, 141N, 169N and 198N forces at a dwell time of 30 seconds on a tablet press (Model C, Carver Inc., USA). The lubricant used was magnesium stearate dispersion in 96% ethanol. On ejection, the tablets were stored for 24 hrs over silica gel to allow for hardening and elastic recovery. The dimensions and weights were determined within 0.01 mm and ±1 mg respectively. Equation 3 was used to calculate the relative densities (D) of the tablet compacts of weight W (g), volume vt (cm^3) and particle density Ps (g/cm^3)

$$D = {}^{W}/_{vt \times Ps} \quad (3)$$

The data obtained were used for the Heckel and Kawakita plots.

Analysis of compaction data

Heckel plot: The compressional properties were determined using the Heckel equation [14]

$$\text{In}\frac{1}{1-D} = KP + A \quad (4)$$

The mean yield pressure P_y of the material was derived from the inverse of the slope K while A is the intercept. D_A was obtained from the intercept using Equation 5:

$$D_A = 1 - e^A \quad (5)$$

The relative density when no pressure is applied (D_o) represents the rearrangement phase due to die filling while D_B (obtained from $D_A - D_B$) is the rearrangement phase at the early stages of compression.

Kawakita plot: The kawakita equation [15] expresses the effect of applied pressure, P on the degree of volume reduction.

$${}^{P}/_{C} = {}^{P}/_{a} + {}^{1}/_{ab} \quad (6)$$

The constant 'a' (obtained from the slope) is the powder porosity without compression and 'b' is a function of the ability of the material to deform plastically. D_I (1-a) which is the initial packed relative density of the tablets pressure when small pressure is applied was obtained. Pk is derived from the reciprocal of b and it represents the pressure required to reduce the powder bed by 50 % [16].

Preparation of tablets

The tablets containing 500 mg of the powders were made by compressing the formulation (Table 1) for 30 seconds at 1.0 tonne with a tablet press (Model C, Carver Inc., USA). The lubricant used for the die and the punches was magnesium stearate dispersion in 96 % ethanol. When the compression process was completed, the tablets were removed from the die and stored over silica gel.

Table 1. Formulation table for metronidazole formulations.

	Formulations			
Ingredients (mg)	**A**	**B**	**C**	**D**
Metronidazole	100	100	100	100
CPS	250	200	-	-
NPS	-	-	250	200
Corn Starch	50	50	50	50
Lactose	100	150	100	150

Evaluation of tablet properties

The tablet hardness was determined by measuring the load required to diametrically break each of the 10 tablets using a Monsanto hardness tester (Copley Scientific Limited, Nottingham, UK) while the mean friability of 20 tablets was obtained with a friabilator (Shivani Scientific Ind., Mumbai, India) set at 25 rpm for 4 min. The time it took each tablet in distilled water maintained at 37 ^{o}C to disintegrate and go through the wire mesh of the disintegration test apparatus (Georgeon, Mumbai) was taken as the disintegration time. The results are given as mean of five determinations. Dissolution test for the tablets was determined using the Veego digital dissolution test apparatus (Veego, India). The dissolution medium used was 900 mLs phosphate buffer solution (pH 6.8) maintained at 37± 0.5 ^{o}C and the rotating speed was 100 rpm. A 5 mL samples were withdrawn at 5, 10, 15, 30, 45 and 60 minutes and replaced with the same volume of fresh medium maintained at the same temperature. The samples withdrawn were filtered through Whatman filter paper and the absorbance of the samples was measured on the spectrophotometer at a wavelength of 233 nm. The test was repeated thrice.

RESULTS AND DISCUSSION

Morphology, FTIR Characterization and thermal properties

The scanning electron micrographs of the starch are presented in Figure 1. The native potato starch (NPS) are predominantly oval in shape with few granules having polygonal shape while the co-processed potato starch (CPS) had more irregular, oval, polygonal and large truncated ellipsoidal granules.

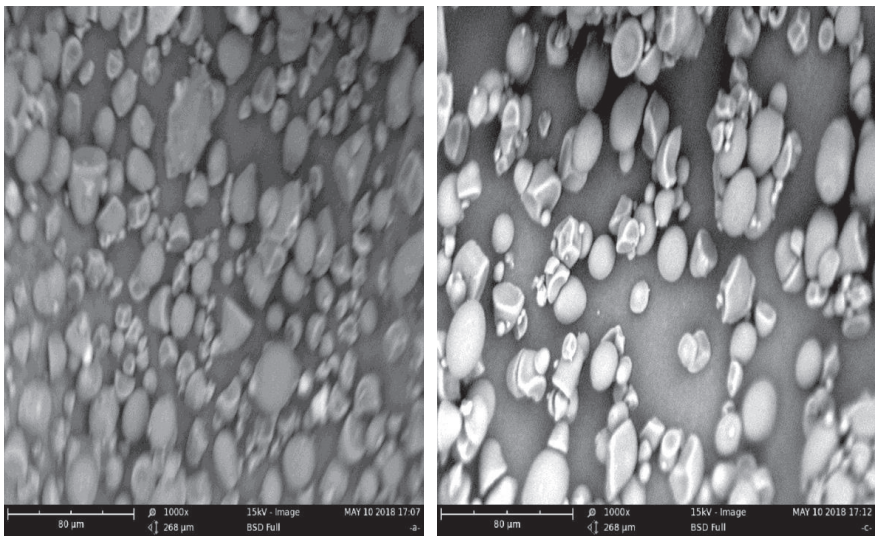

A. SEM of CPS B. SEM of NPS

Figure 1. Scanning electron micrograph of CPS and NPS.

The FTIR spectra of native CPS reveal a broad band at 3265 cm^{-1} attributable to hydrogen bonded –OH (Figure 2). The stretching peak at 2928 cm^{-1} is due to –CH stretching vibration of the amylose and amylopectin present in the starch while the peak at 1640 cm^{-1} is characteristic of tightly bound water molecules [17].

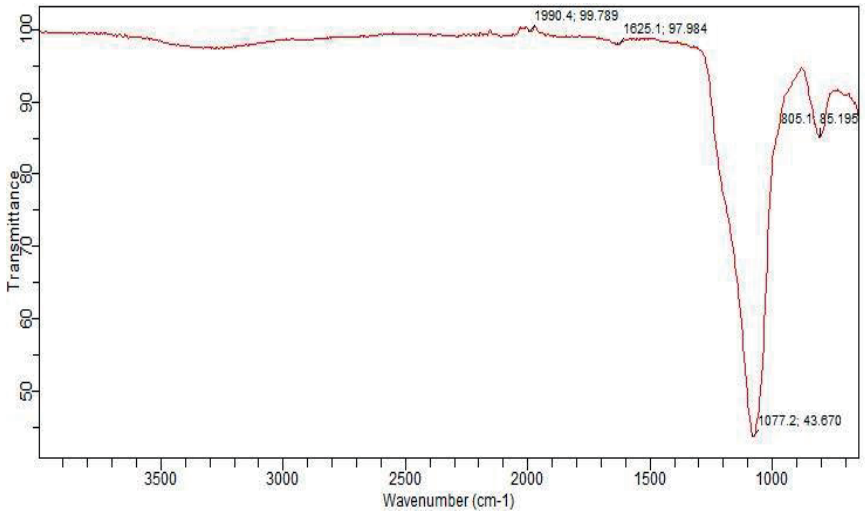

Figure 2a. FTIR spectrum of physical mixture of NPS and silicon dioxide.

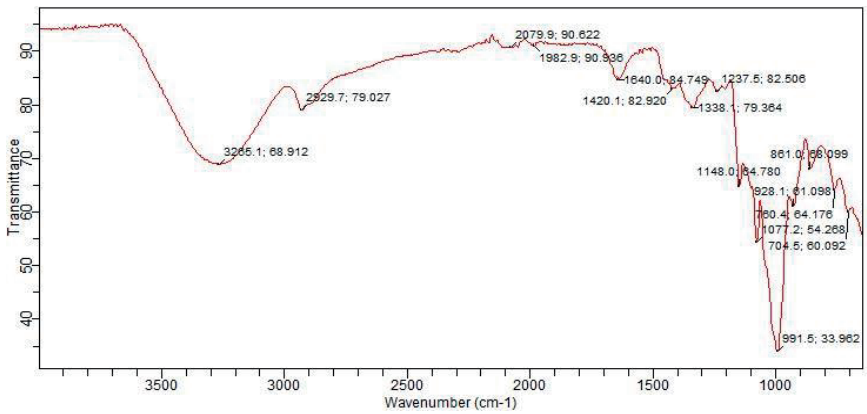

Figure 2b. FTIR spectrum of CPS.

The stretching peaks at 791 and 1077 cm^{-1} is due to the stretching modes in the amorphous regions of the starch [18]. The DSC thermograms presented in Figure 3 show that CPS and NPS exhibited single endothermic peak at 116 ^{o}C which is usually attributed to the melting of amylose- lipid complexes formed when the starches are heated in DSC [19]. These lipids are usually fatty acids and monoglycerides. Starch is a semicrystalline compound which comprises both amylose and amylopectin components. The linear structure of the amylose is responsible for the crystalline region while the amylopectin accounts for the amorphous phase [20-22].

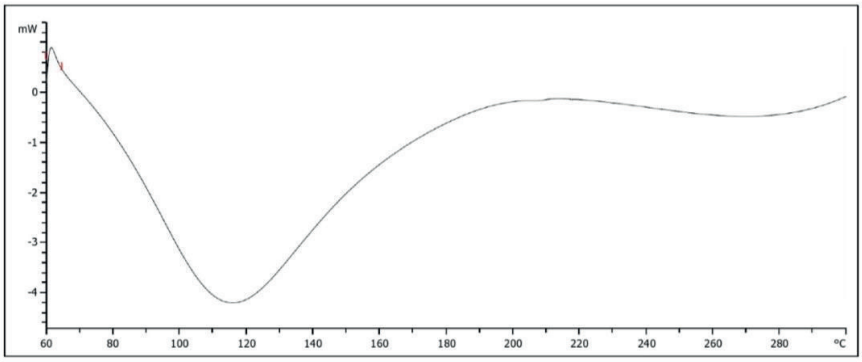

Figure 3a. DSC thermogram of CPS.

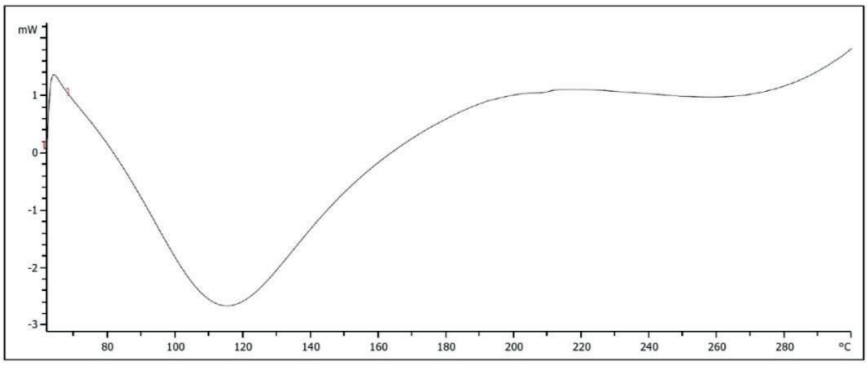

Figure 3b. DSC thermogram of NPS.

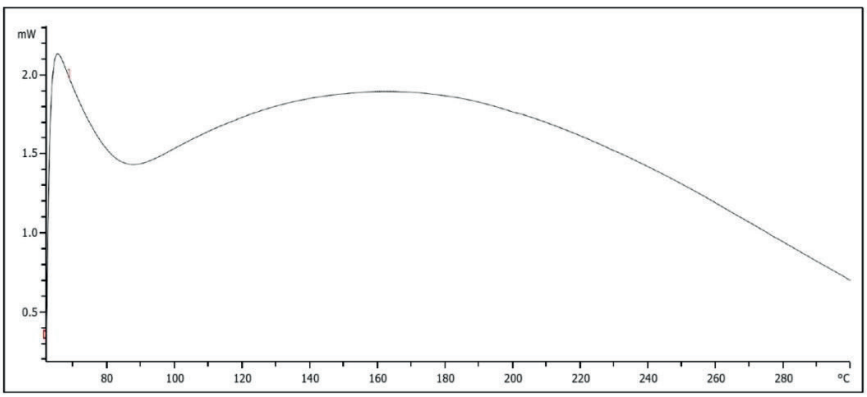

Figure 3c. DSC thermogram of physical mixture of NPS and colloidal silicon dioxide.

Figure 4 which represents the XRD spectra of NPS and CPS confirm the existence of these two phases which is characterized by a broad region between 10° and 27° 2θ containing some distinctive reflections or peaks. Both NPS and CPS exhibited strong reflections at 15 and 24° 2θ and an unresolved doublet at 18° 2θ which is typical of a Type A XRD pattern. The CPS however has a sharp peak with strong intensity at 27° 2θ which is absent in NPS. This could probably be due to a disruption in the granules structure as a result of heating due to co processing. The spectrum of the binary mixture of NPS and colloidal silicon dioxide appears noisy and the peaks are difficult to distinguish.

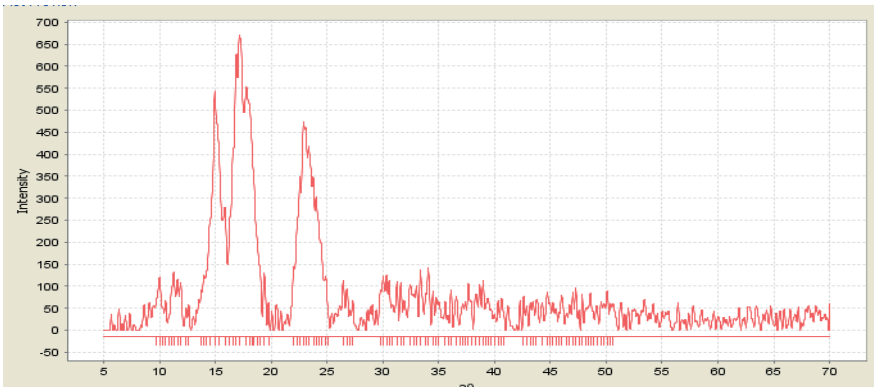

Figure 4a. XRD spectrum of NPS

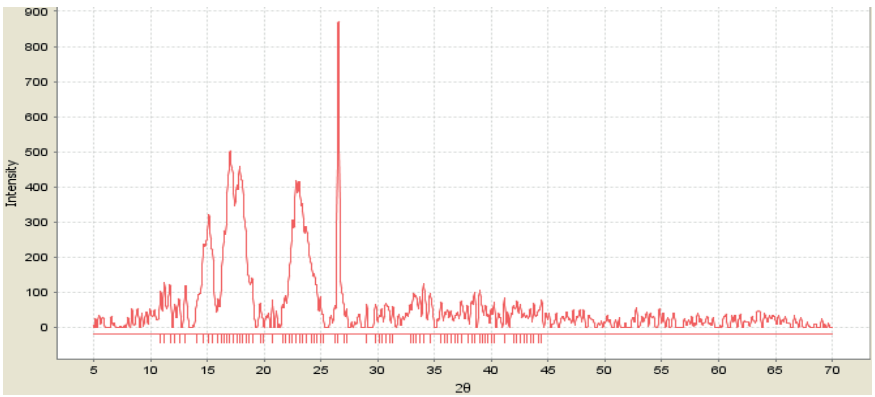

Figure 4b. XRD spectrum of CPS

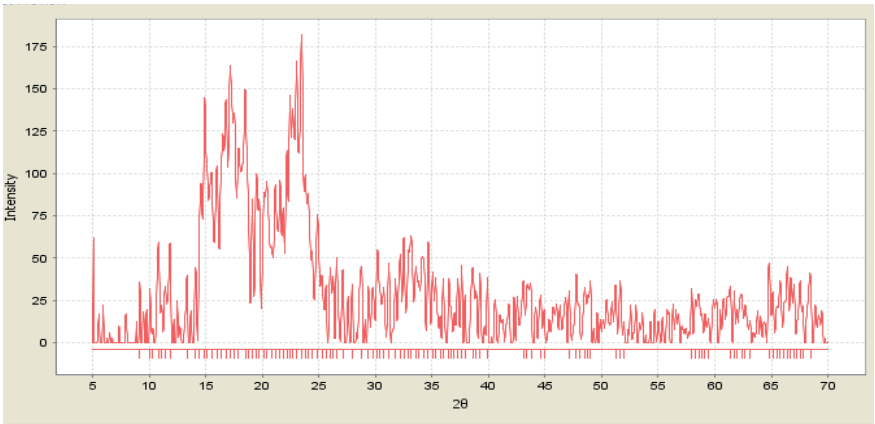

Figure 4c. XRD spectrum of binary mixture of NPS and colloidal silicon dioxide

Physicochemical and compressional properties

The physicochemical properties of pharmaceutical excipients are critical to the properties of the final formulation. Table 2 presents the powder properties of the starches. The angle of repose, Hausners ratio and compressibility index are parameters that indirectly measure the flowability of powders. Generally, materials with angle of repose below 30°, Hausners ratio less than 1.25 and compressibility index below 16% indicate good flow [23].

Table 2. Powder properties of sample materials.

Properties	NPS	CPS	CS
Particle density (g/cm^3)	1.103±0.01	2.197±0.03	0.819±0.01
Bulk density(g/cm^3)	0.56±0.12	0.50±0.03	0.41±0.10
Tapped density (g/cm^3)	0.62±0.05	0.63±0.16	0.56±0.20
Angle of repose (^{0})	24.60	32.70	17.70
Carr's index	9.10	19.10	27.38
Hausner ratio	1.10	1.24	1.37
Swelling index (%)	12.0	12.9	6.35
Porosity (%)	51.1	22.9	51.20
Moisture content (%)	6.7	13.3	6.22
Flow rate (g/s)	2.50	3.61	0.13

The rank for the angle of repose is CPS>NPS>CS. This suggests that co-processing with silicon dioxide did not improve the flow property. This is consistent with the SEM analysis which reveals that CPS has irregularly shaped particles. This increases inter-particulate friction and thus results in increased cohesive forces within the starch particles. Moreover, the high moisture content of CPS might also account for the higher angle of repose. The Hausners ratio and compressibility index values obtained are consistent with the reduction in powder flow in CPS. There was a slight increase in the swelling capacity after co-processing, but the bulk density decreased. The reduction in bulk density might be due to a less dense packing behavior as a result of the irregularly shaped particles. It is important to optimize the moisture content of powder materials because of its effect on stability of pharmaceutical formulations. CPS has high moisture content and requires further drying if it is to be employed in tablet manufacture. Figures 5 and 6 represents Heckel and Kawakita plots respectively. CPS exhibited a Heckel plot shape characteristic of a Type A materials which deforms plastically. The parameters derived from the plots are presented in Table 3. Microcrystalline cellulose (MCC) and dicalcium phosphate dihydrate (DCP) used in this study are model examples of plastically deforming and brittle materials respectively. The Heckel model relates the reduction in powder volume to the applied pressure. Py gives an indication of the plasticity and softness of the materials. A low value shows low resistance to pressure, good densification and fast onset of plastic deformation[16]. The rank order of Py is DCP<NPS<MCC<CPS. This suggests that NPS has a faster onset of plastic deformation than CPS. D_B is the rearrangement phase at the early stages of compression. The ranking of D_B is CPS > NPS > MCC > CS. The high values of D_B in CPS is probably as result of particle de-segmentation. The total degree of densification occurring in a powder bed (D_A) for CPS was more than NPS. The rank order of P_k is CPS<NPS<MCC<DCP. This indicates that the overall plastic deformation was highest in CPS.

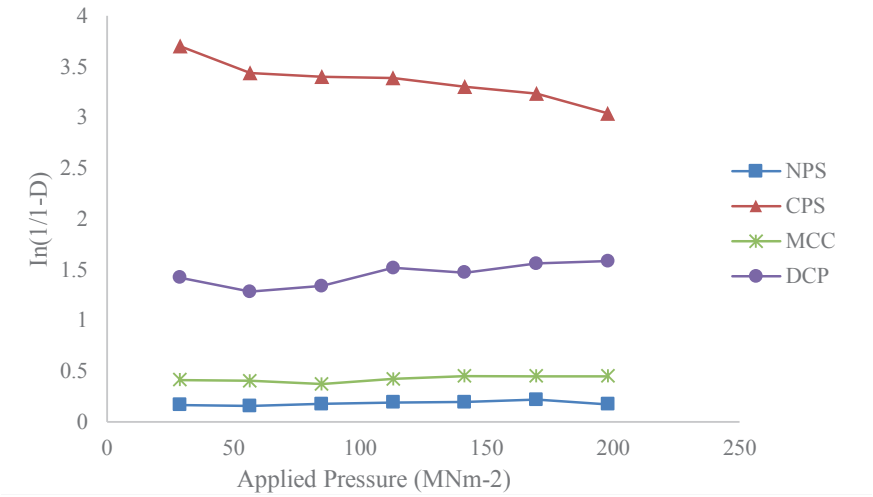

Figure 5. Representative Heckel plot.

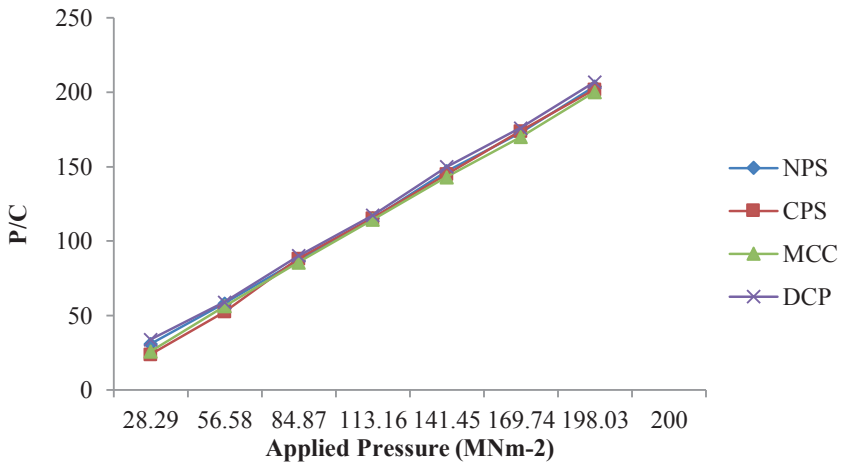

Figure 6. Representative Kawakita plot.

Table 3. Parameters obtained from compression data analysis.

	Heckel Parameters				Kawakita Parameters			
Sample	D_o	P_y	D_A	D_B	a	D_I	b	P_K
NPS	0.501	52.90	0.9220	0.501	0.2527	0.7473	0.2177	4.59
CPS	0.074	250.00	0.1511	0.610	0.2547	0.7453	0.5646	1.77
DCP	0.610	26.70	0.7240	0.074	0.2579	0.7421	0.0109	91.74
MCC	0.087	116.27	0.4910	0.087	0.2517	0.7483	0.0334	29.94

Mechanical properties of metronidazole tablet formulations

The summary of the properties of metronidazole tablets formulated with CPS and NPS are shown in Table 4. The uniformity of weight test is a reflection of the amount of active pharmaceutical ingredient (API) present in a formulation although it does not assure uniformity of the API in all the tablets particularly in low dose formulations. According to the USP "for tablets with weights greater than 324 mg, not more than two tablets should have weights that deviate from the average weight by more than 5%" [24]. Only formulations containing 40 % w/w CPS and 50 % w/w NPS met the compendia specification. Tablets should have enough mechanical strength in order to be able withstand the stress encountered during packaging, transportation and handling. The crushing strength and friability are important parameters that have been used to assess the mechanical strength of tablet formulations [25]. A tablet must have a crushing strength of not less than 4 kg to be considered of satisfactory mechanical strength [26]. The results show that all the formulations have satisfactory strength except formulations containing 40 % w/w CPS. The friability test measures the physical strength of tablets on exposure to attrition or mechanical shock. Conventionally, friability values less than 1 % are considered acceptable [23]. Table 4 shows that all the formulations did not meet the specification and tablets containing CPS are more friable than those formulated with NPS. The crushing strength – friability ratio (CSFR) can also be used to assess the mechanical strength of tablets. Generally, the higher the CSFR, the stronger the tablet (Bakre and Sholuade, 2018). Tablets containing NPS were stronger than formulations containing CPS. All the formulations had disintegration time lower than the British Pharmacopeia [28] specification of 15 min for uncoated tablets. However, tablets formulated with NPS disintegrated faster than formulations having CPS. Generally, formulations containing 40 % w/w starch had lower disintegration time than those containing 50 % w/w starch.

Table 4. Tableting parameters of metronidazole formulations.

Formation Code	Uniformity of weight (mg)	Crushing Strength (kg/cm)	Friability (%)	Disintegration Time (secs)	CSF	T_{50} (secs)	T_{90} (secs)
A	0.401±0.42	4.33±0.23	12.1±0.03	50±0.01	0.36	23.9	42.9
B	0.393±0.05	1.83±0.05	11.4±0.15	23±0.13	0.16	45.7	84.1
C	0.395±0.03	4.67±0.01	10.1±0.04	21±0.04	0.46	26.0	53.8
D	0.393±0.11	5.33±0.03	10.0±0.14	19±0.06	0.53	96.5	182.6

In vitro release properties

The dissolution profile of the metronidazole formulations containing NPS and CPS is shown in Figure 7. The result (Table 4) shows that the rank order of the time taken for 50% (T_{50}) and 90% (T_{90}) drug release was A<C<B<D. Tablets formulated with CPS had faster dissolution than those containing similar concentration of NPS. In addition, the effect of CPS and NPS on dissolution was concentration dependent i.e formulations containing 50%w/w starch had faster dissolution than those formulated with 40 %w/w starch.

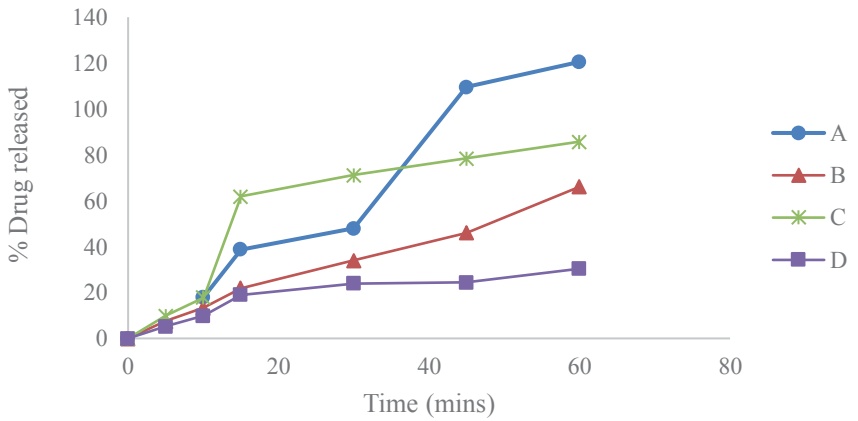

Figure 7. Representative plots of dissolution profile of metronidazole formulations.

Co-processing of potato starch with silicon dioxide represents a simple derivatization procedure that has augmented the compressional and tableting characteristic of the native starch. Although metronidazole tablets containing the co-processed excipient had low mechanical strength, they exhibited faster dissolution than tablets containing similar concentration of the native starch.

CONFLICT OF INTEREST

The authors declare that they don't have any conflict of interest.

REFERENCES

1. Abdellah A.; Noordin M. I.; Ismail W. A. Importance and globalization status of good manufacturing practice (GMP) requirements for pharmaceutical excipients. *Saudi Pharm. J.* **2015**, *23*, 9-13.

2. Zhou Q.; Shi L.; Chattoraj S.; Sun C.C. Preparation and characterization of surface-engineered coarse microcrystalline cellulose through dry coating with silica nanoparticles. *J. Pharm. Sci.* **2012**, *101*, 4258-4266.

3. Koo O.M.Y.; Squibb B. Application challenges and examples of new excipients in advanced drug delivery systems. *Am. Pharm. Rev.* **2011**, *14*, 60-68.

4. Builders P. F.; Mbah C. C.; Mohammed B. B. Preparation and evaluation of carbopol coated maize starch: A novel multifunctional excipient. *Afr. J. Pharm. Pharmacol.* **2017**, *11*, 458-469.

5. Gohel M. C.; Jogani P. D. A review of co-processed directly compressible excipients. *J Pharm. Pharm. Sci.* **2015**, *8*, 76-93.

6. Adetunji O. A.; Odeniyi M. A. Material and compression properties of *Cedrela odorata* gum co-processed with plantain starch and microcrystalline cellulose. *Polim. Med.* **2016**, *46*, 35–43.

7. Mshelia J. G.; Apeji Y. E.; Olayemi O. J. Powder, compaction and tableting properties of co-processed silicified starch. *British J Pharm. Res.* **2015**, *6*, 131-140.

8. Rojas J.; Kumar V. Comparative evaluation of silicified microcrystalline cellulose II as a direct compression vehicle. *Int. J. Pharm.* **2011**, *416*, 120-128.

9. Daraghmeh N.; Rashid I.; Al Omari M. M. H.; Leharne S. A.; Chowdhry B. Z.; Badwan A. Preparation and characterization of a novel co-processed excipient of chitin and crystalline mannitol. *AAPS Pharm. Sci. Tech.* **2010**, *11*, 1558-1571.

10. Builders P. F.; Arhewoh M. I. Pharmaceutical applications of native starch in conventional drug delivery. *Starch.* **2016**, *68*, 864-873.

11. Alebiowu G. Steeping period influence on physical, compressional and mechanical properties of tapioca starch. *J. Pharm. Res.* **2007**, *6*, 139-144.

12. Bakre L. G.; Ajala J. Preliminary evaluation of the physicochemical properties of maize husk, maize silk and cellulose derived from maize husk. *Nig. J. Pharm. Sci.* **2012**, *11*, 21-30.

13. British Standard 1469. British Standard Institution: London. **1970**.

14. Heckel R.W. Density-pressure relationship in powder compaction. *Trans Metal Soc. AIME.* **1961**, 221.

15. Kawakita K.; Ludde K. H. Some considerations on powder compression equations. *Powder Technol.* **1971**, *4*, 61-68.

16. Bakre L. G.; Osideko A.O.; Bamiro O. A. Isolation and characterization of a plant gum from *Chrysophyllum albidium* fruits as pharmaceutical excipient. *J Pharm. Biores.* **2017**, *14*, 22-30.

17. Fang J. M.; Fowler P. A.; Tomkinson J.; Hill C. A. S. The preparation and characterization of series of chemically modified potato starches. *Carbohydr. Polym.* **2002**, *47*, 245–252.

18. Van Soest J. J. G.; Tournois H.; de Wit D.; Vliegenthart J. F. G. Short range structure in (partially) crystalline potato starch determined with attenuated total reflectance Fourier-transform IR spectroscopy. *Carbohydr. Res.* **1995**, *27*, 201-214.

19. Biliaderis C. G. Structures and phase transitions of starch in food systems. *Food Technol.* **1992**, *6*, 98-109.

20. Liu H.; Yu L.; Xie F.; Chen L. Gelatinization of cornstarch with different amylose/amylopec-

tin content. *Carbohydrate Polym.* **2006**, *65*, 357–363.

21. Jane J. Current understanding on starch granule structures. *J. Appl. Glycosci.* **2006**, *53*, 205–213.

22. Tester R. F.; Karkalas J.; Qi X. Starch—composition, fine structure and architecture. *J. Cereal Sci.* **2004**, *39*, 151–165.

23. Kwabena O.; Kwadwo A. M.; Samuel L. K.; Noble K.; Mariam E. B. Development and evaluation of natural gum-based extended release matrix tablets of two model drugs of different water solubilities by direct compression. *Saudi Pharm. J.* **2016**, *24*, 82-91.

24. United States Pharmacopoeia and National Formulary, **2007**. United States Pharmacopoeia XXIII: Rockville U.S.P Convention Inc.

25. Kaleemullah M.; Jiyauddin K.; Thiban E.; Rasha S.; Al-Dhalli S.; Budiasih S.; Gamal O.E.; Fadli A.; Eddy Y. Development and evaluation of Ketoprofen sustained release matrix tablet using *Hibiscus rosa-sinensis* leaves mucilage. *Saudi Pharm. J.* **2017**, *25*, 770–779.

26. Majekodunmi S. O.; Lori E. Lubricating properties of co-processed coconut oil in paracetamol tablets formulation. *British J. Pharm. Res.* **2016**, *14*, 1-10.

27. Bakre L. G.; Sholuade T.O. Formulation and In Vitro Evaluation of Ciprofloxacin Matrix Tablets: Effect of Drug-Polymer Ratio. *Trop. J. Nat. Prod. Res.* **2018**, *2*, 250-253.

28. British Pharmacopoeia Vol. 4. Her Majesty Stationery Office, London. **2003**; 2051.

Acta Pharm. Sci. Vol 57 No: 4. 2019
DOI: 10.23893/1307-2080.APS.05723

Design and Characterization of the Material Attributes of a Co-processed Excipient Developed for Direct Compression Tableting

Yonni Apeji1, [2*], Fatima Haruna[2], Avosuahi Oyi[2], Adamu Isah[2], Teryila Allagh[2]

1 National Institute of Pharmaceutical Education and Research (NIPER), Department of Pharmaceutics, Sector 67, S.A.S Nagar, Punjab 160 062, India.

2 Ahmadu Bello University, Faculty of Pharmaceutical Sciences, Department of Pharmaceutics and Industrial Pharmacy, Zaria, Kaduna State, Nigeria.

ABSTRACT

The objective of the study was to characterize the material attributes of a co-processed excipient and determine its suitability for tableting applications.

A single composite excipient named SGS consisting of tapioca starch (TS), gelatin (GEL) and colloidal silicon dioxide (CSD) was developed by co-processing using the method of co-fusion and its solid-state, powder and mechanical properties evaluated.

Particle morphology revealed spherical shaped particles of SGS with slightly rough surfaces. PXRD was characterized by a halo diffraction pattern consistent with amorphous materials. FT-IR studies demonstrated drug-excipient compatibility. Flow properties of SGS improved in relation to its physical mixture (SGS-PM) and the mechanical properties of SGS was enhanced as a result of co-processing. The outcome of the study demonstrates the suitability of SGS as a tableting excipient.

Keywords: Material attributes, starch, co-processed excipient, tableting

INTRODUCTION

In the formulation of tablets, excipients play a crucial role in ensuring the smooth processing, formation and robust performance of the dosage form. They have been rightly referred to as functional components of a formulation because they influence the manufacturability, stability, bioavailability and

*Corresponding Author: Yonni Apeji, e-mail: yeapeji@abu.edu.ng
Yonni Apeji ORCID Number: https://orcid.org/0000-0002-3116-7570
Fatima Haruna ORCID Number: https://orcid.org/0000-0001-5540-8212
Avosuahi Oyi ORCID Number: https://orcid.org/0000-0002-6232-425X
Adamu Isah ORCID Number: https://orcid.org/0000-0003-4913-1186
Teryila Allagh ORCID Number: https://orcid.org/0000-0002-5814-3499
(Received 16 May 2019, accepted 13 July 2019)

safety of the formulation[1]. Depending on the composition of the formulation, excipients may constitute more than 50 % of the entire formulation. They have been used actively as diluents, binders, disintegrants, glidant, lubricants, colorants etc.2-4 Due to the functional role of excipients in tablet formulation, it is imperative to continually expand the range of excipients available to the pharmaceutical industry to accommodate the diverse challenges encountered in the formulation of novel drug molecules.

Currently, direct compression (DC) method of tablet formulation is gaining much space among manufacturers because it is less demanding, cost effective and does not require much labour when compared to other methods of tableting like wet granulation[5,6]. Nevertheless, the successful processing of formulations containing drugs into tablets by direct compression rests solely on the robustness of the DC excipient employed. DC excipients are required to impart the critical attributes of flowability and compressibility to a formulation to ensure a smooth tableting process that will yield tablets of acceptable quality. Other attributes like solid-state properties and compaction behaviour can influence the functionality of DC excipients in tablet formulation[7,8]. Hence, it has become necessary to develop DC excipients that will fulfil the demands of a robust tableting process.

The concept of developing novel excipients with improved functionality by co-processing has been the focus of several researchers in the last few decades. It is a process where two or more excipients are combined at sub-particle level in optimized proportions using a suitable method to yield a single composite excipient that integrates the advantages of the interacting excipients while minimizing their limitations[5,9–12]. The rationale for co-processing two or more excipients takes into consideration the material properties of the interacting excipients. This factor is crucial because the functionality of the co-processed excipient is determined by the material attributes of the individual excipients. Many studies have been carried out by researchers to co-process excipients including starches, celluloses, gums, chitin and other traditional excipients[13–17]. In our study, native tapioca starch (TS) was co-processed with gelatin (GEL) and colloidal silicon dioxide (CSD) for consideration as a multifunctional excipient in DC formulations. Native starches are inherently weak with poor flow and compression properties[18]. Hence, they are not recommended for DC method of tablet formulation. To enhance the binding properties of TS, GEL has been incorporated to fortify its structural strength. CSD has been used traditionally as a glidant in tablet formulations[19]. Other pharmaceutical applications of CSD as a dispersing agent, suspending agent, emulsion stabilizer, adsorbent and

viscosity controlling agent have been documented in literature[20]. As a glidant, CSD has been added as part of the composition of the co-processed excipient to enhance its flowability. Several studies have shown that the deposition of CSD on particle surfaces during the process of silicification has generated materials with improved functionality relating to disintegration, mechanical resistance and tablet strength[21–23]. Hence, the inclusion of CSD in the formation of the co-processed excipient will enhance the overall performance of the excipient in tablet formulation. Tapioca starch was selected for this study as an alternative to corn starch that has been widely used as a tablet excipient in drug manufacturing. Among the starchy staples, tapioca gives a carbohydrate production which is about 40 % higher than rice and 25 % superior to corn, making tapioca the cheapest source of calories for both human nutrition and animal feeding[25]. It can be obtained in commercial quantities from the root crop of *Manihot esculenta* Crantz grown around the world particularly in Sub-Saharan Africa, Southeast Asia and Latin America but is yet to be fully harnessed by the pharmaceutical industry.

To date, there is yet to be any co-processed excipient that has been developed containing these three excipients. The solid-state, powder and compaction properties of SGS were characterized to evaluate its potential as a multifunctional excipient in direct compression tableting.

METHODOLOGY

Materials

Tapioca starch was obtained as a gift sample from Quality Starch and Chemicals (Tamil Nadu, India), Gelatin (May and Baker Ltd, England), Colloidal silicon dioxide (Cab-o-Sil®, Cabot GmbH, Germany), Ibuprofen (Himedia laboratories Ltd, Mumbai, India). All other materials used were of analytical grade.

Preparation of the co-processed excipient

The co-processed excipient code-named *SGS* was prepared using the method described by Adeoye and Alebiowu[26]. Tapioca starch (90 g) was dispersed in distilled water to obtain a 40 $\%^{w}/_{w}$ suspension and mixed with corresponding quantities of gelatin (7.5 g) and colloidal silicon dioxide (2.5 g) for 5 min. Further mixing continued in a shaker water bath (Julabo SW 23, Seelbach, Germany) set to rotate at a speed of 60 rpm and temperature of 54 ± 2 °C for 15 min. The mixture was homogenized for 5 min at a speed of 11,000 rpm (Ultra Turrax T 25 basic Ika® Werke, India), followed by air-drying initially at room temperature (25 ± 2 °C) for 2 h and then drying completed in the Fluid bed dryer (Retsch TG 100, Germany) at 40 °C for 10 min. The powder obtained was

passed through a sieve of 500 μm, packed into tight sealed containers and kept in the desiccator containing phosphorous pentoxide (P_2O_5) for further studies.

Optical and polarized microscopy

Optical and polarized microscopy of the powder samples were performed with Leica DMLP polarized microscope (Leica Microsystems Wetzlar GmbH, Germany). The images obtained were captured with a JVS colour video camera and analysed using Linksys 32 software. Particle size analysis was carried out by measuring diameter along the longest axis of a minimum of 500 particles for each sample and the d_{10}, d_{50} and d_{90} parameters reported.

Scanning electron microscopy (SEM)

Particle morphology of powder samples were observed under a scanning electron microscope (S-3400, Hitachi Ltd., Tokyo, Japan) operated at an excitation voltage of 10 kV. The powder samples were mounted onto a steel stage using double sided adhesive tape and coated with gold using ion sputter (E-1010, Hitachi Ltd., Japan). Thereafter, SEM images of powder samples were captured at various magnifications.

Powder X-ray diffraction (PXRD)

PXRD analysis of powder samples were recorded at room temperature on Bruker's D8 advance diffractometer (Bruker, Germany) with Cu Kα radiation (1.54 Å), at 40 kV, 40 mA passing through nickel filter. Analysis was performed in a continuous mode with a step size of 0.01 ° and step time of 1 s over an angular range of 2 – 40 ° 2**θ**, using zero background holder. The obtained diffractograms were analysed with DIFFRAC plus EVA (ver.9.0) diffraction software.

Fourier transform infrared spectroscopy (FT-IR)

The FT-IR spectra of all powder samples were recorded from 4000 to 650 cm^{-1} on Perkin Elmer Spectrum 400 spectrometer. Drug-excipient compatibility studies was carried out by running an IR scan of the physical mixture of ibuprofen and SGS in a 1:1 ratio. Analysis of FT-IR spectra was performed using Spectragryph-optical spectroscopy software (ver. 1.2).

True density

The method of helium pycnometry (Pycno 30, Smart Instruments, India) was used to measure the true density of powder samples at 25 ± 2 °C/40 ± 2% RH. The data was collected in triplicate and the mean ± SD was recorded.

Bulk density, Tapped density, Carr's index and Hausner's ratio

Bulk and tapped density parameters for each powder sample were determined according to the USP II method[27]. Carr's index (CI) and Hausner's ratio (HR) were calculated based on equations 1 & 2 using a minimum of three replicates.

$$CI = \frac{TD-BD}{TD} \times 100\ \% \quad \text{.....Eq.1}$$

$$HR = \frac{TD}{BD} \quad \text{.....Eq.2}$$

Angle of repose (AR)

The flow properties of powder samples were assessed by measuring the angle of repose using the granulate flow tester (GTB, Erweka, Germany). Twenty grams (20 g) of the sample powder was poured into the stainless-steel funnel and allowed to flow out through the orifice measuring 10 mm in diameter unto a plate with specified surface forming a cone of powder. The side wall of the built-up cone was measured using an integrated driven laser and the actual angle of repose was calculated and displayed. The experiment was repeated three times and the average recorded (n=3).

Heckel and Kawakita analysis

Powder compacts for each sample were obtained by compressing 400 mg powder weighed individually on a Hydraulic press (Model 3912, Carver Inc., USA) at pressures ranging from 35 – 250 MPa using a 13 mm flat-faced circular punch and die set at a dwell time of 30 s. A minimum of three tablets were compressed at each pressure. The tablets were kept in the desiccator containing phosphorous pentoxide (P_2O_5) for 24 h to allow for elastic recovery prior to analysis. The thickness and diameter of the tablets were measured using a digital micrometre screw gauge (Mitutoyo, Japan). The following parameters were calculated for each tablet: volume, apparent density, relative density and porosity. The data obtained were fitted into the Heckel and Kawakita equations to generate plots used to characterize the compaction profile of the powder samples.

The Heckel model[28] shows the densification of the powder bed during compaction as a function of the applied compression pressure and is presented in Eq. (3):

$$1n\left(\frac{1}{1-D}\right) = KP + A \quad \text{.....Eq.3}$$

where D is the relative density of a compact, K is the Heckel coefficient (slope of a linear part of the curve), P is the applied compression pressure and A is the y-axis intercept. The onset of plastic deformation is defined as the Heckel yield pressure (P_Y) and it is expressed as the reciprocal of the slope, K.

The Kawakita model[29](b describes the relationship between the degree of volume reduction of the powder and the applied pressure and is represented by Eq. 4 below:

$$\frac{P}{C} = \frac{P}{a} + \frac{1}{ab} \quad \text{.....Eq.4}$$

Where C and P represents the degree of volume reduction and compression pressure, respectively. The constant 'a' is the initial porosity of the material at the beginning of compression while the constant 'b' relates to the degree of plasticity of the material. The reciprocal of b or P_K defines the pressure required to reduce the powder bed by 50 %.

The porosity-pressure relationship, tensile strength-pressure relationship and tensile strength-porosity relationship representing compressibility, tabletability and compactibility (CTC) respectively were illustrated with plots generated based on the data obtained from compaction studies[30–32].

Tensile strength

The breaking force required to crush tablets diametrically was measured using a tablet hardness tester (Erweka, USA). The dimensions of thickness and diameter for each tablet were measured using a digital calliper (Digimatic Mitutoyo Corporation, Japan) and fitted into Eq. 5 below to calculate tensile strength[33].

$$\sigma = \frac{2F}{\pi dt} \quad \text{.....Eq.5}$$

Where **σ** is the tensile strength (MM/m^2), F is the breaking force (N), d is the diameter (mm), and t is the thickness of the tablet (mm).

RESULTS AND DISCUSSION

There exists a relationship between the material attributes of an excipient and their functionality in drug product development. Solid-state properties, pow-

der and mechanical properties of an excipient are known to predict its performance in formulation development[7]. Characterization of an excipient's properties is therefore necessary to identify its material attributes that will be a key consideration for its rational selection in drug formulation.

Optical and polarized images of TS and SGS are presented in Fig. 1 (A) – (D). The optical images appear spherical with the polarized images revealing a birefringent pattern (presence of a Maltese cross) consistent with the granular structure of native starches. This implies that co-processing did not affect the granular integrity of TS and hence gelatinization did not occur at the temperature employed for co-fusion. Gelatinization of TS occurs within the range of 55 – 70 ° C and is characterized by loss of birefringence (disappearance of the Maltese cross) and crystallinity[34,35]. Hence, the improvement in the functionality of SGS can be attributed to sub-particle level changes occurring as a result of co-processing TS with GEL and CSD and not to gelatinization of TS. The presence of these other excipients enmeshed in the particle structure of TS modulated its physicomechanical properties without necessary interfering with its granular structure. This confirms that co-processing as a particle engineering technique is entirely a physical process[5,10]"

Particle size analysis carried out by microscopy revealed an increase in particle size of SGS relative to TS evidenced by the parameters, d_{10}, d_{50}, & d_{90} (Table 1). The median particle size (d_{50}) of SGS was 2.4 times more than TS. The polydispersity index (PI) parameter was higher for SGS indicating a broader particle size distribution. Co-processing by co-fusion led to the agglomeration of the three excipients leading to particle size enlargement. Enhancement in the flowability profile of SGS has been linked to the increase in particle size. This outcome agrees with the findings of Adeoye and Alebiowu[26,36] who developed a co-processed excipient using a similar method. It is necessary to control particle size of DC excipients as significant variation in size with the drug may lead to segregation during tableting[5,37].

Table 1. Particle size analysis of TS and SGS

Material	Particle size distribution				
	D_{10}(µm)	D_{50}(µm)	D_{90}(µm)	Range (µm)	Polydispersity index (PI)
SGS	15.5	29	57.8	6.3 - 110.9	1.46
TS	8.9	12.3	16.8	5.6 - 25	0.64

TS – Tapioca starch SGS – Co-processed excipient

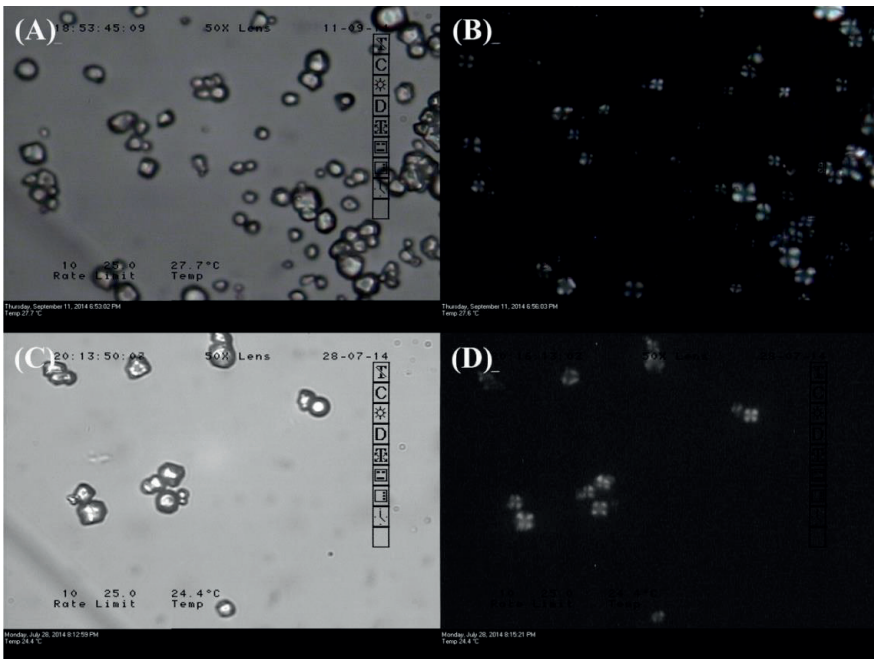

Figure 1. (A) Optical image of TS, (B) Polarized image of TS, (C) Optical image of SGS, (D) Polarized image of SGS.

SEM images of SGS, TS, GEL and CSD are presented in Fig. 2 (A) – (D). Particle morphology of SGS revealed spherical shaped particles with slightly rough surfaces owing to the presence of GEL and CSD in the particle structure of TS. This agrees with the findings of Kittipongpatana and Kittipongpatana[14] who attributed the rough surface morphology of co-processed rice starch and CSD to the homogeneous distribution of CSD on its surface. The surface roughness of SGS may have contributed to its improved tabletability profile when compared to its physical mixture (SGS-PM) due to increase in adhesion between bonding surfaces during compaction[38–40]". The spherical shape of SGS must have been derived to a large extent from TS as the major component of the co-processed excipient. This further explains the improvement in the flow properties of SGS considering the role particle shape plays in the flowability of materials[15].

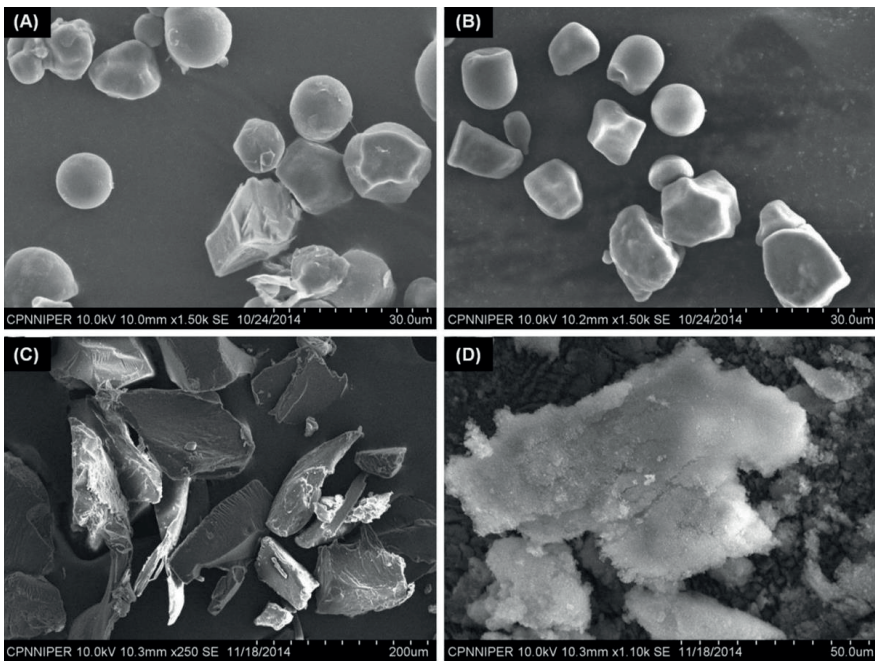

Figure 2. SEM images of (A) SGS, (B) TS, (C) GEL and (D) CSD

An overlay of the PXRD diffraction curves of the individual excipients (TS, GEL and CSD) and the co-processed excipient (SGS) is presented in Fig. 3A. The diffraction patterns of GEL and CSD were characterized by the absence of no peaks indicating that the material is non-crystalline. The diffraction curve of TS revealed a halo pattern which is consistent with amorphous polymers. The broad peaks observed in the diffraction pattern of TS showed that the ma-

terial had some degree of crystallinity. A similar pattern was replicated in the diffraction curve of SGS implying that there was no significant chemical interaction occurring between the excipients during co-processing. PXRD patterns of SGS and SGS-PM displayed in Fig. 3B revealed a halo pattern consistent with amorphous materials[16]. The broad peak occurring at 2θ value of 13 ° can be attributed to the semi-crystalline nature of starch. Consequently, the diffraction patterns of SGS and SGS-PM were superimposable indicating that co-processing did not alter the molecular structure. The sharp diffraction peaks of ibuprofen confirm the crystalline nature of the drug (Fig. 3C). These peaks were maintained in the powder mix of IBU and SGS indicating drug-excipient compatibility.

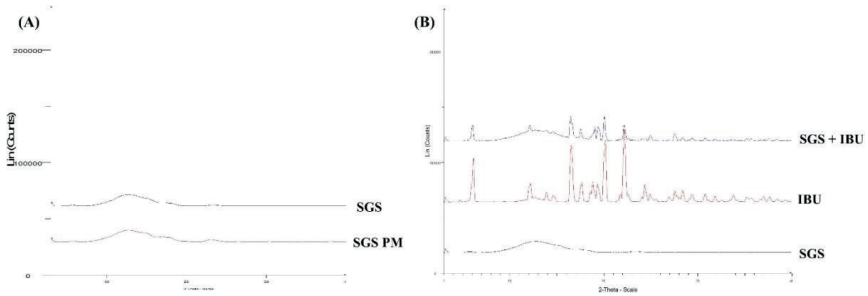

Figure 3. PXRD of (A) SGS and SGS-PM (B) SGS, IBU and SGS + IBU

The FT-IR spectra of SGS, IBU and SGS+IBU are presented as an overlay plot in Fig. 4. The IR spectrum of SGS showed characteristic peaks at 2934, 1636, 1416, 1337, 1150 and 998.6 cm^{-1} corresponding to C-H aliphatic stretch, NH bend, C-N stretch, C-O stretch and C=H bend respectively. The IR spectrum of IBU was characterized by vibrations occurring at 3630 cm^{-1} (OH stretch), 3088, 2954 cm^{-1} (C-H stretch), 1707 cm^{-1} (C=O stretch), and 1183 cm^{-1} (C-O stretch) (Fig. 5C). These peaks were retained in the IR spectrum of a blend of IBU and SGS suggesting that both materials are compatible. Although, changes in the intensity of peaks were observed as a result of dilution effect, the position of these peaks was maintained without a significant shift. Drug-excipient compatibility was therefore confirmed with IR studies.

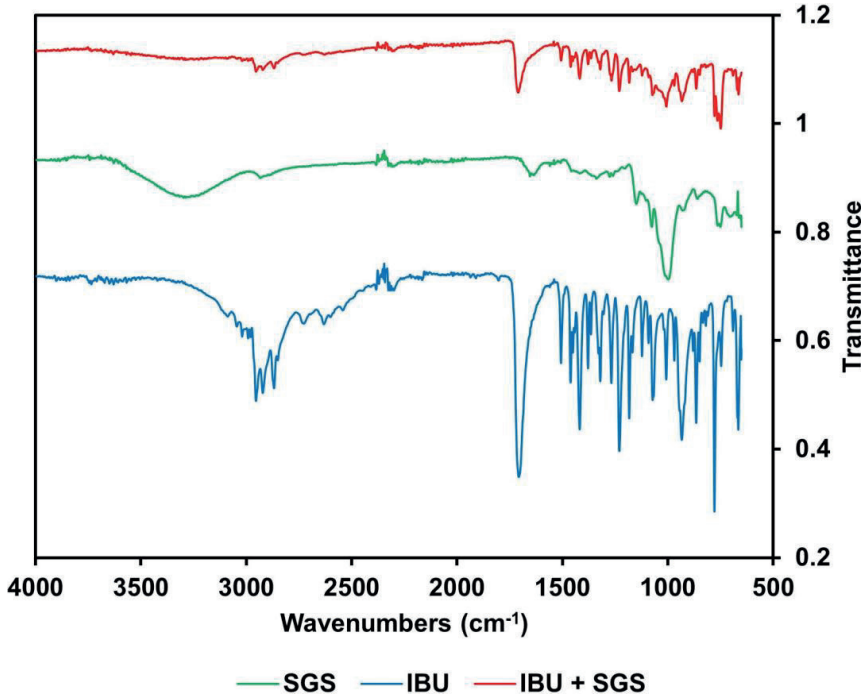

Figure 4. FT-IR overlay of SGS, IBU and SGS+IBU

Table 2 summarizes the powder properties of TS, SGS and SGS-PM. Measurement of angle of repose was used to estimate the flow behaviour of the investigated powders. Values were reported only for SGS as it was not possible to measure the angle of repose of TS and SGS-PM due to poor flowability. The value reported for SGS was 21.6 ° which is an indication of a free-flowing powder. Other parameters measured to estimate powder flow for all three materials were CI and HR which ranged from 14.7 – 23.2 % and 1.17 – 1.30 respectively with SGS having the least values for both parameters. CI and HR parameters of SGS were consistent with the angle of repose as they met the requirements for good flow properties (CI < 20 % and HR < 1.2)[15]roundness, irregularity, equivalent circle diameter (ECD. These parameters give an indirect estimate of the flow behaviour of a material as they measure the degree of packing or consolidation of a powder based on the bulk and tapped densities.

Table 2. Powder properties of TS, SGS and SGS-PM (n = 3)

Properties	TS	SGS	SGS-PM
Angle of repose (°)	Not passable	21.6 (0.29) *	Not passable
Bulk density (g/cm^3)	0.51 (0.02)	0.48 (0.01)	0.54 (0.02)
Tapped density (g/cm^3)	0.65 (0.02)	0.57 (0.02)	0.70 (0.03)
Carr's index (%)	22 (2.64)	14.7 (2.34)	23.2 (2.76)
Hausner's ratio	1.28 (0.04)	1.17 (0.03)	1.30 (0.05)
Porosity (%)	66.5	66.6	63.3
True density	1.52 (0.02)	1.45 (0.02)	1.46 (0.01)

* The values in parentheses represent standard, TS – Tapioca starch, SGS – Co-processed excipient

SGS-PM – Physical mixture of the component excipients of the co-processed excipient in similar proportion

Powder flow is critical to the success of tablet formulation by direct compression. Majority of excipients considered for direct compression are required to impart flowability to the powder blend of the drug and excipient to prevent a wide variation in weight and content uniformity of tablets. One outstanding attribute of co-processed excipients is improved flowability. The study has shown an improvement in the flow functionality of SGS based on AR, CI and HR. Lower values for all three parameters corresponds to better flow properties. It was not possible to measure the angle of repose of TS and SGS-PM because the because of increased interparticulate friction existing between particles of small sizes. The mechanism by which flowability of SGS was improved by co-processing can be attributed to the increase in particle size and porosity giving particles ample space to flow easily. The lower the degree of packing of a powder, the better the flow output of the powder. Hence, powders that are more porous will flow faster compared to less porous powders as confirmed by the bulk and tapped densities of SGS (Table 2) which were relatively low compared to TS and SGS-PM. The improvement in flow properties of SGS as a result of co-processing agrees with the trend observed by other studies performed in the development of co-processed excipients[13–15,26,41]

The Heckel and Kawakita parameters describing the mechanical properties of SGS and SGS-PM are presented in Table 3.

Table 3. Heckel and Kawakita Parameters of SGS and SGS-PM

	Heckel				Kawakita		
Material	P_Y (MPa)	D_A	D_0	D_B	a	b	P_K
SGS	243.90	0.803	0.393	0.410	0.659	0.159	6.299
SGS-PM	285.71	0.736	0.479	0.257	0.607	0.090	11.077

SGS – Co-processed excipient, SGS-PM – Physical mixture of the component excipients of the co-processed excipient in similar proportion

The pressure at which deformation was initiated during compaction corresponds to the mean yield pressure (P_Y) computed as the inverse of the slope of the linear portion of the Heckel plot (Fig. 5A). The P_Y of SGS was lower than that of SGS-PM indicating that a faster onset of plastic deformation had occurred during compression. Lower values of P_Y implies that the material is soft, ductile and readily undergoes plastic deformation while higher values have been implicated in materials that are hard, brittle and resistant to plastic deformation. A lower yield pressure was obtained for SGS relative to SGS-PM implying that it is more compressible and less resistant to deformation during compression into compacts. This may be attributed to the insertion of GEL and CSD into the particle structure of TS which influenced its deformation behaviour giving rise to a material that is more compressible and deforms at a lower yield pressure. The total degree of powder consolidation at the beginning of compression (D_A) was seen to be higher for SGS compared to SGS-PM. This can be attributed to the high degree of particle fragmentation occurring with SGS during compression as evidenced by its high D_B value. Particle fracture at the early stages of compression leads to the generation of smaller particles which rearrange to fit into the pore spaces resulting in a highly consolidated powder bed[42]. The extent of powder consolidation occurring as a result of initial particle rearrangement due to particle movement (D_0) was lower for SGS compared to SGS-PM suggesting that particle fragmentation (D_B) was the major contributor to the total degree of powder consolidation.

The P_K parameter resolved from the Kawakita plot (Fig. 5B) is a measure of the pressure required to contract the volume of the powder bed by 50 % during compaction. A lower value was obtained for SGS in comparison to SGS-PM

indicating a faster onset of compression. The '*a*' parameter which is a measure of compressibility was higher for SGS compared to SGS-PM. Similarly, the '*b*' parameter which corresponds to the total amount of plastic deformation occurring in the powder during compaction was higher for SGS compared to its physical mixture, SGS-PM. The P_K value which represents the compression effort needed to consolidate the powders to 50 % of its initial volume was found to be lower for SGS when compared to its physical mixture, SGS-PM. Overall, the findings of Kawakita analysis is consistent with the observations of the Heckel analysis.

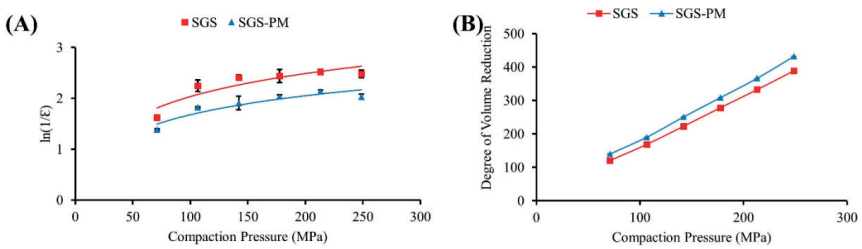

Figure 5. (A) Heckel Plot and (B) Kawakita Plot

The CTC (compressibility, tabletability and compactibility) profile of SGS and SGS-PM is illustrated in Fig. 6A-C. The compressibility plot (Fig. 6A) of the two materials reveals a decrease in the porosity of the compact as the compaction pressure increases. It was observed that the porosity of compacts for both materials did not change significantly beyond 100 MPa. The porosity of SGS compacts were found to be lower when compared to those of SGS-PM at the same compaction pressure implying a greater degree of compressibility in SGS. Compressibility refers to the ability of a powder to undergo volume reduction under the effect of applied pressure and is represented by a porosity-pressure relationship[31,32]

The porosities of SGS compacts were significantly lower than those of SGS-PM across the range of pressures employed implying a greater degree of compressibility. There was an increased capacity for volume reduction during compression of SGS possibly due to the presence of CSD which has been used as a compressibility enhancing agent[17,24]. The presence of GEL in the particle structure of SGS is more likely to have contributed to its compressibility because of its role as a binder which improves the cohesiveness of powder particles during compression thereby lowering the porosity with a corresponding increase in relative density (solid fraction) of the compact. The effect of reduction in po-

rosity during compression brings particles in close proximity thereby increasing the area available for bonding. Compressibility of an excipient therefore plays a significant role in the formation of tablets.

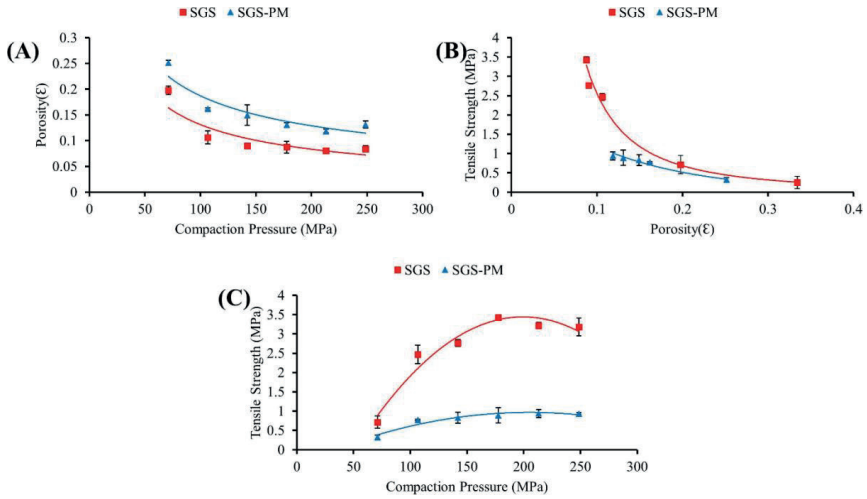

Figure 6. (A) Compressibility plot, (B) Compactibility plot and (C) Tabletability plot.

The compactibility plot illustrated in Fig. 6B demonstrated a pattern of increasing tensile strength of compacts with decrease in porosity for both materials. Compacts of higher tensile strength at the same level of porosity were obtained with SGS in comparison to SGS-PM. Compactibility refers to the ability of a material to form compacts of sufficient mechanical strength and is depicted by tensile strength-porosity relationship[30,31]. For the successful formation of tablets during compression, bonds must be formed between neighbouring particles to convert the loose powder bed into a solid compact. The degree of compactibility of SGS was significantly higher than that of SGS-PM as the tensile strength of SGS compacts produced at the same level of porosity was twice the value obtained with SGS-PM. Hence, there was an improvement in the compactibility of SGS as a result of co-processing leading to an increased bonding strength per unit area.

The tabletability profile of the two materials depicted in Fig. 6C shows the effect of compaction pressure on tensile strength of compacts. There was a corresponding increase in tensile strength of compacts for both materials as the applied pressure increased. The tensile strength of SGS compacts was found to be higher than that of SGS-PM at the same compression pressure. Maximum tensile strength obtained for SGS compacts was 3 MPa compared to less than 1

MPa for SGS-PM at a compaction pressure of 250 MPa. The combined effect of compressibility (bonding area) and compactibility (bonding strength per unit area) must have resulted in the improved tabletability observed with SGS over SGS-PM. Tabletability is the capacity of a powdered material to be transformed into a tablet of specified strength under the effect of compaction pressure[31,40]. The improved tabletability of SGS may have been attributed to its ability to overcome the elastic recovery stage occurring during decompression thereby retaining to a large degree the strength of interparticulate bonds formed during compression. Materials with high particle fragmentation tendency are not prone to immediate elastic recovery because of the minimal elastic energy that is stored during compression[43]. Hence, the combined mechanisms of bonding area and bonding strength (BABS) is necessary for the successful formation of tablets[39,40]. The material attributes of a co-processed excipient (SGS) developed by co-fusion were characterized and found to be suitable for tableting applications in comparison to its parent excipient (TS) and physical mixture (SGS-PM).

REFERENCES

1. Camargo, J. J. R. Assessment of co-processing of cellulose II and silicon dioxide as a platform to enhance excipient functionality. PhD Thesis, University of Iowa, **2011**.

2. Odeku. O. A. Potentials of tropical starches as pharmaceutical excipients: A review. *Starch/Staerke*, **2013**, *65*, 89–106.

3. Emeje, M. O.; Asha, R. Starch. from food to medicine. In: Valdez B, editor. *Scientific, Health and Social Aspects of the Food Industry*. Online, Shanghai, China: InTech China; **2012**, p. 355–380.

4. Rashid, I.; Al-Omari, M. M. H.; Badwan A. A. From native to multifunctional starch-based excipients designed for direct compression formulation. *Starch/Starke*, **2013**, 65(Dc), 552–571.

5. Nachaegari, S. K.; Bansal, A. K. Coprocessed Excipients for Solid Dosage Forms. *Pharm. Technol.* **2004**, (January), 52–64.

6. Rojas, J.; Aristizabal, J.; Henao, M. Screening of several excipients for direct compression of tablets: A new perspective based on functional properties. *J. Basic Appl. Pharm. Sci.* **2013**, *34*, 17–23.

7. Sun, C. C. Materials Science Tetrahedron—A Useful Tool for Pharmaceutical Research and Development. *J. Pharm. Sci.* **2009,** *98*, 1671–1687.

8. Zhou, D.; Qiu, Y. Understanding Material Properties in Pharmaceutical Product Development and Manufacturing: Powder Flow and Mechanical Properties. *J. Valid. Technol.* **2010**, 65–77.

9. Saha, S.; Shahiwala, A. F. Multifunctional coprocessed excipients for improved tabletting performance. *Expert Opin. Drug Deliv.* **2009**, *6*, 197–208.

10. Rojas, J.; Buckner, I.; Kumar, V. Co-processed excipients with enhanced direct compression functionality for improved tableting performance. *Drug Dev. Ind. Pharm.* **2012**, *38*, 1159–1170.

11. Daraghmeh, N.; Chowdhry, B.; Leharne, S.; Omari, M.; Badwan, A. Co-Processed Chitin-

Mannitol as a New Excipient for Oro-Dispersible Tablets. *Mar. Drugs,* **2015**, *13*, 1739–1764.

12. Mshelia, J.; Apeji, Y.; Olayemi, O. Powder, Compaction and Tableting Properties of Co-processed Silicified Starch. *Br. J. Pharm. Res.* **2015**, *6*, 131–140.

13. Daraghmeh, N.; Rashid, I.; Al Omari, M. M. H.; Leharne, S. A.; Chowdhry, B. Z.; Badwan, A. Preparation and characterization of a novel co-processed excipient of chitin and crystalline mannitol. *AAPS PharmSciTech,* **2010**, *11*, 1558–1571.

14. Kittipongpatana, O. S.; Kittipongpatana, N. Preparation and physicomechanical properties of co-precipitated rice starch-colloidal silicon dioxide. *Powder Technol,* **2011**, *217*, 377–382.

15. Ogunjimi, A. T.; Alebiowu, G. Flow and consolidation properties of neem gum coprocessed with two pharmaceutical excipients. *Powder Technol,* **2013**, *246*, 187–192.

16. Sharma, P.; Modi, S. R.; Bansal, A. K. Co-processing of hydroxypropyl methylcellulose (HPMC) for improved aqueous dispersibility. *Int J Pharm*, **2015**, *485*, 348–356.

17. Rojas, J.; Kumar, V. Comparative evaluation of silicified microcrystalline cellulose II as a direct compression vehicle. *Int J Pharm,* **2011**, *416*, 120–128.

18. Odeku, O. A.; Schmid, W.; Picker-Freyer, K. M. Material and tablet properties of pregelatinized (thermally modified) Dioscorea starches. *Eur J Pharm Biopharm* **2008**, *70*, 357–371.

19. Jonat, S.; Albers, P.; Gray, A.; Schmidt, P. C. Investigation of the glidant properties of compacted colloidal silicon dioxide by angle of repose and X-ray photoelectron spectroscopy. *Eur J Pharm Biopharm* **2006**, *63*, 356–359.

20. Jonat, S. The mechanism of hydrophilic and hydrophobic colloidal silicon dioxide types as glidants. PhD Thesis, Eberhard-Karls-Universität Tübingen, **2005**.

21. Tobyn, M. Physicochemical comparison between microcrystalline cellulose and silicified microcrystalline cellulose. *Int J Pharm* **1998**, *169*, 183–194.

22. Edge, S.; Steele, D. F.; Chen, A.; Tobyn, M. J.; Staniforth, J. N. The mechanical properties of compacts of microcrystalline cellulose and silicified microcrystalline cellulose. *Int J Pharm* **2000**, *200*, 67–72.

23. Majerová, D.; Kulaviak, L.; **Růžička, M**.; Štěpánek, F.; **Zámostný, P. Effect of colloidal silica on rheological properties of common pharmaceutical excipients.** *Eur J Pharm Biopharm*. **2016**, *106*, 2-8.

24. Arora, V.; Gupta, V. B.; Singhal, R. Advances in direct compression technology. *Pharma Times* **2007**, *39*, 26–27.

25. Iyali, J. M. Cassava : Nigeria's untapped Goldmine. *Freedom Radio Nigeria*. Available from: http://www.freedomradionig.com/index.php/39-icetheme/editorials/403-cassava-nigeria-s-untapped-goldmine [accessed January 1, 2014].

26. Adeoye, O.; Alebiowu, G. Flow, packing and compaction properties of novel coprocessed multifunctional directly compressible excipients prepared from tapioca starch and mannitol. *Pharm Dev Technol* **2014**, *19*, 901–910.

27. United States Pharmacopoeial Convention. USP Protocol for bulk and tapped densities. *USP/NF*, **2012**.

28. Heckel, R. W. Density-Pressure Relationships in Powder Compaction. *Trans Metall Soc AIME* **1961**, *221*, 671–675.

29. Kawakita, K.; **Lüdde, K. H. Some considerations on powder compression equations.** *Powder Technol* **1971**, *4*, 61–68.

30. Upadhyay, P.; Khomane, K. S.; Kumar, L.; Bansal, A. K. Relationship between crystal structure and mechanical properties of ranitidine hydrochloride polymorphs. *Cryst. Eng. Comm.* **2013**, *15*, 3959–3964.

31. Joiris, E.; Di Martino, P.; Berneron, C.; Guyot-Hermann, A.; Guyot, J. Compression Behavior of Orthorhombic Paracetamol. *Pharm Res* **1998**, *15*, 1122–1130.

32. Khomane, K. S.; More, P. K.; Raghavendra, G.; Bansal, A. K. Molecular understanding of the compaction behavior of indomethacin polymorphs. *Mol. Pharm.* **2013**, *10*, 631–639.

33. Fell, J.; Newton, J. Determination of tablet strength by the diametral-compression test. *J Pharm Sci* **1970**, *59*, 688–691.

34. Sullivan, J. W.; Johnson, J. A. Measurement of starch gelatinization by enzyme susceptibility. *Cereal. Chem.* **1964,** *41*, 73–79.

35. Gomand, S. V.; Lamberts, L.; Derde, L. J.; Goesaert, H.; Vandeputte, G. E.; Goderis B. Structural properties and gelatinisation characteristics of potato and cassava starches and mutants thereof. *Food. Hydrocoll.* **2010**, *24*, 307–317.

36. Adeoye, O.; Alebiowu, G. Evaluation of co-processed disintegrants produced from tapioca starch and mannitol in orally disintegrating paracetamol tablets. *Acta Pol Pharm ñ Drug Res*, **2014**, *71*, 803–811.

37. Mîinea, L. A.; Mehta, R.; Kallam, M.; Farina, J. A.; Deorkar, N. Evaluation and Characteristics of a New Direct Compression Performance Excipient. *Pharm Technol* **2011**, *35*, 1–8.

38. Osei-Yeboah, F.; Sun, C. C. Tabletability Modulation Through Surface Engineering. *J Pharm Sci* **2015,** *104*, 2645–2648.

39. Osei-Yeboah, F.; Chang, S.; Sun, C. C. A critical Examination of the Phenomenon of Bonding Area - Bonding Strength Interplay in Powder Tableting. *Pharm. Res.* **2016**, *33*, 1126–1132.

40. Sun, C. C. Decoding Powder Tabletability: Roles of Particle Adhesion and Plasticity. *J Adhes Sci Technol* **2011**, *25*, 483–499.

41. Chauhan, S. I.; Nathwani, S. V.; Soniwala, M. M.; Chavda, J. R. Development and Characterization of Multifunctional Directly Compressible Co-processed Excipient by Spray Drying Method. *AAPS PharmSciTech* **2017**, *18*, 1293–1301.

42. Apeji, Y. E.; Aluga, D.; Olayemi, O.; Oparaeche, C.; Anyebe, S.; Gamlen, M.; Oyi, A. R. Comparative analysis of co-processed starches developed by three different methods. *Br J Pharm* **2017**, *2*, 1-15.

43. Zhang, J.; Wu, C. Y.; Pan, X.; Wu, C. On identification of critical material attributes for compression behaviour of pharmaceutical diluent powders. *Materials (Basel)* **2017**, *10*, 1–16.

Acta Pharm. Sci. Vol 57 No: 4. 2019
DOI: 10.23893/1307-2080.APS.05724

Formulation and Evaluation of Topical Gel Containing Nanostructured Lipid Carriers Dispersion of an Antifungal Drug

Srinivas Gujjar[1*], Madhavi BLR[1], Roopa Karki[1]

1 Department of Pharmaceutics and Industrial Pharmacy, Acharya & BM Reddy College of Pharmacy, 5 Soldevanahalli, Bengaluru, Karnataka 560107

ABSTRACT

Fungal infection are the common dermatological diseases. Drug delivery systems for topical use have shown significant advantages in targeting the drug to the action site in the body and also reduces the systemic side effects.

In the present study an attempt was made to prepare econazole nitrate loaded nanostructured lipid carrier (NLC). Different formulations were prepared by hot homogenization technique using solid lipid and liquid lipid (GMS, GMO) and surfactants (Poloxamer 188, Poloxamer 407). Formulations were characterized for entrapment efficiency, viscosity, spreadability, pH and *in vitro* drug release.

Entrapment efficiency of formulation F1-F8 was found to be 65.81-74.63%. The drug release of NLC gel followed zero order kinetics. NLC gel were stable at 40 ± 2°C and 75 ± 5% RH. Thus, the prepared NLC gel proved to be a potential candidate as a topical nanoparticulate sustained drug delivery system for econazole nitrate.

Keywords: Nanostructured lipid carrier, Econazole nitrate, Glyceryl monostearate, Glyceryl monooleate, hot homogenization.

INTRODUCTION

Fungal infections are the common dermatological diseases and more than 150 million people are affected with fungal infections, which have impact on human lives. Drug delivery systems for topical use have shown significant advantages in targeting the drug to the action site in the body and also reduces the systemic side effects. With the help of carrier's antifungal drug administration into skin can be improved including vesicular carriers and lipid nanoparticles. [1,2,3]

*Corresponding Author: Srinivas Gujjar, e-mail: srinivasgujjar95@gmail.com
Srinivas Gujjar ORCID Number: https://orcid.org/0000-0002-1439-7489
(Received 23 April 2019, accepted 18 July 2019)

NLC are colloidal nanoparticles produced by mixing liquid lipid (oils) with the solid lipid in which the liquid lipid is either embedded into the solid matrix or localized at the surface of solid particles. These nanoparticles vary in the submicron size range of 10-1000nm[4]. Lipid based drug delivery systems are more prominent because of site specific action[5,6]. As it has the potential to increase the solubility and improve the bioavailability of lipophilic drugs**.** Econazole nitrate (ECN) is an imidazole derivative compound, used primarily in the treatment of superficial infections. Some have reported that econazole nitrate is used for topical administration to treat fungal infections[7]. ECN has low aqueous solubility due to its hydrophobic nature, this can be a drawback on antifungal efficacy, it can be overcome by preparation of nanostructures lipid carriers by using lipid mixture and addition of surfactants and co surfactants for the formulation.

In the present study, an attempt was made to improve the permeability of drug, sustained drug delivery and side effects of the antifungal drug loaded nanostructured lipid carrier containing gel.

METHODOLOGY

Materials

Econazole nitrate was obtained as gift sample from Gufic Biosciences Ltd. Glyceryl monostearate was purchased from Central Drug House(P), Ltd. New Delhi. Glyceryl monooleate was purchased from Yarrow Chem Products, Mumbai. Poloxamer 188 and poloxamer 407 was purchased from Yarrow chem Ltd. All the other chemicals used were of analytical grade.

Methods

Selection of lipid phase

5 mg of Econazole nitrate was dispersed in mixture of melted lipid (5 g) and hot distilled water (5 ml) and Stirred continuously for 30 minutes under magnetic stirring and temperature maintained above 10° C melting point of lipid. Then aqueous phase was separated by ultracentrifugation at 5500 rpm and drug content was analyzed[7,8]

Melting point determination

Melting point of econazole nitrate was determined by using Thiele's tube method. Melting point of a drug sample has been the first indication of purity of the sample. The presence of relatively small amount of impurity can be detected by a lowering as well as widening in the melting point range.

Compatibility studies

FTIR analysis

FTIR spectral studies were carried out for pure drug econazole nitrate, freshly prepared and six months old 1:1 SDs and individual substances to check the compatibility between drug and polymers using Bucker Tensor-27 (Bucker, Germany)

Differential Scanning Calorimeter (DSC)

DSC studies were carried out on DSC Q60, Shimadzu, Japan. Sealed and perforated aluminum pans were used in the experiments for all samples. Temperature calibrations were performed using indium as standard. An empty pan sealed in the same way as for the sample was used as a reference. The entire samples were run in nitrogen atmosphere at a scanning rate of 10° C/ min from 50-300°C. By comparing the DSC curves of a pure drug sample with that of formulation, the presence of an impurity can be detected in a formulation[9].

Preparation of econazole nitrate loaded nanostructured lipid carriers

Econazole nitrate loaded nanostructured lipid carriers were prepared by using hot homogenization method. The solid lipid and liquid lipid were melted to approximately 10° C above its melting point; Econazole nitrate was dispersed in this molten lipid mixture. An aqueous phase was prepared by dissolving poloxamer 188 and poloxamer 407 as cosolvent in distilled water. The hot aqueous phase was added to the molten lipid mixture under magnetic stirring with same temperature maintained homogenized using Ultra Turax Homomgenizer Then obtained solution was kept in lyophilizer to get the final product (econazole nitrate nanostructured lipid carriers)[10-15].

Table 1. Formulation chart of econazole nitrate nanostructured lipid carriers

Formulation code	Econazole nitrate (g)	Glyceryl mono stearate (g)	Glyceryl monooleate (ml)	Poloxamer 188 (g)	Poloxamer 407 (g)	Distilled water (ml)
F1	0.1	1	1	0.5	2	100
F2		1	2	1.0	1.5	100
F3		1	3	1.5	1.0	100
F4		1	4	2	0.5	100
F5		1	5	0.5	0.5	100
F6		1	6	1.0	1	100
F7		1	7	1.5	1.5	100
F8		1	8	2	2	100

Preparation of nanostructured lipid carrier gel of econazole nitrate

2 g of carbopol was weighed and transferred slowly into 100 ml distilled water taken in a beaker. This solution was stirred at 200 rpm for 3 h under magnetic stirring. To this 10 g base gel, calculated amount of lyophilized nanostructured lipid carrier of econazole nitrate was added and stirred at 100 rpm for 2 h; followed by the addition of methyl paraben and propyl paraben. Triethanolamine about 1-3 drops was added to get the proper gel consistency[16-18].

Table 2. Formulation of Econazole nitrate-NLC gel

Sl.No.	Ingredients	Quantity taken
1	Carbopol	2 g
2	Methyl Paraben	0.2 g
3	Propyl Paraben	0.3 g
4	Optimized econazole nitrate-nanostructured lipid carrier (F3)	192mg
5	Triethanolamine	q.s.
6	Distilled water	Upto 100 ml

Evaluation of econazole nitrate NLC

Particle size analysis

The particle size of nanostructured lipid carrier (NLC), were measured by using Malvern Zeta sizer Nano ZS-90. Before analysis, nanosuspension was further diluted with HPLC graded water followed by sonication for 30 min. The mean particle size was decisived from the particle size distribution data.

Zeta potential

Zeta potential is defined as a measure of the magnitude of the electrostatic or charge repulsion or to allure between particles in liquid suspension. Its measurement will give detailed insight into the causes of dispersion, or flocculation, aggregation and can be applied to enhance the composition of dispersions, emulsions and suspensions. The unit of zeta potential is usually milli volt (mV). Before analysis, nanosuspension was further diluted with HPLC graded water followed by sonication for 30 min[19,20].

Scanning electron microscopy (SEM)

SEM photographs were taken for the prepared nanoparticles using a scanning electron microscope (Carl Zeisus FESEM model number: Ultra 55 USA.**)** at different required magnifications at room temperature. The photographs were analyzed for morphological characteristics.

Drug entrapment efficiency

The prepared NLC dispersion was centrifuged at 6000 rpm for 30 min at 4°C using REMI cooling centrifuge. Then the free drug content was evaluated by using supernatant liquid. The entrapment efficiency (%) of drug was calculated by the following equation[21].

$$\% \text{ Entrapment Effiency} = \frac{\text{Total drug loaded-Free drug content}}{\text{Total drug loaded}} \text{ x } 100$$

Loading Capacity

Loading capacity is the amount of drug loaded per unit weight of the nanoparticles, indicating the percentage of mass of the nanoparticles that is due to the encapsulated drug.

Loading capacity can be calculated by the amount of total entrapped drug divided by volume of water that is required to re-suspend the nanoparticles[22].

$$\text{Loading capacity} = \frac{\text{Total drug loaded-Free drug content}}{\text{Volume of water required to resuspend Nanostructured lipid carrier}}$$

In vitro drug release for econazole nitrate nanostructured lipid carrier

The *in vitro* drug release profile of econazole nitrate loaded NLC were studied using vertical diffusion cell. The dialysis membrane was soaked overnight in the pH 5.5 phosphate buffer. Then calculated amount of product was kept in the donor compartment above the dialysis membrane. 250 ml of pH 5.5 phosphate buffer was taken in 250 ml beaker. Then the beaker was placed over a magnetic stirrer, the temperature and rpm was maintained at 34±0.5°C and 100 rpm throughout the study. Samples (5 ml) were withdrawn at predetermined intervals of time (1, 2, 3, 4, 5, 6, 7, and 8 h) and replaced with equal amounts of fresh buffer. After suitable dilution the samples were analyzed for drug concentration by UV spectrophotometer at 271 nm[23,24].

In vitro drug release for econazole nitrate nanostructured lipid carrier gel

The *in vitro* drug release profile of nanostructured lipid carrier gel of econazole nitrate and the standard econazole nitrate gel were studied using Franz diffusion cell. About 0.1 g of gel was kept on the dialysis membrane was mounted over the donor compartment and fixed on it. The dialysis membrane was soaked overnight in pH 5.5 phosphate buffer. The receptor compartment was filled with the buffer. Then the beaker was placed over a magnetic stirrer, the temperature and rpm was maintained at 37±0.5°C and 100 rpm throughout the study. Samples (5 ml) were withdrawn at predetermined intervals of time (1, 2, 3, 4, 5, 6, 7 and 8 h) and replaced with equal volume of fresh buffer. After suitable dilution the samples were analyzed for drug concentration by UV spectrophotometer at 271 nm[25,26,27].

Kinetic analysis of drug release

To reveal the kinetics of drug release from the NLC gel, the results obtained from *in vitro* release studies was fitted to various kinetic models such as Zero-order, First-order, Higuchi and Krosmeyer Peppas model. The precedent for selecting the most convenient model was based on a goodness-of-fit test[28].

Evaluation of econazole nitrate loaded nanostructured lipid carrier gel

Spreadability

The spreadability of formulations was determined by using horizontal glass plate method. A standard weight (5 g) was tied to the upper glass plate and about 1 g of econazole nitrate nanostructured lipid carrier gel was placed between two horizontal glass plates. The whole set was hold in the vertical position. The time required for the plate to slide off from the other plate was noted. The spreadability was calculated from the formula[21].

Spreadability = M ∗ L/ T

M = Weight tied to upper slide (g)

L = Length of glass slide (cm)

T = Time taken (sec)

pH determination

Before the analysis pH meter is calibrated using pH 4.0, 7.0 and 9.2 standard solutions. After the calibration the glass electrode was immersed in the gel (50 g) and the pH was noted[21].

Viscosity

Viscosity of the nanostructured lipid carrier gel was determined by using Brookfield viscometer. The temperature of the gel was maintained at 25°C. Helipath T-bar Spindle no. 96F was fixed to viscometer and immersed in the beaker containing 50 g of NLC gel. The viscometer was operated at different rpm and reading was noted in centipoises (cps)[21].

Drug content estimation

Accurately weighed 1 g of the gel transferred to the 100 ml of volumetric flask containing 20 ml of phosphate buffer pH 5.5. The volumetric flask was shaken for 30 min and the volume was made up to 100 ml with phosphate buffer pH 5.5 solution. After suitable dilution, the sample was analyzed using Agilent technologies carry 60 UV- visible spectrophotometer at 271 nm.

Skin irritation study

The experimental protocol for the skin irritation study was approved by Institutional Animal Ethics Committee. Skin irritation study was carried out using 6 rats of either sex weighing between 200-250 g. The animals were kept in

polypropylene cages with free access to a standard laboratory diet and water. Animals were divided into 2 groups of 3 animals each. Hairs were depleted from the abdominal region using scissors and blade. After hair depletion, gel was applied and covered with cotton bandage. The reaction at the site of application was studied and scored[29,30].

Stability studies

Stability studies were carried out on most satisfactory formulation as per ICH guidelines at 40±2°C and 75 ±5% RH. The most satisfactory formulation stored in a sealed in aluminum foil. These were stored at room temperature. After 3 months, particle size, zeta potential, entrapment efficiency, *in vitro* drug release of most satisfactory formulation was determined[31,32].

RESULTS AND DISCUSSION

Preformulation study

Melting point determination

The melting point of econazole nitrate was determined by Thiele's tube method and the melting point range was found to be 161-162°C.

Compatibility study - FTIR study

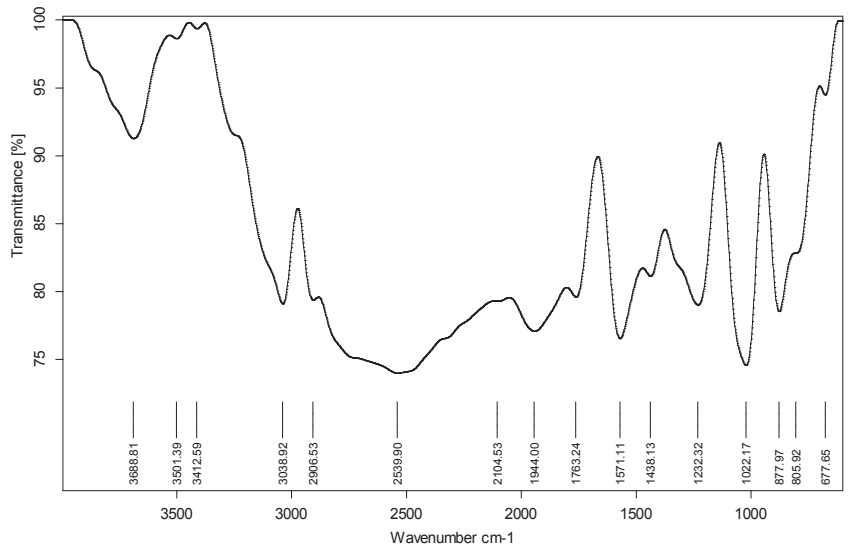

Figure 1. FTIR spectrum of econazole nitrate

Figure 2. FTIR spectrum of econazole nitrate + GMS

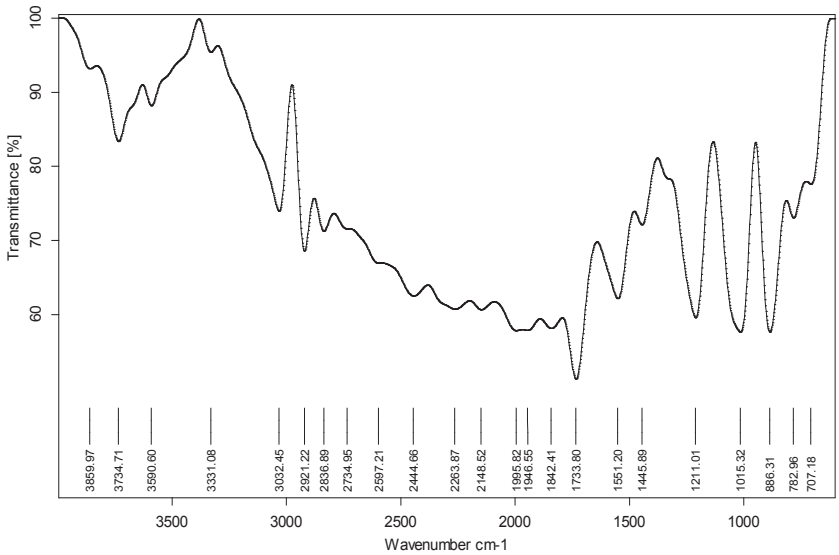

Figure 3. FTIR spectrum of econazole nitrate+ GMO

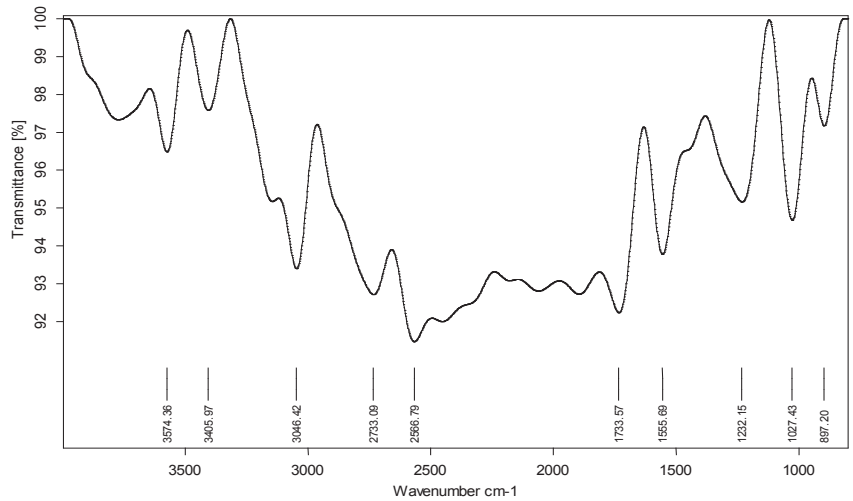

Figure 4. FTIR spectrum of econazole nitrate+ carbopol

FTIR spectra of econazole nitrate and its combination with glyceryl monostearate and also with glyceryl monooleate were shown in Fig:1,2,3,4. From the obtained spectra it was observed that the characteristics peaks of econazole nitrate (1763cm-1, 1022cm-1, 877cm-1) were present in the combination spectra thus indicating the compatibility of the drug with the lipids used. It shows that there was no significant change in the chemical integrity of the drug and spectral data and it complies with IP.

3.1.2 DSC study

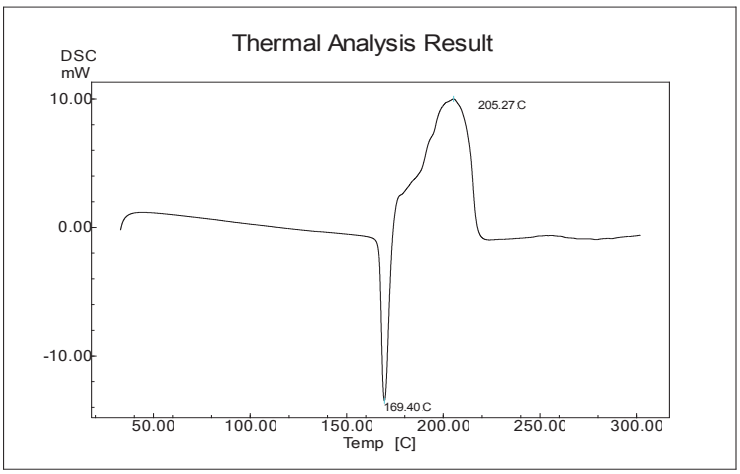

Figure 5. DSC thermogram of econazole nitrate

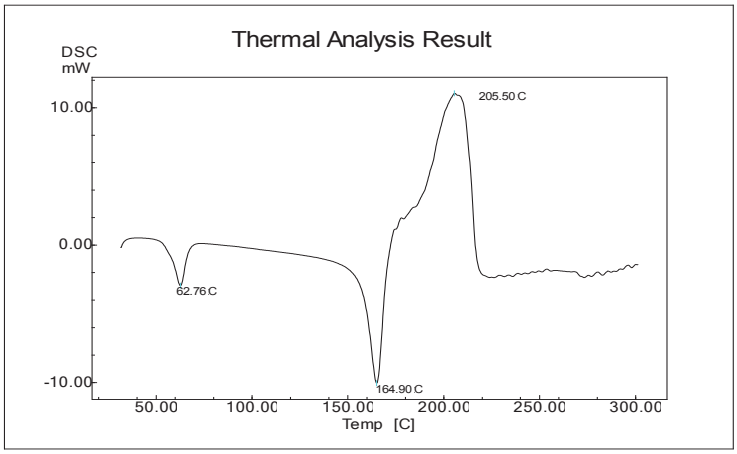

Figure 6. DSC thermogram of econazole nitrate + GMS

DSC spectrum of pure drug econazole nitrate exhibit a sharp endothermic peak at 169.40°C (Fig:5,6) and the mixture of glyceryl monostearate and drug shown a blunt endothermic peak at 164.90°C. These results infer that the compatibility between the lipids and drug.

Evaluation parameters of Nanostructured lipid carrier - Particle size, polydispersity index and zeta potential

Table 3. Physicochemical characteristics of NLC F1-F8

Formulation code	Particle size* (nm) Mean ± SD	Polydispersity index* Mean ± SD	Zeta potential* (mV) Mean ± SD
F1	142.1±0.92	0.27±0.01	-22.16±0.32
F2	162.8±0.28	0.32±0.002	-41.8±0.35
F3	153.3±0.66	0.34±0.002	-47.4±0.32
F4	160.24.5±5	0.38±0.002	-26.36±0.30
F5	182.73±0.45	0.32±0.0025	-31.46±0.25
F6	173.4±0.88	0.39±0.005	-30.53±0.35
F7	142.83±0.60	0.354±0.003	-25.43±0.35
F8	134.8±0.65	0.36±0.003	-27.4±0.3

*n=3

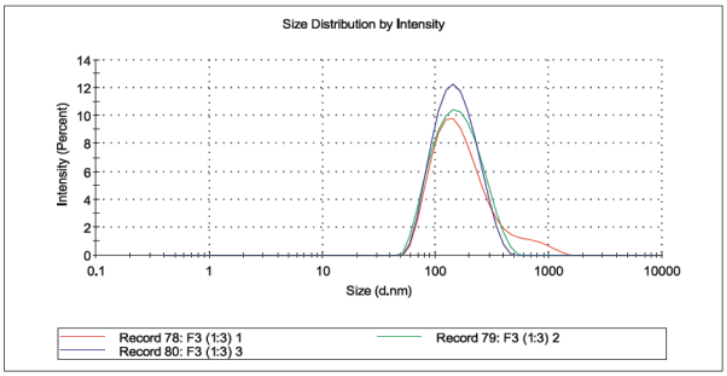

Figure 7. Particle size distribution of F3 formulation

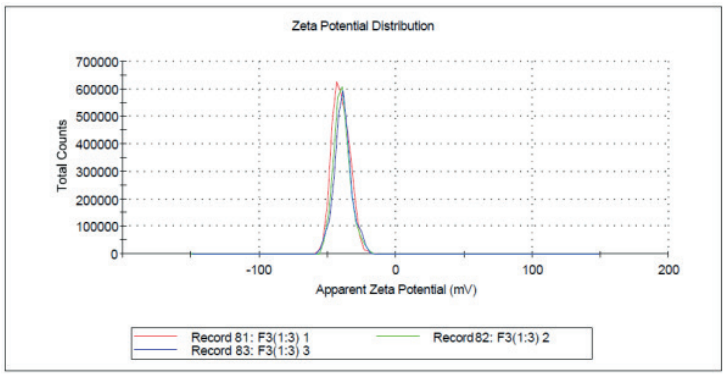

Figure 8. Particle size distribution of F3 formulation

Average particle sizes of econazole nitrate NLC were found in the range of 134.83 nm to 182.8 nm. It showed that the particles were in nanometre range. The polydispersity index (PDI) was found in the range of 0.27 to 0.39 for glyceryl monostearate and glyceryl monooleate as mentioned in (Table 3). This showed the polydispersity of particle was below 1 which infers the more homogeneity of the particles. The stability of the econazole nitrate nanostructured lipid carrier was evaluated by measuring the zeta potential of the NLC. The zeta potential of the formulations ranges from -22.16 to -47.4 mV. The zeta potential of best formulation F3 was found to be -47.4 mV which indicates that the formulation was stable has been given in (Table 3 and Fig:7,8). From the observations it was found that the nanostructured lipid carrier has been good homogeneity because polydispersity index was found to be less than one. The zeta potential is negative due to presence of negative surface charge of the drug.

Surface morphology

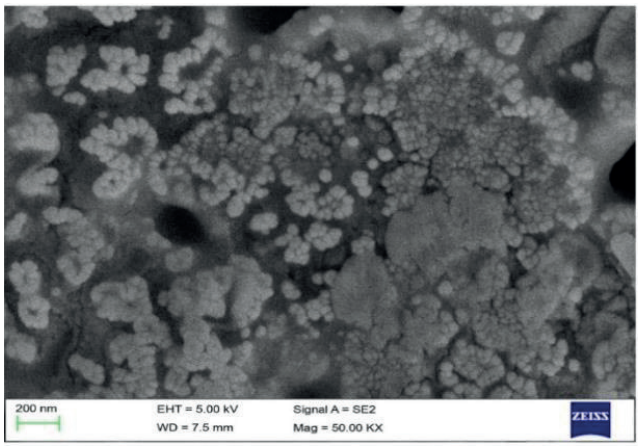

Figure 9. SEM micrograph of F3 at 50KX magnification

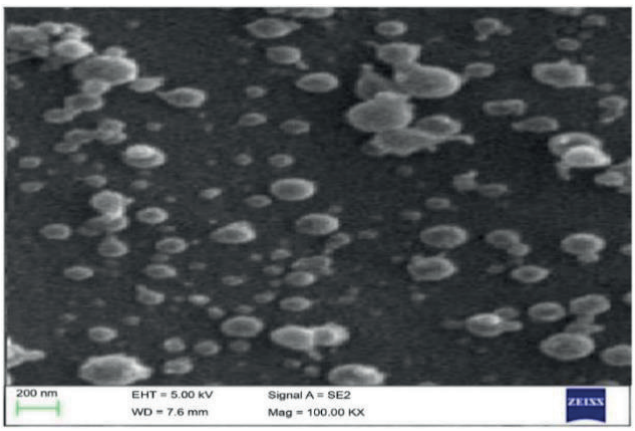

Figure 10. SEM of F3 at 100KX magnification

The morphological observation of sample under the SEM revealed that nano-structured lipid carrier of econazole nitrate are spherical in shape with different sizes ranging from 50.87 nm to 200.54 nm as shown in fig: 9,10.

Drug entrapment efficiency % and loading capacity

Table 4. Drug entrapment efficiency of nanostructured lipid carrier (F1-F8)

Formulation code	Drug entrapment efficiency* (%) Mean±SD	Loading capacity* (mg/ml) Mean±SD
F1	70.96±0.042	1.65±0.0009
F2	65.81±1.02	1.8±0.02
F3	67.29±0.05	1.6±0.01
F4	68.29±0.39	1.70±0.0009
F5	67.54±0.024	1.50±0.0005
F6	68.42±0.045	1.62±0.001
F7	72.89±0.056	1.61±0.0012
F8	74.63±0.04	1.58±0.0010

Highest entrapment efficiency of econazole nitrate NLC was found to be 74.63±0.04%. As the lipid concentration was increased the entrapment efficiency also increased, Table 4.

In vitro diffusion study of nanostructured lipid carrier of econazole nitrate

Table 5. *In vitro* drug release data of formulations F1-F4

Time (h)	Percentage cumulative drug released* (%) Mean±SD			
	F1	F2	F3	F4
1	12.49±0.47	12.07±0.46	10.82±0.2	7.56±0.39
2	18.75±0.38	23.17±0.38	12.21±0.47	8.76±0.31
3	29.56±0.75	28.08±0.67	15.36±0.49	12.12±0.39
4	36.31±0.77	35.81±0.75	17.96±0.27	16.79±0.52
5	42.52±0.65	39.5±0.92	35.02±0.87	27.4±0.62
6	51.74±1.15	47.38±1.01	46.46±0.96	33.4±0.69
7	65.78±1.24	53.9±1.09	52.92±1.07	56.38±0.85
8	74.43±1.38	69.45±1.27	66.8±1.03	66.75±1.05

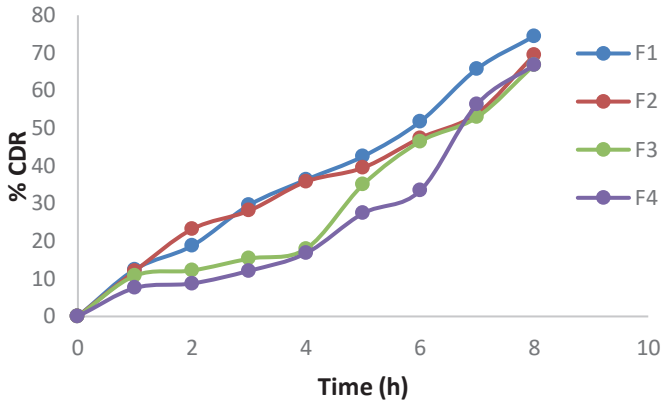

Figure 11. Percentage cumulative drug released profiles of formulations F1-F4

Table 6. *In vitro* drug release data of formulations F5-F8

Time (h)	Percentage cumulative drug released (%) Mean±SD			
	F5	F6	F7	F8
1	6.4±0.28	5.7±0.29	5.35±0.17	5.42±0.15
2	8.07±0.34	7.12±0.24	6.96±0.23	6.3±0.17
3	10.58±0.33	9.4±0.24	9.4±3.0.37	8.57±0.2
4	14.54±0.46	12.42±0.26	12.19±0.5	12±0.47
5	24.69±0.18	22.35±0.35	19.96±0.5	19.91±0.48
6	31.24±0.28	28.82±0.14	27.52±0.62	28.49±0.75
7	43.24±0.48	41.51±0.71	40.47±0.39	39.5±0.83
8	55.23±0.66	52.19±1.04	50.33±0.54	48.81±0.99

Figure 12. Percentage cumulative drug released profiles of formulations F5-F8

In vitro drug released study was carried out for 8 h for formulation F1-F8. The cumulative percent drug release after 8 h was found. At low lipid concentration in F1=43.47, % drug release was found to be 74.43%, whereas at high lipid concentration in F8=68.70, % drug release was found to be 48.81%. % Decrease in drug release was found as the liquid lipid is increased, this may be due to high viscous and thickness of lipid layer, Table no: 5,6 and Fig: 11,12.

Evaluation of nanostructured lipid carrier gel of econazole nitrate, spreadability, pH, drug content and viscosity

Table 7. Profile of ECN-NLC gel in terms of spreadability, pH, drug content and viscosity data's

Formulation code	Spreadability coefficient (g.cm/sec) Mean±SD	pH Mean±SD	Drug content (%) Mean±SD	Viscosity (cps)
NLC gel of econazole nitrate	0.467±0.0374	6.84±0.045	74.08±0.51	15372±35.72

In vitro drug diffusion study of nanostructured lipid carrier gel of econazole nitrate

Table 8. ECN-NLC gel in terms of *in vitro* diffusion study

Time (h)	Percentage drug released (%) Mean±SD
	NLC gel of ECN
1	9.2940±0.61
2	11.4372 ±0.33
3	16.813±0.57
4	26.488±1.29
5	31.364±1.28
6	33.6301±0.36
7	42.1698±2.10
8	50.557±2.64

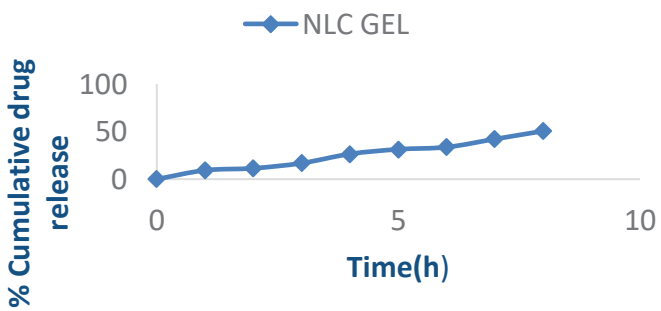

Figure 13. % Cumulative drug released profile of ECN-NLC gel

The cumulative percent drug release from the nanostructured lipid carrier gel showed 50.55±2.64 after 8 h of diffusion study given in (Table 8 and Fig:13. This may be because of the NLC gel containing the drug loaded lipid particles. The penetration of the drug, concentrates on the skin and remains localized for a longer period of time, thus enabling drug targeting to the skin.

Skin irritation study

The primary skin irritation index was found to 0.00 for erythema, Eschar and edema formation in the rats of control group, test group I and test group II. From the results of primary skin irritation index, it was concluded that there is no skin irritation in rats.

Stability study

Table 9. Stability studies of nanostructured lipid carrier loaded econazole nitrate

Days	Spreadability* (g.cm/sec) Mean±SD	Viscosity* (cps) Mean±SD	pH* Mean±SD	Percentage drug released* (%) Mean±SD
30	0.335 ± 0.010	15351 ± 17.00	6.7 ± 0.07	50.33±0.12
60	0.338±0.011	15324 ± 22.12	6.7±0.10	49.67±0.17
90	0.315±0.01	15283 ± 10.44	6.7±0.1	49.32±0.20

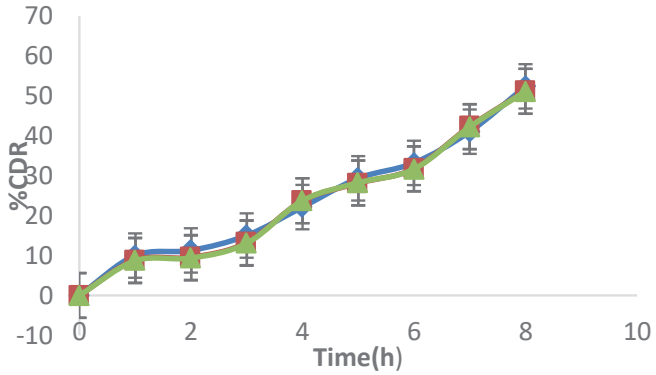

Figure 14. Drug release profile of ECN-NLC

Nanostructured lipid carrier gel of Econazole nitrate These studies revealed that NLC gel of Econazole nitrate was stable in terms of spreadability, pH, viscosity and cumulative percent drug release after storage for three months at 40±2°C, 75±5% RH. There was no significant difference after 3 months of stability study as given in Table 9 and Fig:14.

By Hot homogenization method ECN-NLC gel reduces particle size, improves stability due to Glyceryl monostearate, Glyceryl monooleate, Poloxamer108 and 407 and Carbopol 934P and therefore it is favourable for topical delivery system. The developed formulation overcomes and alleviates the drawbacks (drug loading, skin irritation) and limitations of econazole nitrate formulations.

REFERENCES

1. Bseiso, A.E.; Nasr.; Sammour, O.; Gawad, N. Recent advances in topical formulation carriers of antifungal agents. *Indian. J. Dermatol. Venerol. Leprol.* **2015**, *81*, 457-63.

2. Sevgi, G.; Sedef, M.; Aksu, B. New formulation strategies in topical antifungal therapy. *J. Cosmet. Dermatol. Sci.* **2013**, *3*, 56-65.

3. Robert, M.; Yogeshvar, N.K. New developments in topical antifungal therapy. *Am. J. Drug. Deliv.* **2006**, *4*, 231-47.

4. Sonia, T.; Silvia, M.; Cassano, R. Solid lipid nanoparticles for antifungal drugs delivery for topical applications. *Ther. Deliv.* **2016**, *7*, 639-47.

5. Dhruv, K.P.; Tanaji, D.N.; Sushikumar, S.P. Nano-lipid carriers for topical application: Current Scenario. *Asian. J. Pharm.* **2016**, *9*, 1-9.

6. Kaur, N.; Sharma, K.; Bedi, N. Topical nanostructured lipid carrier-based hydrogel of mometasone furoate for the treatment of psoriasis. *Pharm. Nanotech.* **2018**, *6*, 133-43.

7. Indian pharmacopoeia, Government of India, Ministry of Health and Family Welfare. 8th ed.; Indian Pharmacopoeia Commission: Ghaziabad, **2018**; pp 1267.

8. Goel, A.; Shaweta, S.; Kaur, N.; Anupam, S. Pharmacokinetic data and solubility profile of antifungal drugs. *Int. J. Pharma. Professionals. Res.* **2011**, *2*, 256-65.

9. Daniel, A.R.; Maria, V.M.; Frattini, A.; Soazo, M.; Alicia, G.L.; Marisa, S. Design, characterization, and *in vitro* evaluation of antifungal polymeric films. *AAPS. Pharm. Sci. Tech.* **2013**, *14*, 64-73.

10. Tejasa, U.; Senthil, V. Nanostrucutured lipid carrier system for the treatment for skin disease- a review. *JSM. Nanotechnol. Nanomed.* **2017**, *5*, 1-6.

11. Nighojkar, P.A.; Devi, S.K.U.; Pund, K.V.; Gadakh, R.T.; Shinde, M.G. Formulation and development of betamethasone dipropionate NLCs enriched gel. *Int. J. Pharm. Sci. Res.* **2017**, *3*, 3522-3529.

12. Dandagi, P.M.; Dessai, G.A.; Gadad, A.P.; Desai, V.B. Formulation and evaluation of nanostructured lipid carrier (nlc) of lornoxicam. *Int. J. Pharm. Sci.* **2014**, *6*, 73-77.

13. Akbari, J.; Saeedi, M.; Semnani, K.M.; Rostamkaeli, S.S.; Asadi, M.; Addo, K.A. A design of naproxen solid lipid nanoparticles to target skin layers. *Colloids. Surf. B. Biointerfaces.* **2016**, *145*, 626-633.

14. Gajanan, S.S.; Guru, P.M. Design and Evaluation of Miconazole Nitrate loaded Nanostructured Lipid Carriers (NLC) for improving the Antifungal therapy. *J. Appl. Pharm Sci.* **2013**, *3*, 46-54.

15. Praveen, K.; Anil, K.P.; Raj, K.P.; Singh, S.G. Formulation and evaluation of ethosome for econazole nitrate as a model drug to enhanced transdermal delivery. *Int. J. Pharm. Drug. Anal.* **2016**, *4*, 140-146.

16. Prachi, B.S. Preparation and evaluation of clotrimazole Nanostructured lipid carrier for

topical delivery. *Int. J. Pharm. Bio. Sci.* **2013**, *4*, 407-416.

17. Shashank, J.; Niketkumar, P.; Mansi, K.S.; Pinak, K.; Namrata, V. Recent advances in lipid-based vesicles and particulate carriers for topical and transdermal application. *J. Pharm. Sci.* **2016**, *106*, 423-445.

18. Loveelen, K.; Guleri, K. Topical gel: A recent approach for novel drug delivery Asian. *J. Bio. Pharm. Sci.* **2013**, *3*, 1-5.

19. Joshi, M.; Patravale, V. Formulation and evaluation of NLCs based gel of Valdecoxib. *Drug. Dev. Ind. Pharm.* **2008**, *32*, 911-918.

20. Gaba, B.; Fazil, M.; Khan, S.; Ali, A.; Baboota, S.; Ali, J. Nanostructured lipid carrier system for topical delivery of terbinafine hydrochloride. *Bull. Fac. Pharm. Cairo. Univ.* **2015**, *53*, 147–159.

21. Uthaman, S.; Maya, S.; Jayakumar, R.; Cho-Su C. Carbohydrates based nanogels as drug and gene delivery system. *J. Nanosci. Nanotechnol.* **2014**, *14*, 694-702.

22. Patel, D.; Dasgupta, S.; Dey, S.; Ramani, Y.R.; Ray, S.; Mazumder, B. NLCs based gel for topical delivery of aceclofenac: preparation, characterization *in vivo* evaluation. *Sci. Pharm.* **2012**, *80*, 749-764.

23. Joaquim, S.C.; Antonio, B.M.; Lyda, H.B.; Nelvis, V.C.; Jonna, Z.L.; Nuria, B.F. Skin permeation of econazole nitrate formulated in an enhanced hydrophilic multiple emulsion. *Wiley.* **2016**, *60*, 166-177.

24. Hussian, A.; Abdus, S.; Singh, S.K.; Ahsan, M.N.; Haque, M.W.; Faruk, A. Nanoemulsion gel-based topical delivery of an antifungal drug: *in vitro* activity and *in vivo* evaluation. *Drug. Deliv.* **2016**, *23*, 642-657.

25. Jayaraja, K.; Selvadurai, M.; Subramani, P. *In vitro* and *in vivo* evaluation of microspheres loaded topical gel delivery system of ketoconazole in male rats against *Candida glabrata*. *J. Pharm. Sci. & Res.* **2014**, *6*, 376-381.

26. Gautam, S.; Mahaveer, S. Review: *in-vitro* drug release characterization models. *Int. J. Pharma. Res.* **2011**, *2*, 77-84.

27. Bhaskar, K.; Anbu, J.; Ravichandiran, V.; Venkateswarlu, V.; Rao, Y.M. Lipid nanoparticles for transdermal delivery of Flurbiprofen: formulation, *in vitro, ex vivo* and *in vivo* studies. *J. Lipid. Res.* **2009**, *8*, 1-15.

28. Prakash, R.; Rao, N.G. Formulation, Evaluation and anti-inflammatory activity of topical Etoricoxib gel. *Asian. J. Pharm. Clinical. Res.* **2010**, *3*, 126-129.

29. More, H.B.; Sakharwade, N.S.; Tembhurne, V.S.; Sakarkar, M.D. Evaluation for skin irritancy testing of developed formulations containing extract of *Butea monosperma* for its topical application. *Int. J. Toxicol. Appl. Pharmacol.* **2013**, *3*, 10-13.

30. Tiruwa, R. A review on nanoparticles- preparation and evaluation parameters. *Indian J. Pharm. Bio. Res.* **2015**, *4*, 27-31.

31. Junyapraset, V.B.; Teeranachaideekul, V.; Souto, E.B.; Boonme, P.; Muller, RH. Q10- loaded NLCs versus nanoemulsion: stability, rheology and *in vitro* skin permeation. *Int. J. Pharm.* **2009**, *377*, 207-214.

32. Poonam, V.; Kamla, P. Nanosized ethanolic vesicles loaded with Econazole nitrate for treatment of deep fungal infections through topical gel formulation. *Nanomedicine.* **2012**, *8*, 489-496.

Acta Pharm. Sci. Vol 57 No: 4. 2019
DOI: 10.23893/1307-2080.APS.05725

Formulation and Evaluation of Acetylsalicylic Acid Suppositories using Capra hircus (Goat) Fat and Its Binary Blends

Olusola I. Aremu[1, 4*], John Paul Adjuzie[1], Olubunmi J. Olayemi[1], Judith E. Okoh[1], Kokonne E. Ekere[1], Omolola T. Fatokun[2], Martins O. Emeje[1,3]

1 Department of Pharmaceutical Technology and Raw Materials Development, National Institute for Pharmaceutical Research and Development, Abuja, Nigeria.

2 Department of Medicinal Plant Research and Traditional Medicine, National Institute for Pharmaceutical Research and Development, Abuja, Nigeria.

3 Centre for Nanomedicine and Biophysical Drug Delivery, National Institute for Pharmaceutical Research and Development, Abuja, Nigeria.

4 Department of Pharmaceutics and Industrial Pharmacy, Faculty of Pharmaceutical Sciences, University of Ilorin, Ilorin, Nigeria.

ABSTRACT

A study has been made on the formulation and evaluation of Acetylsalicylic acid (ASA) suppositories using Goat fat (GF) and its binary blends with Palm Kernel oil and Liquid Paraffin.

Cocoa butter was used as the standard reference suppository base. Rectal suppositories containing ASA (300 mg) in pre-calibrated mould were prepared by fusion method and evaluated for appearance, crushing strength, weight variation, melting point, liquefaction time, content uniformity and *in-vitro* release using standard procedures.

Liquefaction or disintegration time (minutes) followed this order: ACB(4.40±0.84) <AGL(6.20±0.83) <AGP(7.14±0.84) < AGF(11.45±2.20) while cumulative drug release (%) is AGP> AGF >AGL>ACB ($p<0.05$). Results obtained indicated that the bases used generally could be ranked in the order of GL > GP > GF > CB ($p<0.05$) in terms of favourable physicochemical properties investigated.

The foregoing indicates that GL or GP has promising potential and could be a substitute suppository base in the formulation of ASA suppositories.

Keywords: Formulation, Suppositories, Acetylsalicylic acid, Goat fat, Palm Kernel oil

*Corresponding Author: Olusola Aremu, e-mail: solabanks@yahoo.com
Olusola Aremu ORCID Number: https://orcid.org/0000-0002-3890-1256
Olubunmi Olayemi ORCID Number: https://orcid.org/0000-0001-5759-7176
Judith Okoh ORCID Number: https://orcid.org/0000-0001-7789-4776
Kokonne Ekere ORCID Number: https://orcid.org/0000-0001-8876-9284
Omolola Fatokun ORCID Number: https://orcid.org/0000-0002-9939-3371
Martins Emeje ORCID Number: https://orcid.org/0000-0002-0202-5426
(Received 15 May 2019, accepted 04 August 2019)

INTRODUCTION

Meat production worldwide has been estimated to increase annually by 1.9 % excluding nations like China where meat is not consumed often.[1] Consequently, the amount of waste or byproducts such as fats obtained from this industry has been increasing. Animal fats are lipid materials that can be obtained from pigs, cows and goats and it has been proven that, the biological source of the fat affects its characteristics[2] ; for human health concerns, attention has shifted to the application of these fats in non-food industries such as manufacture of soaps, fatty acids lubricants, feedstuffs, candle waxes and liniments.[3] They also find wide application in cosmetics, pet food, animal food, biodiesel production and pharmaceutical industry.[4,5] Pharmaceutical uses of animal fat have been extensively investigated [6,7,8,9,10] and the findings showed that goat fat is a cheap raw material which is suitable in developing several drug delivery systems. Nnamani *et al*[11] investigated the functional properties of goat fat in topical nano-drug delivery systems and concluded that goat fat is an effective lipid drug carrier. The study by Esimone *et al*[12] demonstrated the effectiveness of goat fat and shea butter in encapsulating benzyl penicillin in liposphere formulations. However, they reported that the presence of goat fat in one of such formulations impacted its stability. Goat fat has also been exploited as a co-lubricant in tablet formulations and found to improve granule flow and packing into the tablet die resulting in production of compact tablets.[13] In another study, Momoh *et al*[14] investigated the use of goat fat and phospholipids admixture in the formulation of solid-lipid nanoparticles. Their results showed that the drug-loaded nanoparticles improved drug bioavailability and therapeutic activity. In a similar but different study, herbospheres of *Vernonia amygdalina* prepared by using a lipid matrix containing the combination of goat fat (70 %) and Phospholipon 90H (30 %) were observed to be significantly more effective in inhibiting the growth of *Staphylococcus aureus* than Tetracycline. The emulsifying effect of goat fat has also been reported.[15,16,17] One study demonstrated the capability of the admixtures of goat fat and melon oil employed in the formulation of self-nanoemulsifying systems (SNEDDS) to deliver indomethacin.[18]

Rectal drug delivery though unconventional, is an apt substitute for oral drug administration, because it circumvents unwanted gastrointestinal (GIT) side effects, reduces hepatic first pass effect and problems relating to drug absorption. They are also beneficial for patients who cannot tolerate oral drugs due to reasons like vomiting or age; particularly the young children. Suppositories are solid medicated formulations designed to be inserted into the rectum where

they melt, dissolve or disperse and elicit local or systemic effect. Suppository bases are carriers of active medicaments that are incorporated into suppository formulations; they are usually hydrophilic or lipophilic. The bases determine the rate of drug release and absorption from suppository formulations as well as the onset of drug action, as such, appropriate bases are selected for suppository formulations.

Acetylsalicylic acid (ASA) is a non-steroidal anti- inflammatory drug (NSAID) with analgesic, antipyretic, anti-inflammatory and antiplatelet properties. It elicits these effects by inactivating cyclooxygenase enzymes (COX-1 and 2) required for prostaglandin synthesis.[19] Low dose acetylsalicylic acid irreversibly blocks the formation of thromboxane A2 in platelets, producing an inhibitory effect on platelet aggregation.[20] Oral NSAIDS like acetylsalicylic acid cause upper and lower GIT disorder such as gastric ulcers due to direct irritation of the gastric mucosa.[21] As a result of various challenges to oral medication of ASA as enunciated above including problem of emesis in critically ill patient, other dosage forms such as suppository maybe considered to avoid these drawbacks. Therefore, acetylsalicylic acid suppositories will be formulated by using goat fat, goat fat/palm kernel oil (3:1) and goat fat/liquid paraffin (3:1) admixtures and their effects on the physicochemical properties of the suppositories will be compared.

METHODOLOGY

Materials used include Acetylsalicylic acid powder (Sigma, Germany), Aluminum foil (Novena 85 foil, China), Liquid paraffin (BDH Chemicals ltd, Poole, England), Palm Kernel Oil, Cocoa butter, Hydrochloric acid (Emprove-Exp Merck, Germany), Goat fat obtained from a batch processed in the laboratory, Distilled water (National Institute for Pharmaceutical Research and Development, Laboratory, Nigeria).

Extraction process

The goat fat was extracted from its adipose tissue. The extraneous parts of it (adipose tissue) was manually separated and the separated fat thereafter was mashed together by using mortar and pestle. The mashed sample was melted using water bath and filtered through a 250-mesh sieve. The extracted fat was stored in a refrigerator until further use.

Gas Chromatography-Mass Spectrometry (GC-MS) analysis of Goat fat

The protocol of Okhale *et al,*[12] was adopted in carrying out this analysis. Shimadzu QP-2010 GC with QP-2010 Mass Selective Detector [MSD, operated in the EI mode (electron energy=70 eV) was used within the scan range of 45 and 400 amu, a scan rate of 3.99 scans/sec], and Shimadzu GCMS solution data system. The Gas chromatography column used was Optima-5 ms fused silica capillary with 5 % phenyl-methylpolysiloxane stationary phase, with length of 30 m, 100 internal diameter of 0.25 mm and film thickness of 0.25 **µm**. The carrier gas was helium with flow rate of 1.61 mL/min. The program used for Gas chromatography oven temperature was 180 °C at a rate of 10 °C/min, then held at 180°C for 2 min, followed by 18-280 °C at a rate of 15 °C/min, which was again held at 280 °C for 4 min. The injection port temperature was 250 °C while detector temperature was 280 °C. The goat fat sample was diluted; 1/100 v/v in hexane then 1.0 **µL** was injected using autosampler and in the split mode with ratio of 10:90. Individual constituents of the goat fat were identified by comparing their mass spectra with known compounds and NIST Mass Spectral Library (NIST 11).

Preparation of Acetylsalicylic acid suppositories using different bases

The bases used were goat fat, goat fat/palm kernel oil (3:1) and goat fat/liquid paraffin (3:1) and cocoa butter. Fusion method was employed in the production of the suppositories in pre-calibrated mould with different bases. Required quantities of the bases were weighed into a beaker and placed in a water bath at about 43°C to melt. Acetylsalicylic acid was weighed into a beaker (300mg per suppository); portion of melted base was mixed with the drug and then the required amount of base was added and the content of the beaker was stirred at about 39°C by using a magnetic stirrer until homogenous. The mixture was poured into the mould cavities until overflowed; the cavities were filled with the melted base as the solidifying mixture was shrinking. The mould content was allowed to solidify after which the mould was unscrewed. The suppositories were removed and wrapped in aluminum foils until further analysis was carried out.

Evaluation of Suppositories

Appearance (visual characterization)

Ten randomly selected suppositories (from each batch) were examined as a whole and also after splitting them longitudinally; the colour, odour, shape as

well as presence or absence of fissuring, pitting, exudation, sedimentation and migration of active ingredients were assessed.

Weight variation

The weight variation test was carried out according to British Pharmacopoeia.[22] Twenty suppositories were randomly selected from each batch of the formulations, weighed individually using an analytical balance (Mettler Toledo, Switzerland), the mean weights and standard deviations were calculated.

Hardness/Crushing test

The crushing strength, a measure of mechanical strength or hardness of the suppository was determined using the hardness tester (Erweka GmbH Germany). Three suppositories were randomly selected from each batch. The force under which each suppository cracked was recorded.

Liquefaction time

From each batch, one suppository was placed in a beaker with a thermometer inserted and placed in a thermo regulated heating mantle to maintain the temperature at 39 ± 1°C. The time taken for the suppository to completely melt was recorded as the liquefaction time. Three suppositories from each batch were evaluated for this purpose.

Melting point determination

The melting point of the suppositories was determined according to method reported by Adebayo and Akala[23]. -Briefly, a suppository, randomly selected from each batch, was placed in a beaker with a thermometer inserted. The beaker was placed on a water bath and regulated to a gradual temperature increase of 1°C/2 min. The temperature at which the suppository sample began to melt was taken as the melting point. The results obtained were average of quintuplicate determinations.

Content uniformity

The method of Setnikar and Fontani[24] was adopted with some modifications. Three suppositories were randomly selected from each batch and assayed for drug content individually. The suppository was placed in a beaker containing 60 mL of 0.1N HCl solution that was pre-heated to and maintained at 37 ± 1°C. The suppository was allowed to melt. The mixture was made up to 100 mL and then stirred at 100 rpm for 5 minutes using magnetic stirrer and filtered through a cotton plug. This volume was essential to allow for sink condition in order that the required amount of drug may be released from the product into

the medium. The absorbance of 5mL of filtrate was measured using UV-Vis spectrophotometer (Jenway 6505, UK) at 230 nm. The concentration of the acetylsalicylic acid in the solution was calculated using a standard Beer- Lambert curve obtained from the plot of absorbance against several dilute concentrations ranging from 2 x 10 −5 to 5 x 10 2 µg/mL as shown in Figure 1.

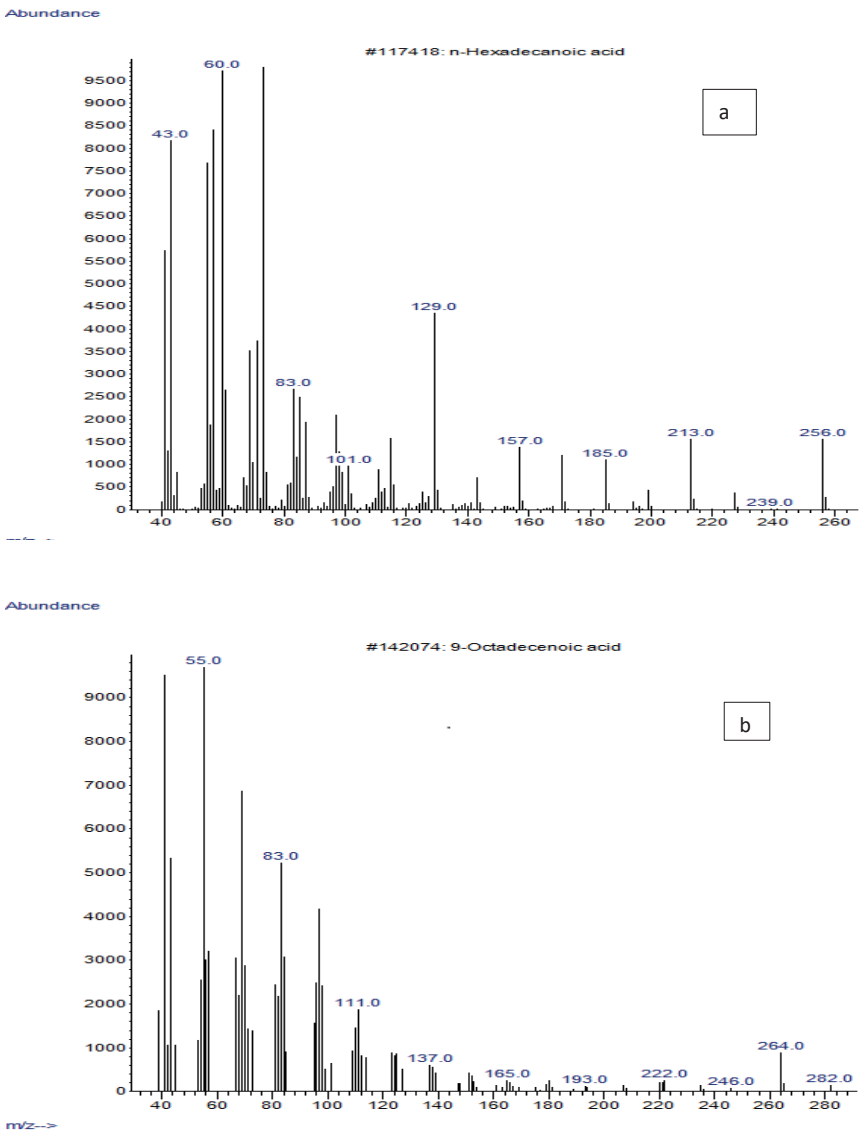

Figure 1. Gas chromatography spectra of goat fat showing the saturated fatty acids (a) hexadecanoic acid and (b) octadecanoic acid.

Release studies

The release studies were carried out using a magnetic stirrer assembly. A 100 mL quantity of 0.1N HCl solution was maintained on the magnetic stirrer assembly at temperature of 37± 1°C. One suppository from each batch was placed in the solution and the magnetic stirrer was set at 50 rpm. 5mL portion of the release medium was withdrawn at an interval of 5 minutes and was filtered through a cotton plug. The volume of the release medium was kept constant by replacing the amount withdrawn with 0.1N HCl after each withdrawal. Absorbance of 5 mL of filtered portions was determined using UV-Vis spectrophotometer (Jenway 6505, UK) at 230 nm.

RESULTS AND DISCUSSION

Gas Chromatography (GC)/Mass Spectroscopy (MS) has long been used for the selective qualitative and quantitative analysis of non-polar compounds particularly fatty acids with long chain alkyl groups. The detection of structural molecular ions generated from the MS source provides more sensitive and selective assay of varied arrays of fatty acids present in lipid samples.[25] The GC-MS spectra in Figure 1 shows that goat fat contains mainly long chain fatty acids and methyl esters; chiefly cis-vaccenic acid (52.29 %), saturated fatty acids such as octadecanoic acid (38.26 %), hexadecanoic acid also known as palmitic acid (8.46 %) and alcohols. Vaccenic acid (VA) is a positional and geometric isomer of oleic acid, and is reported as the predominant trans-isomer in ruminant fats. The chemical and physical stability, non-reactive and widely compatible properties of these fatty acids confer on goat fat the properties of a good suppository base. The outcome of various physicochemical assessments carried out on the suppositories is presented in Table 1. The goat fat extracted was off white coloured solid with characteristic odour. The formulated suppositories were solid at room temperature and assessed to be consistent in appearance with no air bubbles. The dissected suppositories have no holes or were not brittle and as such were not fragile. This implies that they could withstand transportation and other mechanical stresses they may be exposed to.[26]

Table 1. Suppository formulations and their composition

Ingredients	AGF	AGL	AGP	ACB
Acetyl salicylic acid	0.30 g	0.30 g	0.30 g	0.30 g
Goat fat to	39.35 g	-	-	-
Goat fat + Liquid paraffin (3:1) to	-	37.44	-	-
Goat fat + Palm kernel oil (3:1) to	-	-	39.10	-
Cocoa butter to	-	-	-	39.80

AGF= acetylsalicylic acid + goat fat, AGL= acetylsalicylic acid + Goat fat/ liquid paraffin (3:1), AGP= acetylsalicylic acid + goat fat/palm kernel oil (3:1), ACB= acetylsalicylic acid + cocoa butter

The physicochemical properties of the suppositories that are presented in Table 2 shows that all of the suppositories conform to BP requirement for weight uniformity. Not more than two individual suppositories deviated from the average weight by more than 5% and no suppository differed from the average weight by more than 10%.[22] The relative standard deviations (RSD) of the mean weight of the suppositories were less than 3.5%. Results of the crushing strength shows that, there were significant ($p<0.05$) differences between the values obtained for the suppositories and the placebo; with the order of strength being Goat fat alone; GF (3.43N) > Goat fat and liquid paraffin; GL (3.11N) > Goat fat and Palm kernel oil; GP (2.39N) and Goat fat + Acetylsalicylic acid; AGF (8.01N) > Goat fat and liquid paraffin + Acetylsalicylic acid AGL (6.54N) > Goat fat and palm kernel oil + Acetylsalicylic acid; AGP (3.27N) for placebo and medicated suppositories respectively. Although there is no official requirement as regards the acceptable values for the crushing strength of suppositories, it is nonetheless recognized that, crushing strength helps in identifying the mechanical strength of suppositories during handling, packaging and shipping. The mechanical strength can be valuable to avoid problems with formulations in which the melting point has been depressed by inclusion of either active pharmaceutical ingredient or an adjuvant.

Table 2. Physicochemical parameters of the suppositories

Physicochemical parameters	AGF	GF	AGL	GL	AGP	GP	ACB	CB
Shape	Torpedo	Torpedo	Torpedo	Torpedo	Torpedo	Torpedo	Torpedo	Torpedo
Colour	White	Off-white	Off-white	Off-white	Off-white	Ash	Light yellow	Light yellow
Mean weight (g)	2.05±0.03	-	2.01±0.02	-	2.02±0.02	-	2.01±0.01	-
Hardness (N)	8.01±0.28	3.48±0.85	6.54±0.57	6.11±0.28	3.27±0.57	2.39±0.39	-	-
Melting point (°C)	36.70±0.06	38.30±0.03	38.20±0.36	38.30±0.70	37.30±0.15	36.60±0.76	31.00±0.61	30.10±0.71
Liquefaction time (min)	11.45±2.20	14.47±2.10	6.20±0.83	6.25±2.30	7.14±0.84	7.11±0.64	4.40±0.84	3.20±0.63
Displacement value	1.35	-	1.87	-	1.29	-	1.12	-

AGF= Acetylsalicylic acid + Goat fat; GF= Goat fat, AGL= Acetylsalicylic acid + Goat fat/Liquid Paraffin (3:1); GL= Goat fat/Liquid Paraffin (3:1); AGP= Acetylsalicylic acid + Goat fat/Palm kernel oil (3:1); GP= Goat fat/Palm kernel oil (3:1); ACB= Acetylsalicylic acid + Cocoa butter; CB= Cocoa butter

Acceptable or "good" crushing strength values are suggested to be in the range between 17.7 and 19.6 N; although the results obtained from this present study are not within this range, it was noted that, throughout the period of this study, the suppositories remained non-brittle and solid at room temperature except for those that were formulated with cocoa butter. This suggest that they can withstand the mechanical rigours of handling and transportation. The inclusion of acetylsalicylic acid increased the crushing strengths of the suppositories, probably because of its high concentration (300mg) in the bases. However, crushing strength of formulations with cocoa butter could not be determined due to its instability during production. It is a known fact that cocoa butter could exist in different polymorphic forms depending on the exposure to varying temperature conditions. The melting points of AGF, AGL and AGP are 36.7, 38.2 and 37.3°C respectively (Table 2).

These values fall within the acceptable range for suppository formulations. The melting points of AGF was observed to be lower than its respective placebo base which is 38.3°C while that of AGL and AGP are higher than their respective placebo bases, 37.3 and 36.6 °C respectively. The change in temperature is probably as result of the inclusion of the active ingredient which may affect

the release of the drug.27 The melting point of cocoa butter with the drug is 31°C as shown in Table 2; this is low for storage in tropic conditions. The liquefaction times for all suppositories showed significant ($p<0.05$) difference with an order of AGF (11.45±2.20)> AGP (7.14±0.84)>AGL (6.20±0.83); however all of these values fall within the acceptable limits as suggested by Saho o[28] which says that liquefaction time influences drug absorption after release and subsequently influences the time it takes for the drug to reach peak plasma concentration.

Invariably there is a better patient compliance unlike when there is a prolonged liquefaction time. On the other hand, a suppository that takes a longer time to liquefy may exert irritant action on the rectal mucosa and as such increase release time and delay onset of action. Drug content of all the suppositories was computed from the calibration curve given in Figure 2.

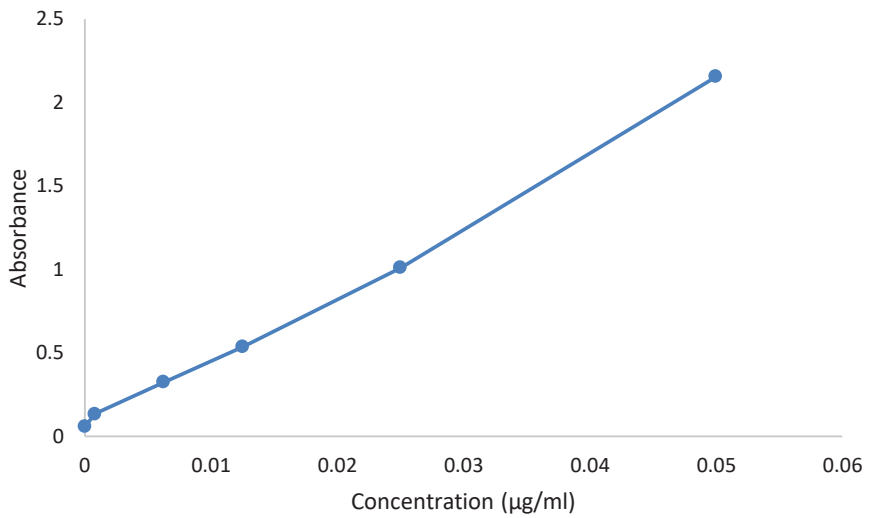

Figure 2. Calibration curve of Acetyl salicylic acid in 0.1 N HCl

The mean drug content for AGF and AGL suppositories met the USP requirement for the content uniformity. The mean drug content of these two batches fall within (96.7- 99.2%) as seen in Figure 3. This is an indication of even dispersion of active ingredient in the base. In some other instances inconsistency in active ingredient content in suppositories is usually due to the improper mixing of the molten bases or due to sedimentation of the drug by gravity during production.[29] This factor may account for why AGP and ACB mean drug content of 84.5 and 94.6% respectively was outside the acceptable range. The

most important thing is to realize that for the patient, the release characteristics are the determining properties towards the therapeutic success. What must be targeted is an optimal bioavailability which for the formulator means ensuring optimal and reproducible release *in vitro*/*in vivo*. As can be seen in Figure 4, there is no significant difference ($p<0.05$) in the rate and extent of release of the medicament from AGP, AGL and AGF. It can be concluded that there is little or no affinity between the bases and the medicament. Barring other physiological conditions of the rectum, there is relative assurance that the drug will be available biologically to elicit its action. The case is different for ACB (Figure 4); where the rate and extent of release was the least of all the bases interrogated in this study. It goes to suggest that, there might be some level of affinity between the drug and this base.

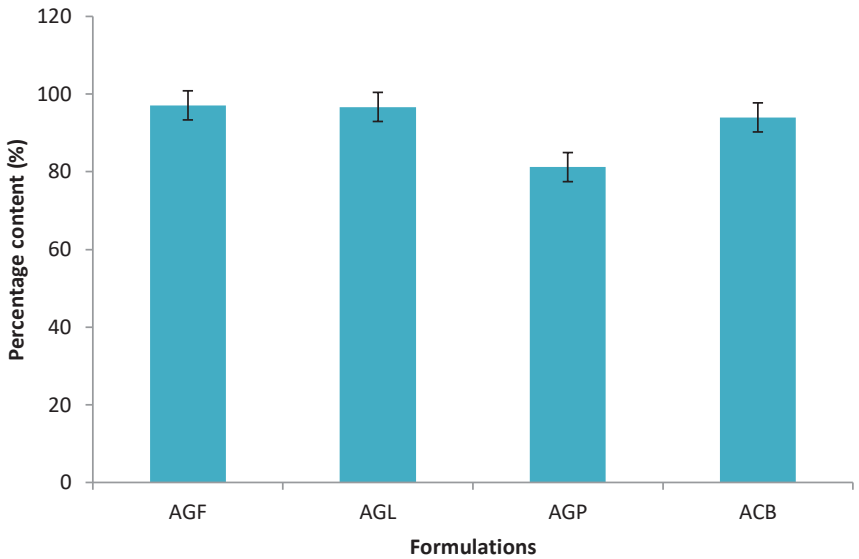

Key: AGF= Acetylsalicylic acid + Goat fat; AGL= Acetylsalicylic acid + Goat fat/Liquid paraffin (3:1); AGP= Acetylsalicylic acid + Goat fat/Palm kernel oil (3:1); ACB= Acetylsalicylic acid + Cocoa butter

Figure 3. Percentage content of acetylsalicylic acid suppositories

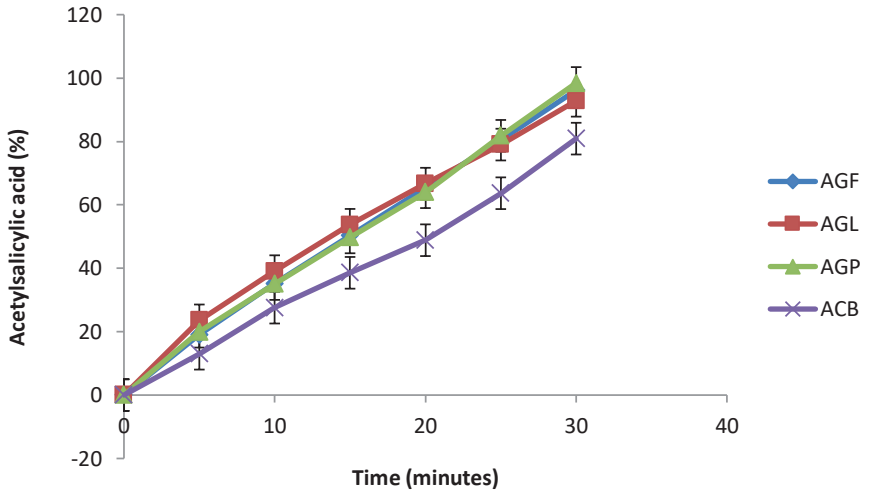

AGF= Acetylsalicylic acid + goat fat; AGL= Acetylsalicylic acid + Goat fat/ Liquid Paraffin (3:1);

AGP= Acetylsalicylic acid + Goat fat/Palm kernel oil (3:1); ACB= Acetylsalicylic acid + Cocoa butter

Figure 4. Release profile of Acetylsalicylic acid suppositories

Drug release kinetics studies were analyzed using Zero-order, First-order and Higuchi release models as shown in Table 3. Adjusted Coefficient of Determination (R adjusted) was used in selecting the best-fit release method. AGF (R2=0.999), AGL (R2=0.998), AGP (R2=0.998) and ACB (R2=0.993) were found to follow Zero-order model. AGL (R2=0.992) fitted also perfectly on Higuchi model.

The release mechanism of acetylsalicylic acid from the suppositories was analyzed with Korsmeyer-peppas model. The release exponents, n, for all the formulations range from 0.76 to 0.98. These values of 'n' for all the formulations were greater than 0.5 suggesting non-Fickian diffusion mechanisms of drug release from the suppositories. It indicates that the release of drug from the bases involves melting of the base and partitioning of the drug between the molten base and the dissolution medium. Non-Fickian diffusion mechanism is able to ensure better release of the medicament, faster absorption and timely onset of action.

Table 3. Release rate constant and model fitting parameters for release kinetics of different Acetylsalicylic acid suppository formulations

Release Kinetic models	Selection parameters	AGF	AGL	AGP	ACB
Zero order	K_0 (min)	3.068	2.737	3.145	2.616
	R^2	0.999	0.998	0.998	0.992
First order	K_1 (mg/min)	0.027	0.023	0.027	0.029
	R^2	0.943	0.945	0.959	0.939
Higuchi	K_H (mg/min$^{-1/2}$)	23.70	21.23	24.03	20.09
	R^2	0.986	0.992	0.976	0.967
Korsmeyer-Peppas	K_{KP} (mg/min^n)	0.901	0.762	0.885	0.986
	R^2	0.999	0.999	0.997	0.996

AGF= Acetylsalicylic acid + Goat fat; AGL= Acetylsalicylic acid + Goat fat/ Liquid paraffin (3:1); AGP= Acetylsalicylic acid + Goat fat/Palm kernel oil (3:1); ACB= Acetylsalicylic acid + Cocoa butter

From the results of this study, Acetylsalicylic acid suppositories were successfully prepared using single and binary blends of goat fat with palm kernel oil, liquid paraffin and cocoa butter. Any of the blends; goat fat and liquid paraffin or goat fat and palm kernel oil, may be a very good substitute to the more expensive bases used in formulation of suppositories. The *in vivo* performance tests of the optimized formulations is ongoing in our laboratory and will form a separate report.

The Acetylsalicylic acid suppositories prepared using single and binary blends of goat fat with palm kernel oil, liquid paraffin and cocoa butter showed that, any of the two blends may be a very good substitute to the more expensive bases. The *in vivo* performance of the optimized formulations is ongoing in our laboratory and will form a separate report.

CONFLICT OF INTEREST

The authors declare no conflict of interest.

ACKNOWLEDGEMENT

The authors are grateful to the technical staff in the Department of Pharmaceutical Technology and Raw Materials Development, National Institute for Pharmaceutical Research and Development (NIPRD), Abuja, Nigeria for their input in the course of this work.

REFERENCES

1. Food and Agriculture Organization (FAO). Food Outlook; Biannual Report on Global Food Markets; Food and Agriculture Organization of the United Nations: Rome, Italy, **2017**; pp. 1–142.

2. National Research Council. Fat Content and Composition of Animal Products. Washington, DC: Printing and Publishing Office, National Academy of Science, **1976**; pp 203.

3. Food and Agriculture Organization. Definition and classification of commodities: 14 vegetable and animal oils and fats. **1994**; http://www.fao.org/waicent/faoinfo/economic/faodef/fdef14e.htm.

4. Rivera, J. A.; Sebranek, J. G.; Rust, R. E.; Tabatabai, L. B. Composition and Protein Fractions of Different Meat By-Products Used for Pet Food Compared with Mechanically Separated Chicken (MSC). *Meat Sci.* **2000**, *55*, 53–59.

5. Gokul, R. S.; Ranjitha, J. Comprehensive Study on Biodiesel Produced from Waste Animal Fats-A Review. *J. Environ. Sci. & Tech.* **2018**, *11*, 157-166.

6. Attama, A. A.; Nkemnele, M. O. *In Vitro* Evaluation of Drug Release from Self Micro-Emulsifying Drug Delivery Systems Using a Novel Biodegradable Homolipid from *Capra hircus*. *Int. J. Pharm.* **2005**, *304*, 4-10.

7. Attama, A. A.; Muller-Goymann, C. C. A Critical Study of Novel Physically Structured Lipid Matrices Composed of a Homolipid from *Capra hircus* **and Theobroma Oil.** *Int. J. Pharm.* **2006**, *322*, 67-78.

8. Attama, A. A.; Schicke, B. C.; Paepenmuller, T.; Muller-Goymann, C. C. Solid Lipid Nanodispersions Containing Mixed Lipid Core and a Polar Heterolipid: Characterization. *Eur. J. Pharm. & Biopharm.* **2007**, *67*, 48-57.

9. Attama, A. A.; Muller-Goymann, C. C. Effect of Beeswax Modification on the Lipid Matrix and Solid Lipid Nanoparticle Crystallinity. *Colloids Surf. A Physicochem. Eng. Asp.* **2008**, *315*, 189-195.

10. Attama, A. A.; Igbonekwu, C. N. *In Vitro* Properties of Surface-Modified Solid Lipid Microspheres Containing an Antimalarial Drug: Halofantrine. *Asian Pac. J. Trop. Med.* **2011**, *4*, 253-258.

11. Nnamani, P. O.; Ibezim, E. C.; Attama, A. A.; Adikwu, M. U. Piroxicam-Loaded P90glylated Tallow Fat-Based Solid Lipid Microparticles: Characterization and in vivo evaluation. *Nig. J. Pharm. Res.* **2010**, *8*, 19-35.

12. Esimone, C. O.; Attama, A. A.; Osonwa, U. E.; Nwakile, C. D.; Onochie, F. T. O. Formulation and Evaluation of Goat Fat and Shea Butter Based Lipospheres of Benzyl Penicillin. *Int. J. Pharm. Sci. & Res.* **2012**, *3*, 1022-1027.

13. Majekodunmi, S. O.; Matthew, E. B. Evaluation of Goat Fat as Potential Co-Lubricant in Pharmaceutical Tablet Dosage Form. *IOSR J. Pharm.* **2014**, *4*, 01-09.

14. Momoh, M.; Attama, A. A.; Kunle, O. O. Formulation *In Vitro* and *In Vivo* Evaluation of SRMS-Based Heterolipid-Templated Homolipid Delivery System for Diclofenac Sodium. *Drug Deliv.* **2014**, *23*, 907-915.

15. Attama, A. A.; Nzekwe, I. T.; Adikwu, M. U.; Onugu, O.; Nnamani, P. O. The Use of Solid Self-Emulsifying Systems in the Delivery of Diclofenac Sodium. *Int. J. Pharm.* **2003**, *262*, 23-28.

16. Attama, A. A.; Mpamaugo, V. E. Pharmacodynamics of Piroxicam from Self-Emulsifying

Lipospheres Formulated with Homolipids Extracted from *Capra hircus*. *Drug Deliv*. **2006**, *13*, 133-137.

17. Usha, S. B. M.; Kiranmai, M. I.; Indira, Y. 2012. Self-Emulsifying Tablets of Ibuprofen: Design, Optimization and Evaluation. *Res. J. Pharm. Biol. Chem. Sci*. **2012**, *3*, 0975-8585.

18. Obitte, N. C.; Ofokansi, K. C.; Nzekwe, I. T.; Esimone, C. O.; Okoye, I. E. Self-nanoemulsifying Drug Delivery Systems Based on Melon Oil and its Admixture with a Homolipid from *Bos Indicus* for the Delivery of Indomethacin. *Trop. J. Pharm. Res*. **2011**, *10*, 299-307.

19. Toth, L.; Muszbek, L.; Komaromi, I. Mechanism of the Irrevervisible Inhibition of Human Cyclooxygenase-1 by Aspirin as Predicted by QM/MM Calculations. *J. Mol. Graph. Model*. **2013**, *40*, 99-109.

20. Vonkeman, H. E.; Mart, A. F. J. Non-steroidal Anti-inflammatory Drugs: Adverse Effects and their Prevention. *Semin Arthritis Rheum*. **2010**, *39*, 294-312.

21. Aalykke, C.; Lauristen, K. Epidemiology of NSAID Related Gastroduodenal Mucosal Injury. *Best Pract. Res. CL. GA*. **2001**, *15*, 705-722.

22. British Pharmacopoeia. British Pharmacopoeia Office: MHRA, 151 Buckingham Palace road, London SW1W9SZ; 2013.

23. Adebayo, A. S.; Akala, E. O. Kinetics Model for the *In Vitro* Release of a Hydrophilic Drug (Amodiaquine) from Fat-Based Suppositories. *Int. J. Arts Technol*. **2005**, *2*, 1-11.

24. Setnikar, I.; Fontani F. Content Uniformity in Rectal Suppositories. *J. Pharm. Sci*. **1970**, *59*, 1319-1324.

25. Field, C. J.; Blewett, H. H.; Proctor, S.; Vine, D. Human health benefits of vaccenic acid. *App. Physio. Nut. Metab*. **2009**, *34*, 979-991.

26. Ofoefule, S. I.; Chukwu, A.; Nwankwo, C.; Orisakwe, O. E. *In-Vitro* Properties of Ciprofloxacin Suppositories Formulated with Glycerogelatin and Theobroma Oil Bases. *Boll. Chim. Farm*. **1998**, 137, 341-344.

27. Taylor, O.; Igwilo, C. I.; Adeoye, D. I.; Awosika, O. O. *In Vitro* Release of Paracetamol from Various Suppository Formulations of Purified Shea Butter. *J. Pharm. Sci. Pharm. Pract*. **1993**, *2*, 93-99.

28. Sahoo, C. K.; Sudhakar, M.; Ramana, D. V; Satyanarayana, K. A Discussion on Quality Control of Suppositories. *MJPMS*. **2017**, *6*, 1618.

29. Carter, S. J. Dispensing for Pharmaceutical Students. CBS Pub., Delhi, **1987**; pp. 231-252.

Acta Pharm. Sci. Vol 57 No: 4. 2019
DOI: 10.23893/1307-2080.APS.05726

Investigation of the Anti-inflammatory and Hypoglycaemic Effects of Macaranga hurifolia Beille (Eurphorbiaceae) Extract on Wistar albino Rats

Peter Segun[1*], Morenike Gbadebo[1], Modupe Adebowale[1], Katherine Olufolabo[1], Adediwura Fred-Jaiyesimi[1]

1 Department of Pharmacognosy, Faculty of Pharmacy, Olabisi Onabanjo University, Sagamu 8 Campus, Nigeria.

ABSTRACT

Macaranga hurifolia Beille (Euphorbiaceae) is used in Nigerian ethnobotany for treating several diseases. This work was designed to determine the phytochemical composition, as well as, investigate the anti-inflammatory and hypoglycaemic activities of *Macaranga hurifolia* extract (MHE). MHE was evaluated for its anti-inflammatory and antidiabetic potentials using the egg albumin inflammatory model and alloxan-induced diabetic rat model, respectively. MHE produced both dose-dependent and time-dependent inhibition of oedema development with its maximum effect (69.6%) produced at the dose of 300 mg/kg. The acute *in vivo* antidiabetic study revealed that MHE produced significant hypoglycaemic effects at doses of 200 mg/kg (54% reduction) and 400 mg/kg (59% reduction), comparable to glibenclamide (5 mg/kg) which caused a 42% decrease, while all the treatment groups produced at least 25% reduction in blood glucose level for the chronic study. This study established, for the first time, the anti-inflammatory and antidiabetic potentials of *Macaranga hurifolia*.

Keywords: Alloxan, diabetes mellitus, egg albumin, inflammation, *Macaranga hurifolia*

INTRODUCTION

Diabetes mellitus (DM) continues to impose a major threat on global human

*Corresponding Author: Peter Segun, e-mail: segun.peter@oouagoiwoye.edu.ng
Peter Segun ORCID Number: 0000-0002-2177-4609
Morenike Gbadebo ORCID Number: 0000-0002-5664-8397
Modupe Adebowale ORCID Number: 0000-0002-0944-0702
Katherine Olufolabo ORCID Number: 0000-0003-3054-9339
Adediwura Fred-Jaiyesimi ORCID Number: 0000-0002-5906-9155
(Received 17 April 2019, accepted 08 August 2019)

health affecting around 25% of the world population and the number of people suffering from this ailment is projected to reach 439 million by 2030[1,2]. DM is a major metabolic disorder characterized by improper management of carbohydrate and lipid metabolism by insulin, often leading to high blood glucose levels. This ailment may either result from the autoimmune destruction of the pancreatic islet beta cells leading to inadequate endogenous production of insulin; a condition known as type 1 DM or the impaired insulin secretion and/or insulin resistance; a condition commonly referred to as type 2 DM[3]. Inflammation, the response of viable tissues to injury, involves several mechanisms including enzyme activation, release of mediators, extravasations of fluid, and tissue breakdown and repair. Non-steroidal anti-inflammatory drugs (NSAIDs) have been the main stay in the treatment of inflammation, although adverse effects on the gastric mucosa and kidney have limited their therapeutic success.

Hyperglycaemia, a major feature of DM, is often linked with increase oxidative stress and inflammatory responses. In particular, excessive flow of glucose through the aldose reductase metabolic pathway leads to the oxidation of NADPH to $NADP^+$ and the reduction of NAD^+ to NADH[4,5]. This change in redox potential leads to cell hypoxia, acceleration of glycolysis, increase production of superoxide and the eventual activation of the protein kinase C (PKC)[6]. The activation of PKC reduces the availability of nitric oxide, causes endothelial dysfunction leading to the release of several endothelial inflammatory biomarkers including Von Willebrand factor (VWF), interleukin-6 (IL-6), tumor necrosis factor-alpha (TNF-α), intercellular adhesion molecule-1 (ICAM-1), thromboxane A2 (TA2)[7,8]. Several studies have shown that oxidative stress and inflammatory responses play key roles in the development of microvascular and macrovascular complications in diabetic patients as many of the important pro-inflammatory mediators have been reported to be present in high amount in diabetic patients[9].

Despite the great progress made in orthodox medicine towards the management of DM as exemplified in the discovery and development of current antidiabetic agents including sulfonylureas, biguanides, thiazolidinediones and α-glucosidase inhibitors[10], complications such as weight gain, hypoglycaemia, dropsy and drug-resistance that often arise from the use of these agents have necessitated the search for alternative treatment for DM[11]. Consequently, there is a great need for the discovery of novel molecules, especially from natural sources such as medicinal plants, that can tackle the problem posed by DM.

Macaranga hurifolia Beille (Euphorbiaceae) is a short tree up to 12 m high that is found in forest and savannah regions of Cameroon, Nigeria and Sierra

Leone. It is commonly referred to as *'owolewa'* by the Yoruba speaking people of southwestern Nigeria[12]. It is used traditionally for its medicinal values and as its branches are widely used as fire woods. In traditional folklore medicine, *M. hurifolia* is used to treat cough and diabetes, to relieve oedema in pregnant women and as a purgative. Although several studies have investigated the phytochemical constituents and the bioactivities of numerous *Macaranga* species including *M. barteri* and *M. schweinfurthii*[13-17], the literature is void of report on the phytochemical constituents, anti-inflammatory and antidiabetic potentials of *M. hurifolia*. Therefore, the aim of this study is to determine the phytochemical composition, as well as, investigate the hypoglycaemic and anti-inflammatory activities of *M. hurifolia* extract (MHE).

METHODOLOGY

Materials

The fresh leaves of *M. hurifolia* were collected in March 2018 in Epe (6° 35' 2.83" N and 3° 59' 0.10" E, altitude 42 m), Lagos State, Nigeria. The plant identification and authentication were carried out by Mr A. S. Odewo at the Forest Herbarium Unit, Forestry Research Institute of Nigeria (FRIN), Ibadan, Nigeria where an herbarium specimen with voucher number FHI 111956 has been deposited. The plant's name was checked at http://www.theplantlist.org (assessed on 27th, April 2018). All chemicals and reagent used were of analytical grade and purchased from Sigma Co. UK.

Animals

Male Wistar albino rats, 220 -250 g, obtained from Babcock University, Ilishan, Nigeria, were used for this study. The animals were bred and housed in the animal house, Faculty of Pharmacy, Olabisi Onabanjo University. The animal house was well ventilated with room temperature between 25 and 29 °C and had a 12 h light-dark cycle and were housed in groups. The rats were fed with rodent commercial diet and water *ad libitum* and allowed to acclimatise to laboratory environment for one week prior to the experiment. The animals were maintained in accordance with the guidelines of the International Guidelines for Care and Use of Laboratory Animals[18] and approval from the Animal Ethical Committee was obtained.

Preparation of crude extract

The air-dried, powdered leaves of *M. hurifolia* were macerated with 80% methanol at room temperature (25-29 °C) and filtered. The obtained filterate was concentrated *in vacuo* at 35 °C using rotary evaporator. The extract (yield: 8.1 %) was stored in a clean amber bottle and kept in a refrigerator at 4 °C prior to use.

Phytochemical screening

The presence of various secondary metabolites in the plant was investigated using standard procedures[19]. The chemical groups of compounds tested were alkaloids, anthraquinones, cardiac glycosides, flavonoids, reducing sugars, saponins, steroids and tannins.

Anti-inflammatory activity

For the determination of the anti-inflammatory potential of MHE, the egg albumin inflammatory model described previously in the literature was adopted with slight modifications[20]. Briefly, thirty male Wistar rats were divided into six groups each group containing five rats. The rats were starved for 12 h prior to the experiment and also deprived of water to reduce possible fluctuations in oedematous response. To induce inflammation, fresh egg albumin (0.1 mL) was injected into the subplantar surface of the right hind paw of each animal and allowed to stay for 1 h prior to treatment with extract/drug. The extract was administered to group 1, group 2, group 3 and group 4 at doses of 300 mg/kg, 150 mg/kg, 75 mg/kg and 37.5 mg/kg, respectively. Group 5 which served as the positive control group received diclofenac (50 mg/kg), while the negative control group (group 6) received normal saline. All treatments were administered using an oral canula. The paw circumference was estimated using cotton thread method[21] with measurements made prior to the start of the experiment and subsequently every 30 min after treatment with extract/drug for a total of 120 min.

Induction of Type 2 DM in rats and drug administration

Investigation of the effect of *M. hurifolia* extract (MHE) on type 2 DM rats was carried out following a procedure described earlier in the literature[22]. The rats were fasted overnight before the commencement of the experiment. Thereafter, intraperitoneal administration of alloxan monohydrate solution (dissolved in normal saline) at a dose of 140 mg/kg body weight was given to the rats. Forty-eight hours after alloxan injection, the fasting blood glucose level (FBG) was measured and rats with FBG level above 250 mg/dL were considered diabetic and used for further investigations. For the examination of the anti-hyperglycaemic potential of MHE, the rats were divided into six groups of five rats each. Group 1, which served as the normal control group, were normoglycaemic rats that received normal saline at a dose of 1 mL/kg. Group 2, the diabetic control group, comprised of diabetic rats that received no treatment. Group 3 which served as the standard treatment group were rats that received a treatment of glibenclamide at a dose of 5 mg/kg. Groups 4, 5 and 6 were administered MHE at doses of 100, 200 and 400 mg/kg, respectively. All the groups were treated

appropriately for seven days. Blood samples were obtained from the tail veins of the experimental animals using a sterile lancet and the blood glucose levels measured at 0h, 1h, 3h, 6h and 24h after drug administration on the first day, using a glucometer (One-Touch®). Treatment with MHE and measurement of the blood glucose level was subsequently conducted daily for seven days.

Statistical analysis

Results obtained were expressed as mean ± standard error of mean (n = 5) and the data were analysed using the student's t-test and values of $p < 0.05$ were considered statistically significant.

RESULTS AND DISCUSSION

DM is a major predisposing factor to the formation of myocardial infarction, cerebrovascular accident and peripheral vascular diseases and recent studies have reported that diabetic sufferers are almost five times more probable of developing heart diseases and stroke that non-diabetic individuals[6,23]. In the recent times, emphasis has been laid on the discovery of newer drugs for the treatment of DM and inflammation from traditional medicine, especially from medicinal plants, due to the untoward effects of the currently available synthetic medications. In this study, the anti-inflammatory and hypoglycaemic effects of *Macaranga hurifolia* leaves extract (MHE) was investigated.

The analysis of the phytochemical constituents of MHE revealed that it contains several secondary metabolites including alkaloids, flavonoids, saponins and tannins (Table 1). These metabolites 7which have been reported in other members of the *Macaranga* genus[16,17,24], may be responsible for its observed bioactivity. In addition, saponins and tannins have been reported to possess anti-inflammatory activity in several *in vivo* models[25].

Table 1. Phytochemical constituents of *M. hurifolia* methanol extract (MHE)

Phytochemicals	Results
Alkaloids	+++
Anthraquinones	-
Cardiac glycosides	-
Flavonoids	++
Saponins	++
Sterols	-
Tannins	+

- = absent; + = present; ++ = abundant

The subplantar administration of egg albumin into the right hind paw of male Wistar rats elicited oedema which peaked at 60 min post administration of the agent. MHE caused both dose-dependent and time-dependent inhibition of oedema development. The maximum inhibition of oedema development (69.6%) was produced at the dose of 300 mg/kg at the 120 min interval, an effect comparable but not significantly different from that elicited by 50 mg/kg diclofenac (73.1%) at the same time interval (Table 2). Previous research have shown that induction of oedema elicited by egg albumin is mediated by the release of vasoactive substances, especially histamine and serotonin[26]. The significant inhibitory effect on rat paw development exhibited by MHE suggest that the extract may likely inhibit the release and/or actions of histamine and serotonin.

The hypoglycaemic effect of MHE and glibenclamide (positive control) are shown in Tables 2 and 3. From the acute *in vivo* antidiabetic study designed to evaluate the effect of MHE over a short period of time, it was observed that DHE at a dose of 200 mg/kg and 400 mg/kg significantly reduced the blood glucose level of diabetic rats by 54% and 59%, respectively, over the 24 h period, comparable to glibenclamide (5 mg/kg) which caused a 42% decrease over the same treatment period (Table 3). Several studies have reported that a reduction in the blood glucose level by 25% is to be considered as a significant hypoglycaemic effect[27-29].

Table 2. Anti-inflammatory effects of MHE on egg albumin-induced rat paw oedema

Treatment groups	Dose (mg/kg)	Paw thickness (mm)[a]				% inhibition
		30 min	60 min	90 min	120 min	
Normal saline	10 (mL/kg)	3.26 ± 0.38	3.23 ± 0.12	3.16 ± 0.15	2.86 ± 0.26	-
MHE	37.5	3.66 ± 0.23	3.33 ± 0.52	3.13 ± 0.51	3.00 ± 0.43	12.5
MHE	75	3.56 ± 0.10	3.03 ± 0.32	2.56 ± 0.38	2.90 ± 0.23	30
MHE	150	3.8 ± 0.26	3.40 ± 0.20	2.90 ± 0.17	2.72 ± 0.40	56.3
MHE	300	3.56 ± 0.10	2.60 ± 0.26	2.66 ± 0.17	2.70 ± 0.10	69.6
Diclofenac	50	3.36 ± 0.66	3.33 ± 0.58	3.13 ± 0.66	2.90 ± 0.36	73.1

[a]Values are expressed as mean ± standard error of mean of five rats per group.
* denotes percentage inhibition of oedema development with respect to the control.

Table 3. Acute effect of *M. hurifolia* crude extract (MHE) on fasting glucose level in alloxan-induced diabetic rats

Treatment groups	Fasting blood glucose (mg/dL)[a]				
	0 h	1 h	3 h	6 h	24 h
Group 1	110.0 ± 11.2	105.0 ± 11.2	96.0 ± 4.0	98.5 ± 4.4	68.3 ± 6.8
Group 2	332.3 ± 10.8	369.8 ±7.8	362.5 ± 9.9	354.5 ± 5.1	436.0 ± 16.1
Group 3	415.5 ± 16.1	373.8 ± 22.4	359.0 ± 15.7	304.0 ± 17.3	241.5 ± 15.5[b] (41.9%)*
Group 4	260.7 ± 16.0	371.0 ±15.8	160.3 ± 16.5[b]	227.8 ± 16.9[b]	218.5 ± 7.8[b] (15.96%)*
Group 5	444.5 ±16.4	415.5 ± 16.5	370.5 ± 13.7	272.5 ± 7.4[b]	205.5 ± 11.7[b] (53.76%)*
Group 6	347.3 ±15.5	279.0 ± 16.9[b]	195.6 ±12.5[b]	166.0 ± 9.3[b]	143.6 ± 8.4[b] (58.61%)*

[a]Values are expressed as mean ± standard error of mean of five rats per group. bStatistically different from the diabetic control ($P < 0.05$). Group 1 were normoglycaemic rats; group 2 were diabetic rats that received no treatment; group 3 were diabetic rats that received a treatment of glibenclamide at a dose of 5 mg/kg; groups 4, 5 and 6 were diabetic rats that were given TBE at doses of 100, 200 and 400 mg/kg, respectively. *denotes percentage reduction of the blood glucose level with respect to the time 0 h.

For the chronic antidiabetic model (seven days treatment period), all the treatment groups had reduction in the blood glucose levels more than 25%, with the diabetic rats administered with DHE at doses of 200 mg/kg been the most significant (73%), compared to glibenclamide that resulted in 69% decrease in blood glucose level (Table 4).

Table 4. Chronic effect of *M. hurifolia* crude extract (MHE) on fasting glucose level in alloxan-induced diabetic rats

Treatment groups	Fasting blood glucose (mg/dL)		
	Day 1	Day 2	Day 3
Group 1	68.3 ± 6.8	89.8 ± 11.1	90.3 ± 9.12
Group 2	436.0 ± 16.1	366.5 ± 20.5	378.3 ± 12.6
Group 3	241.5 ± 15.5[b]	315.8 ± 13.5	225.5 ± 13.6[b]
Group 4	218.5 ± 7.8[b]	285.5 ± 10.9[b]	308.3 ± 17.5
Group 5	205.5 ±11.7[b]	326.6 ± 16.3	285.3 ± 18.5
Group 6	143.6 ± 8.4[b]	188.8 ± 11.3[b]	181.8 ± 10.9[b]

Day 4	Day 5	Day 6	Day 7
85.5 ± 13.1	86.0 ± 9.34	87.7 ± 7.99	85.8 ± 6.89
368.0 ± 14.9	364.0 ± 14.7	346.8 ± 17.5	344.5 ± 19.39
234.8 ± 11.6[b]	206.8 ±10. 9[b]	163.0 ± 17.3[b]	130.5 ± 19.5[b] (68.7%)*
217.5 ± 12.4[b]	243.0 ± 22.8	236.0 ± 15.3	182 ± 11.7[b] (30.2%)*
268.0 ± 17.8	198.3 ± 15.2[b]	147.3 ± 12.6[b]	118.6 ± 17.0[b] (73.3%)*
247.5 ± 1.8	202.8 ± 14.9[b]	161.8 ± 11.2	107.7 ± 18.2[b] (69.0%)*

[a]Values are expressed as mean ± standard error of mean of five rats per group. bStatistically different from the diabetic control ($P < 0.05$). Group 1 were normoglycaemic rats; group 2 were diabetic rats that received no treatment; group 3 were diabetic rats that received a treatment of glibenclamide at a dose of 5 mg/kg; groups 4, 5 and 6 were diabetic rats that were given TBE at doses of 100, 200 and 400 mg/kg, respectively. *denotes percentage reduction of the blood glucose level with respect to the time 0 h.

To the best of our knowledge, this is the first report on the anti-inflammatory and antidiabetic activities of the methanol extract of the leaves of *Macaranga hurifolia*. Other members of this genus have been reported to display antidiabetic effects. For instance, the chloroform fraction of the leaves of *M. barteri* lowered the blood glucose level in alloxan induced diabetic rats, with lupeol acetate responsible for the antidiabetic property of the leaves[30]. In addition, macatannins A and B isolated from the leaves of *M. tanarius* displayed remarkable α-glucosidase inhibitory activity[31].

This study has demonstrated the anti-inflammatory and antidiabetic activities of the methanol extract of *Macaranga hurifolia*. Further work is ongoing to isolate, purify and structurally elucidate the compounds that are responsible for the observed biological activity of the extract, and this will be reported in due course.

ACKNOWLEDGEMENTS

The authors express their profound gratitude to the technologists at the Department of Pharmacognosy, Faculty of Pharmacy, Olabisi Onabanjo University who assisted with the various aspects of this research.

REFERENCES

1. Shaw, J. E.; Sicree, R. A.; Zimmet, P. Z. Global estimates of the prevalence of diabetes for 2010 and 2030. *Diabetes Research and Clinical Practice* **2010,** *87*, 4-14.

2. Rahimi, M. A. Review: anti diabetic medicinal plants used for diabetes mellitus. *Bull. Env. Pharmacol. Life Sci.* **2015,** *4*, 163-180.

3. Abo, K. A.; Fred-Jaiyesimi, A. A.; Jaiyesimi, A. E. A. Ethnobotanical studies of medicinal plants used in the management of diabetes mellitus in South Western Nigeria. *J. Ethnopharmacol.* **2008,** *115,* 67-71.

4. Tangvarasittichai, S. Oxidative stress, insulin resistance, dyslipidemia and type 2 diabetes mellitus. *World J. Diabetes* **2015,** *6*, 456.

5. Asmat, U.; Abad, K.; Ismail, K. Diabetes mellitus and oxidative stress—a concise review. *Saudi Pharm. J.* **2016,** *24,* 547-553.

6. Kayama, Y.; Raaz, U.; Jagger, A.; Adam, M.; Schellinger, I. N.; Sakamoto, M.; Suzuki, H.; Toyama, K.; Spin, J. M.; Tsao, P. S. Diabetic cardiovascular disease induced by oxidative stress. *Int. J Mol. Sci.* **2015,** *16*, 25234-25263.

7. Pop-Busui, R.; Ang, L.; Holmes, C.; Gallagher, K.; Feldman, E. L. Inflammation as a therapeutic target for diabetic neuropathies. *Curr. Diabetes Rep.* **2016,** *16,* 29.

8. Roy, M. S.; Janal, M. N.; Crosby, J.; Donnelly, R. Markers of endothelial dysfunction and inflammation predict progression of diabetic nephropathy in African Americans with type 1 diabetes. *Kidney Int.* **2015,** *87,* 427-433.

9. Gupta, S.; Maratha, A.; Siednienko, J.; Natarajan, A.; Gajanayake, T.; Hoashi, S.; Miggin, S. Analysis of inflammatory cytokine and TLR expression levels in Type 2 diabetes with complications. *Scientific reports* **2017,** *7,* 7633.

10. Adaramoye, O.; Amanlou, M.; Habibi-Rezaei, M.; Pasalar, P.; Moosavi-Movahedi, A. Methanolic extract of African mistletoe *(Viscum album*) improves carbohydrate metabolism and hyperlipidemia in streptozotocin-induced diabetic rats. *Asian Pac. J. Trop. Med.* **2012,** 427-433.

11. Tahrani, A. A.; Piya, M. K.; Kennedy, A.; Barnett, A. H. Glycaemic control in type 2 diabetes: targets and new therapies. *Pharmacol. Therapuetics* **2010,** *125,* 328-361.

12. Burkill, H. The flora of west tropical Africa. *Kew, Royal Botanic Gardens, United Kingdom* **1985**, 211.

13. Ogbole, O. O.; Segun, P. A.; Adeniji, A. J. *In vitro* cytotoxic activity of medicinal plants from Nigeria ethnomedicine on rhabdomyosarcoma cancer cell line and HPLC analysis of active extracts. *BMC Comp. Alt. Med.* **2017,** *17*, 494.

14. Ogbole, O. O.; Akinleye, T. E.; Segun, P. A.; Faleye, T. C.; Adeniji, A. J. *In vitro* antiviral activity of twenty-seven medicinal plant extracts from southwest Nigeria against three serotypes of echoviruses. *Virol. J.* **2018,** *15,* 110.

15. Segun, P.; Ogbole, O.; Ismail, F.; Nahar, L.; Evans, A.; Ajaiyeoba, E.; Sarker, S. Bioassay-guided isolation and structure elucidation of cytotoxic stilbenes and flavonols from the leaves of *Macaranga barteri. Fitoterapia* **2019,** *134,* 151-157**.**

16. Ogbole, O.; Segun, P.; Akinleye, T.; Fasinu, P. Antiprotozoal, antiviral and cytotoxic properties of the Nigerian mushroom, *Hypoxylon fuscum* Pers. Fr.(Xylariaceae). *Acta Pharm. Sci.* **2018,** *56,* 43-56.

17. Segun P. A.; Ogbole, O. O.; Akinleye, T. E.; Faleye, T. C.; Adeniji, A. J. *In vitro* anti-enteroviral activity of stilbenoids isolated from the leaves of *Macaranga barteri*. *Nat. Prod. Res.* **2019,**

18. Bayne, K. Developing guidelines on the care and use of animals. *Annals New York Acad. Sci.* **1998,** *862*:105-110.

19. Prashant, T.; Bimlesh, K.; Mandeep, K.; Gurpreet, K.; Harleen, K. Phytochemical screening and extraction: a review. *Int. Pharm. Sci.* **2011,** *1,* 98-106.

20. Okoli, C.; Akah, P.; Nwafor, S.; Anisiobi, A.; Ibegbunam, I.; Erojikwe, O. Anti-inflammatory activity of hexane leaf extract of *Aspilia africana* CD Adams. *J. Ethnopharmacol.* **2007,** *109*, 219-225.

21. Akindele, A.; Adeyemi, O. Antiinflammatory activity of the aqueous leaf extract of *Byrsocarpus coccineus*. *Fitoterapia* **2007,** *78,* 25-28.

22. Zheng, T.; Shu, G.; Yang, Z.; Mo, S.; Zhao, Y.; Mei, Z. Antidiabetic effect of total saponins from *Entada phaseoloides* (L.) Merr. in type 2 diabetic rats. *J. Ethnopharmacol.* **2012,** *139*, 814-821.

23. Hoffman, R. Vascular endothelial dysfunction and nutritional compounds in early type 1 diabetes. *Curr. Diabetes Rev.* **2014,** *10*, 201-207.

24. Ngoumfo, R. M.; Ngounou, G. E.; Tchamadeu, C. V.; Qadir, M. I.; Mbazoa, C. D.; Begum. A.; Ngninzeko, F. N.; Lontsi, D.; Choudhary, M. I. Inhibitory effect of macabarterin, a polyoxygenated ellagitannin from *Macaranga barteri*, on human neutrophil respiratory burst activity. *J. Nat. Prod.* **2008,** *71*, 1906-1910.

25. Akindele, A.; Oladimeji-Salami, J.; Usuwah, B. Antinociceptive and anti-inflammatory activities of *Telfairia occidentalis* hydroethanolic leaf extract (Cucurbitaceae). *J. Med. Food* **2015,** *18*, 1157-1163.

26. Adeyemi, O.; Okpo, S.; Okpaka, O. The Anti-nociceptive effect of the methanolic extract of *Acanthus montanus*. *J. Ethnopharmocol.* **2004,** *90*, 45-48.

27. Murthy, T.; Kommineni, M.; Mayuren, C. Influenceof losartan on the hypoglycemic activity of glimepiride in normal and diabetic rats. *Ther. Adv. Endocrinol. Metab.* **2013,** *4*, 133-138.

28. Xing, R.; He, X.; Liu, S.; Yu, H.; Qin, Y.; Chen, X.; Li, K.; Li, R.; Li, P. Antidiabetic activity of differently regioselective chitosan sulfates in alloxan-induced diabetic rats. *Mar Drugs* **2015,** *13*, 3072-3090.

29. Sathya, S.; Kokilavani, R.; Gurusamy, K. Hypoglycemic effect of *Gymnema sylvestre* (Retz.,) R.Br leaf in normal and alloxan induced diabetic rats. *Anc. Sci. Life* **2008,** *28*, 12-14.

30. Fred-Jaiyesimi, A. A.; Bamidele, B. I. Lupeol acetate from *Macaranga barteri* Mull.-Arg leaf lowers blood glucose level in alloxan induced diabetic rats. *Nig. Quart. J. Hosp. Med.* **2016,** *26*, 368-371.

31. Maria, D. P. T.; Gunawan, P.; Jun, K. Novel a-glucosidase inhibitors from *Macaranga tanarius* leaves. *Food Chem.* **2010,** *123,* 384-389.

Acta Pharm. Sci. Vol 57 No: 4. 2019
DOI: 10.23893/1307-2080.APS.05727

A Novel Bioactive Compounds of 2-Azetidinone Derived from Pyrazin Dicarboxylic Acid: Synthesis and Antmicrobial Screening

Ahmed Neamah Ayyash[1*], Hadeel Qais Abdalrazzaq Habeeb[2]

1 Department of Applied Chemistry, College of Applied Sciences, University of Fallujah, Anbar, Iraq. 2Department of Nursing, Al-Farabi University College, Baghdad, Iraq.

ABSTRACT

A series of novel 2-azetidinons entitled N, N'-bis[3-chloro-2-oxo-4-(substituted pyridine-2-yl)-azetidin-1-yl] pyrazine-2,3-dicarboxamide and N,N'-bis[3,3-dichloro-2-oxo-4-(substitutedpyridine-2-yl)-azetidin-1-yl] pyrazine-2,3-dicarboxamide have been synthesized from the relating newly Schiff bases by [2+2] cycloaddition reaction in good yields. Starting with pyrazine-2,3-dicarboxylic acid which was converted to the corresponding diester in absolute ethanol and glacial acetic acid as a catalyst. After that, the hydazinolysis of resulted diester with hydrazine hydrate afforded dicarbohydrazide which further treated with different substituted pyridine-2-carbaldehyde to give new Schiff bases. These new Schiff bases were reacted with chloroacetochloride and (or) dichloroacetochloride in presence of trimethylamine in DMF solvent under reflux and stirring to yield new derivatives of titled compounds. The structural assignments were estimated from their spectroscopic analysis such as IR,^{1}H NMR, ^{13}C NMR, and C, H, N elemental analysis. The newly prepared 2-azetidinones have been screened for their antimicrobial activity and some of them revealed excellent antibacterial and antifungal activities.

Keywords: 2-Azetidinones, Antimicrobial, Pyrazine-2,3-dicarboxylic acid, Schiff bases, Synthesis.

INTRODUCTION

2-Azetidinones, also called (β-lactam) compounds are classified as an important class of heterocyclic compounds whish are consist the most structural feature of β-lactams antibiotics such as; penicillin, cephalosporin and clavu-

*Corresponding Author: Ahmed N. Ayyash, e-mail: ahmed_198232@yahoo.com
Ahmed Neamah Ayyash ORCID Number: 0000-0003-3407-7295
(Received 15 July 2019, accepted 22 August 2019)

lanic acid.[1,2] Because of the biological properties of 2-azetidinone compounds as antibiotics, antimicrobial, and anti-inflammatory,[3-7] as well as the chemical importance as an intermediate for synthesis of many bioactive compounds,[8] a remarkable attraction and the main framework for all interested researchers toward synthesis and discover of new 2-azetidinone derivatives. Many of the current antimicrobial drugs has becoming less effective versus microbe resistance. Herein, it was necessary to synthesis and development of new antimicrobial agents which may be possess more activity against these strains resistant.[9] However, by the literature survey, many various procedures were reported to prepare a new derivative of substituted azetidin-2-one with powerful biological activity. For example, benzimidazolyloxazolyl 2-azetidinone derivatives has been prepared with good yields.[10] Also, a series of 2-azetidinone derivatives have been prepared from their corresponding azomethine compounds and triethyl amine in presence of chloroacetyl chloride.[11] Moreover, the cyclocondensation of azolylindol Schiff bases and chloroacetyl chloride afforded new derivatives of 3-chloro-azetidin-2-one.[12] More recently, other new 2-azetidinones derivatives have been prepared by cycloaddition reaction of some Schiff bases with triethylamine and chloroacetyl chloride, the newly products exhibited good antibacterial activity.[13] (Fig. 1).

So, based on the facts above and as a part of our interesting, this present work aims to design and development of new 2-azetidinone derivatives and investigation of their antimicrobial activities.

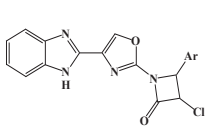

benzimidazolyloxazolyl 2-azetidinones [10]

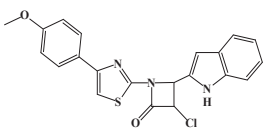

3-chloro-4-(1H-indol-2-yl)-1-(4-(4-methoxyphenyl)thiazol-2-yl)azetidin-2-one [12]

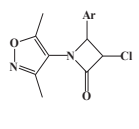

4-aryl-3-chloro-1-(3,5-dimethyl-4-isoxazol-2-yl)-azeidine-2-one [13]

Figure 1. Some of the recently prepared of 2-azetidinone derivatives.

METHODOLOGY

Chemicals and all reagents and solvents have been used as received from their suppliers BDH, Fluka, Merck, and Sigma-Aldrich companies without more purification. The reactions progress was monitored on pre-coated aluminum plates by thin layer chromatography (TLC) technique. Melting points were measured in Celsius degree on open-capillary Electro thermal apparatus and are uncorrected. IR spectra were recorded on FTIR Shimadzu (8400s) spec-

trophotometer using KBr disc. The spectra of ^{1}H NMR and ^{13}C NMR have been outlined with Bruker spectrometer in DMSO-d_6 solvent, (400 and 100 MHz), respectively, and expressed as part per million (δ ppm) downfield from tetramethylsilane (TMS as an internal standard reference). Elemental analysis of the (C, H, N) percentages were found with Elemental Analyzer Model (Fison EA1108). For chemical structures drawing, Chem Draw Ultra (6.0) software application was operated.

***General procedure for the preparation of dimethyl pyrazine-2,3-dicarboxylate,* 2:** The standard esterification procedure was applied to convert pyrazine-2,3-dicarboxylic acid **1** into corresponding diester **2.**[14]

***General procedure for the preparation of pyrazine-2,3-dicarbohydrazide,* 3:** According to the Smith procedure,[15] compound **3** was prepared by hydrazinolysis of **2.**

***General procedure for the synthesis of N'², N'³-bis[(E)(substituted-pyridine-2-yl) methylidene] pyrazine-2,3-dicarbohydrazide,* 4a-e:** A solution of (2 mmol) of appropriate pyridine-2-carbaldehyde in 20 mL of absolute ethanol was added to (1 mmol) of compound **3** and 3-4 drops of glacial acetic acid (GAA). The mixture was refluxed under stirring for 3h. After cooling at room temperature for 24h., the precipitated solid was filtered, washed with water, dried, and purified by recrystallization from ethanol.

General procedure for the synthesis of N,N'-bis[3-chloro-2-oxo-4-(substitutedpyridine-2-yl)-azetidin-1-yl] pyrazine-2,3-dicarboxamide, 5a-e: A solution (2 mmol) of chloroacetyl chloride and (2 mmol) of trimethylamine (TEA) in 10 mL of DMF was added with stirring to (1 mmol) of the suitable newly prepared Schiff base **4a-e** and refluxed for 4-5 h. under stirring, then the reaction flask contents were kept to cool and poured onto crushed ice. The solid was separated off by filtration, dried and recrystallized from dimethylsufoxide (DMSO).

General procedure for the synthesis of N,N'-bis[3,3-dichloro-2-oxo-4-(substitutedpyridine-2-yl)-azetidin-1-yl] pyrazine-2,3-dicarboxamide, 6a-e: The same procedure mentioned above for compounds **5a-e** was applied for compounds **6a-e** except the dichloroacetyl chloride was used instead of chloroacetyl chloride.

Table 1. Physicochemical properties of all synthesized compounds

Compound	R	Yield (%)	m.p (°C)	M.wt. (g/mol.)	Empirical Formula	Anal. (calcd.) / found %
2		87	155 (dec.)	196.16	$C_8H_8N_2O_4$	(C, 48.98; H, 4.11; N, 14.28) / C, 48.92; H, 4.08; N, 14.25
3		82	117-118	196.17	$C_6H_8N_6O_2$	(C, 36.74; H, 4.11; N, 42.84) / C, 36.80; H, 4.14; N, 42.89
4a	H	69	188-189	374.36	$C_{18}H1_4N_8O_2$	(C, 57.75; H, 3.77; N, 29.93) / C, 57.70; H, 3.73; N, 29.88
4b	5-CH_3	73	203-205	402.41	$C_{20}H_{18}N_8O_2$	(C, 59.69; H, 4.51; N, 27.85) / C, 59.62; H, 4.48; N, 27.82
4c	5-OCH_3	66	212-214	434.41	$C_{20}H_{18}N_8O_4$	(C, 55.30; H, 4.18; N, 25.79) / C, 55.24; H, 4.15; N, 25.75
4d	3-OH	81	241-242	406.36	$C_{18}H_{14}N_8O_4$	(C, 53.20; H, 3.47; N, 27.58) / C, 53.17; H, 3.45; N, 27.54
4e	3-Cl	68	198-200	443.25	$C_{18}H_{12}Cl_2N_8O_2$	(C, 48.77; H, 2.73; N, 25.28) / C, 48.72; H, 2.70; N, 25.24
5a	H	72	188-189	527.32	$C_{22}H_{16}Cl_2N_8O_4$	(C, 50.11; H, 3.06; N, 21.25) / C, 50.08; H, 3.04; N, 21.22
5b	5-CH_3	74	191-194	555.37	$C_{24}H_{20}Cl_2N_8O_4$	(C, 51.90; H, 3.63; N, 20.18) / C, 51.87; H, 3.61; N, 20.14
5c	5-OCH_3	65	199-201	587.37	$C_{24}H_{20}Cl_2N_8O_6$	(C, 49.08; H, 3.43; N, 19.08) / C, 49.03; H, 3.40; N, 19.05
5d	3-OH	79	256-259	559.32	$C_{22}H_{16}Cl_2N_8O_6$	(C, 47.24; H, 2.88; N, 20.03) / C, 47.21; H, 2.86; N, 20.00
5e	3-Cl	69	190-192	596.21	$C_{22}H_{14}Cl_4N_8O_4$	(C, 44.32; H, 2.37; N, 18.79) / C, 44.27; H, 2.34; N, 18.74
6a	H	78	203-204	596.21	$C_{22}H_{14}Cl_4N_8O_4$	(C, 44.32; H, 2.37; N, 18.79) / C, 44.28; H, 2.37; N, 18.75
6b	5-CH_3	82	218-220	624.26	$C_{24}H_{18}Cl_4N_8O_4$	(C, 46.18; H, 2.91; N, 17.95) / C, 46.13; H, 2.88; N, 17.91
6c	5-OCH_3	72	227-228	656.26	$C_{24}H_{18}Cl_4N_8O_6$	(C, 43.92; H, 2.76; N, 17.07) / C, 43.88; H, 2.73; N, 17.05
6d	3-OH	85	259-262	628.21	$C_{22}H_{14}Cl_4N_8O_6$	(C, 42.06; H, 2.25; N, 17.84) / C, 42.01; H, 2.22; N, 17.81
6e	3-Cl	70	187-189	665.10	$C_{22}H_{12}C_{l6}N_8O_4$	(C, 39.73; H, 1.82; N, 16.85) / C, 39.69; H, 1.80; N, 16.82

RESULTS AND DISSCUSION

1,3,4-Trisubstituted-2-Azetidinone derivatives **5a-e** and **6a-e**, as well as their Schiff bases **4a-e** have been synthesized according to the synthetic route that predicted in Scheme 1.

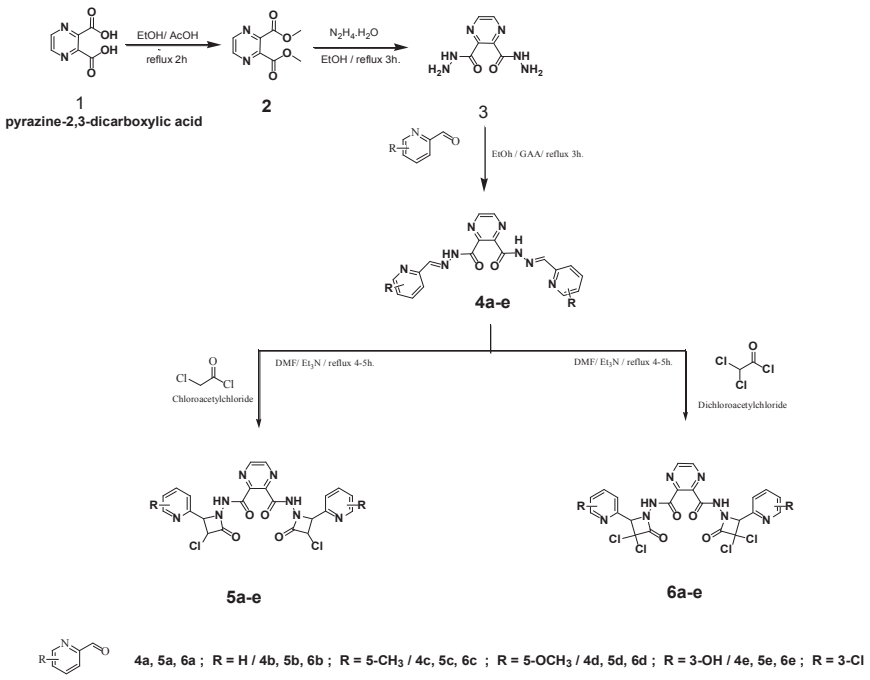

Scheme 1. General synthetic pathway of the target compounds.

At the beginning, a standard esterification method was applied to convert pyrazine-2,3-dicarboxilic acid **1** to the corresponding diester compound **2** with good yield. Then the hyrazinolysis of 2 in refluxing ethanol afforded diacarbohydrazide **3** which further condensed with some derivatives of pyridine-2-carbaldehyde in acidic medium of absolute ethanol solution under reflux and stirring to yield new azomethine (Schiff bases) derivatives **4a-e**. Finally, the new derivatives of target 2-azetidinone compounds **5a-e** were synthesized by [2+2] cycloaddition reaction between chloroacetochloride and newly prepared Schiff bases in presence of triethylamine (TEA) in DMF under reflux. By the same procedure, the other designed 2-azitidinones **6a-e** have been prepared in presence of dichloroacetochloride instead of chloroacetochloride as a ketene compound according to an imine-ketene mechanism, Scheme 3. [16]

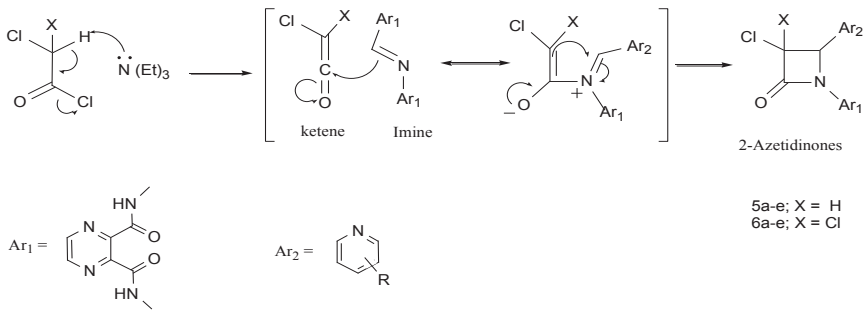

Scheme 2. Proposed mechanism for 2-azetidinones derivatives 5a-e and 6a-e.

The chemical structures of all newly synthesized compounds have been established from their IR, ^{1}H NMR, and ^{13}C NMR which gave the comfortable results for the desired structures. FTIR spectrum of **2**, (Fig. 2) showed the absence the bands due to hydroxyl group stretching vibration of raw material while the new bands were observed at 2955 cm^{-1} and 1687 cm^{-1} which belonging to the stretching vibrations of aliphatic C-H and ester carbonyl C=O groups, respectively. On the other hand, the more significant peak due to carboxylic acid protons of raw material was disappeared in the ^{1}H NMR spectrum of compound **2**, by contrast the methoxy protons as a singlet signal was noted at 3.98 ppm, (Fig. 3).

Concerning compound 3, the FTIR spectrum showed stretching absorption bands due to NH_2 and NH group in the region 3441-3283 cm^{-1} and another band at 1682 cm^{-1} corresponded to amidic C=O group, (Fig. 4). Furthermore, ^{1}H NMR spectrum of 3 confirmed the presence of NH and NH_2 protons when new signals were recorded at 7.52 ppm and 2.50 ppm as shown in (Fig. 5).

As for newly Schiff bases **4a-e**, ^{1}H NMR spectrum of **4a** and **4c**, (Fig. 6 and Fig. 7) revealed the more characteristic peak of azomethine proton (CH=N) at 8.04 and 7.84 ppm, respectively. In addition to the microanalysis, IR and ^{1}H NMR spectra, the ^{13}C NMR spectra of newly synthesized 2-azetidinones **5a-e** and **6a-d** as shown in (Fig. 9) and (Fig. 10), respectively**,** displayed several signals with full coincidence of the proposed structures beside the other spectral data which are given in Table 2.

Biological Studies

Antimicrobial activities of the newly compounds **5a-e** and **6a-e** have been screened against two bacterial strains*; Staphylococcus Sciuri* as gram positive *and Escherichia Coli* as gram negative, as well as against fungal strains; *Candida Albicans* and *Aspergillus Flavus*, by diffusion method.[17] The tested compounds were dissolved in dimethyl sulfoxide (DMSO) to prepare 100 µg/mL concentration. The plates of bacterial culture were incubated at 37 °C for 24h. while for fungal culture were incubated at 25 °C and tested after 72 h. Cefuroxime and fluconazole were used (as antibacterial and antifungal drugs), respectively. The growth inhibition ability of the tested compounds was measured as inhibition zone diameter in milliliters. The results are listed in Table 3, showed good to excellent activities of the examined newly 2-azetidinones.

Table 2. Spectral data of all synthesized compounds

Spectral data
2) ***dimethyl pyrazine-2,3-dicarboxylate*** IR (KBr, cm^{-1}): 3086 (Ar. C-H), 2955 (Ali. C-H), 1687 (ester C=O),1645 (C=N), 1290 (C-O-C). ^{1}H NMR (DMSO-d_6, δ, ppm): 9.52-9.28 (s, 2H, 2-pyrazine), 3.52 (s, 6H, OCH_3).**3)** ***pyrazine-2,3-dicarbohydrazide*** IR (KBr, cm^{-1}): 3441-3283 (NH), 3088 (Ar. CH), 1682 (C=O), 1654 (C=N), 1280 (C-N). ^{1}H NMR, (DMSO-d_6, δ, ppm): 9.43 (s, 2H, 2- Pyrazine), 7.52 (s, 2H, NH), 2.50 (s, 4H, NH_2).
4a) ***N'²,N'³-bis[(E)-(pyridine-2-yl)methylidene]pyrazine-2,3-dicarbohydrazide*** IR (KBr) (v, cm^{-1}): 3386-3182 (NH), 3085 (Ar. C-H), 1679 (C=O), 1642 (C=N), 1594 (C=C), 1238-1108 (C-N). ^{1}H NMR (400 MHz, DMSO-d6) δ (ppm): 6.95 (s, 2H, NH), 7.47 (s, 2H, N=CH), 7.87-8.82 (m, 8H, pyridine Ring), 9.37 (s, 2H, 2-pyrazine).
4b) ***N'²,N'³-bis[(E)-(5-methylpyridine-2-yl)methylidene]pyrazine-2,3-dicarbohydrazide*** IR (KBr) (*υ*, cm^{-1}): 3349-3162 (NH), 3095 (Ar. C-H), 2988 (Ali. C-H), 1672 (C=O), 1642 (C=N), 1595 (C=C), 1230-1110 (C-N). ^{1}H NMR (400 MHz, DMSO-d_6) δ (ppm): 2.49 (s, 6H, Ar-CH_3), 6.25 (s, 2H, NH), 7.35 (s, 2H, N=CH), 7.99-8.86 (m, 6H, pyridine Ring), 9.46 (s, 2H, 2-pyrazine).
4c) ***N'²,N'³-bis[(E)-(5-methoxypyridine-2-yl)methylidene]pyrazine-2,3-dicarbohydrazide*** IR (KBr) (*υ*, cm^{-1}): 3404-3210 (NH), 3092 (Ar. C-H), 2995 (Ali. C-H), 1685 (C=O), 1650 (C=N), 1587 (C=C), 1232-1110 (C-N). ^{1}H NMR

(400 MHz, DMSO-d_6) δ (ppm): 3.42 (s, 6H, Ar-OCH_3), 7.04 (s, 2H, NH), 7.21 -7.84 (m, 6H, pyridine Ring and s, 2H, N=CH), 8.54 (s, 2H, 2-pyrazine).

4d) ***N'²,N'³-bis[(E)-(3-hydroxypyridine-2-yl)methylidene]pyrazine-2,3-dicarbohydrazide*** IR (KBr) (*υ*, cm^{-1}): 4487 (OH), 3349-3210 (NH), 3082 (Ar. C-H), 1678 (C=O), 1640 (C=N), 1595 (C=C), 1222-1108 (C-N). ^{1}H NMR (400 MHz, DMSO-d_6) δ (ppm): 4.88 (s, 2H, Ar. OH), 6.83 (s, 2H, NH), 7.72 (s, 2H, N=CH), 7.80-8.85 (m, 6H, pyridine Ring), 9.60 (s, 2H, 2-pyrazine).

4e) ***N'²,N'³-bis[(E)-(3-chloropyridine-2-yl)methylidene]pyrazine-2,3-dicarbohydrazide*** IR (KBr) (*υ*, cm^{-1}): 3382-3195 (NH), 3088 (Ar. C-H), 1680 (C=O), 1656 (C=N), 1590 (C=C), 1248-1115 (C-N), 721 (C-Cl). ^{1}H NMR (400 MHz, DMSO-d_6) δ (ppm): 6.71 (s, 2H, NH), 7.04 (s, 2H, N=CH), 7.97-8.85 (m, 6H, pyridine Ring), 9.52 (s, 2H, 2-pyrazine).

5a) ***N,N'-bis[3-chloro-2-oxo-4-(pyridine-2-yl)-azetidin-1-yl] pyrazine-2,3-dicarboxamide*** IR (KBr) (*υ*, cm^{-1}): 3249-3181 (NH), 3095 (Ar. CH), 1722 (C=O, β-lactam), 1668 (C=O, sec. amide), 1642 (C=N), 1598 (C=C), 721 (C-Cl). ^{1}H NMR (400 MHz, DMSO-d_6) δ (ppm): 4.40 (s, 2H, NC_3H, β-lactam), 6.72 (s, 2H, C_3H-Cl, β-lactam), 7.38-7.62 (m, 8H, Ar. H, and 2H, NH), 9.35 (s, 2H, 2-pyrazine). ^{13}C NMR (100 MHz, DMSO-d_6) δ (ppm): 62.8 (N-CH-C-Cl, azetidine ring), 65.8 (C-Cl azetidine ring), 120.2-137.4 (aromatic carbons), 143.2 (C-N pyridine ring), 152.5 (C=N, pyridine ring), 163.2 (N-C=O, azetidine ring), 169.5 (HNCO-Ar).

5b) ***N,N'-bis[3-chloro-2-oxo-4-(5-methylpyridine-2-yl)-azetidin-1-yl]pyrazine-2,3-dicarboxamide*** IR (KBr) (*υ*, cm^{-1}): 3345-3210 (NH), 3080 (Ar. CH), 2995 (Ali. CH), 1710 (C=O, β-lactam), 1665 (C=O, sec. amide), 1638 (C=N), 1588 (C=C), 724 (C-Cl). ^{1}H NMR (400 MHz, DMSO-d_6) δ (ppm): 2.48 (s, 6H, Ar. CH_3), 4.85 (s, 2H, NC_3H, β-lactam), 5.80 (s, 2H, C_3H-Cl, β-lactam), 7.24-8.72 (m, 6H, Ar. H, and 2H, NH), 8.86 (s, 2H, 2-pyrazine). ^{13}C NMR (100 MHz, DMSO-d_6) δ (ppm): 21.2 (Ar. CH_3), 62.5 (N-CH-C-Cl, azetidine ring), 66.2 (C-Cl azetidine ring), 120.2-138.7 (aromatic carbons), 141.8 (C-N pyridine ring), 155.0 (C=N, pyridine ring), 163.4 (N-C=O, azetidine ring), 169.8 (HNCO-Ar).

5c) ***N,N'-bis[3-chloro-2-oxo-4-(5-methoxypyridine-2-yl)-azetidin-1-yl]pyrazine-2,3-dicarboxamide*** IR (KBr) (*υ*, cm^{-1}): 3249-3181 (NH), 3097 (Ar. CH), 2988 (Ali. CH), 1698 (C=O, β-lactam), 1675 (C=O, sec. amide), 1648 (C=N), 1590 (C=C), 719 (C-Cl). ^{1}H NMR (400 MHz, DMSO-d_6) δ (ppm): 3.71 (s, 6H, Ar. OCH_3), 5.02 (s, 2H, NC_3H, β-lactam), 5.48 (s, 2H, C_3H-Cl, β-lactam), 7.38-8.28 (m, 6H, Ar. H, and 2H, NH), 9.08 (s, 2H, 2-pyrazine). ^{13}C NMR (100 MHz, DMSO-d_6) δ (ppm): 54.8 (Ar. OCH_3), 62.8 (N-CH-C-Cl, azetidine ring),

64.0 (C-Cl azetidine ring), 121.0-137.9 (aromatic carbons), 149.4 (C-N pyridine ring), 157.5 (C=N, pyridine ring), 164.2 (N-C=O, azetidine ring), 170.3 (HNCO-Ar).

5d) ***N,N'-bis[3-chloro-2-oxo-4-(3-hydroxypyridine-2-yl)-azetidin-1-yl]pyrazine-2,3-dicarboxamide*** IR (KBr) (υ, cm^{-1}): 3442 (OH), 3342-3152 (NH), 3087 (Ar. CH), 1712 (C=O, β-lactam), 1664 (C=O, sec. amide), 1644 (C=N), 1598 (C=C), 722 (C-Cl). ^{1}H NMR (400 MHz, DMSO-d_6) δ (ppm): 4.04 (s, 2H, Ar. OH), 4.96 (s, 2H, NC_3H, β-lactam), 5.30 (s, 2H, C_3H-Cl, β-lactam), 7.25-8.15 (m, 6H, Ar. H, and 2H, NH), 8.82 (s, 2H, 2-pyrazine). ^{13}C

NMR (100 MHz, DMSO-d_6) δ (ppm): 62.6 (N-CH-C-Cl, azetidine ring), 64.5 (C-Cl azetidine ring), 120.5-138.8 (aromatic carbons), 151.2 (C-N pyridine ring), 163.2 (C=N, pyridine ring), 164.2 (N-C=O, azetidine ring), 170.8 (HNCO-Ar).

5e) ***N,N'-bis[3-chloro-2-oxo-4-(3-chloropyridine)-azetidin-1-yl] pyrazine-2,3-dicarboxamide*** IR (KBr) (υ, cm^{-1}): 3395-3252 (NH), 3010 (Ar. CH), 1708 (C=O, β-lactam), 1671 (C=O, sec. amide), 1653 (C=N), 1591 (C=C), 721 (C-Cl). ^{1}H NMR (400 MHz, DMSO-d_6) δ (ppm): 4.84 (s, 2H, NC_3H, β-lactam), 5.52 (s, 2H, C_3H-Cl, β-lactam), 7.11-7.98 (m, 6H, Ar. H, and 2H, NH), 8.92 (s, 2H, 2-pyrazine). ^{13}C NMR (100 MHz, DMSO-d_6) δ (ppm): 63.2 (N-CH-C-Cl, azetidine ring), 63.8 (C-Cl azetidine ring), 119.8-136.8 (aromatic carbons), 152.8 (C-N pyridine ring), 161.8 (C=N, pyridine ring), 164.4 (N-C=O, azetidine ring), 170.2 (HNCO-Ar).

6a) ***N,N'-bis[3,3-dichloro-2-oxo-4-(pyridine-2-yl)-azetidin-1-yl] pyrazine-2,3-dicarboxamide*** IR (KBr) (υ, cm^{-1}): 3385-3168 (NH), 1712 (C=O, β-lactam), 3098 (Ar. CH), 1674 (C=O, sec. amide), 1661 (C=N), 1601 (C=C), 721 (C-Cl). ^{1}H NMR (400 MHz, DMSO-d_6) δ (ppm): 4.80 (s, 2H, NC_3H, β-lactam), 7.35-8.62 (m, 8H, Ar. H, and 2H, NH), 9.45 (s, 2H, 2-pyrazine). ^{13}C NMR (100 MHz, DMSO-d_6) δ (ppm): 72.3 (N-CH-C-Cl_2, azetidine ring), 92.3 (C-Cl_2 azetidine ring), 120.8-137.8 (aromatic carbons), 148.4 (CH=C-N pyridine ring), 154.6 (N-C=O, azetidine ring), 163.2 (C-C=N-C, pyridine ring), 169.8 (HNCO-Ar).

6b) ***N,N'-bis[3,3-dichloro-2-oxo-4-(5-methylpyridine-2-yl)-azetidin-1-yl]pyrazine-2,3-dicarboxamide*** IR (KBr) (υ, cm^{-1}): 3282-3144 (NH), 3083 (Ar. CH), 2992 (Ali. CH), 1704 (C=O, β-lactam), 1666 (C=O, sec. amide), 1639 (C=N), 1596 (C=C), 722 (C-Cl). ^{1}H NMR (400 MHz, DMSO-d_6) δ (ppm): 2.26 (s, 6H, Ar. CH_3), 4.79 (s, 2H, NC_3H, β-lactam), 7.38-8.82 (m, 6H, Ar. H, and 2H, NH), 9.22 (s, 2H, 2-pyrazine). ^{13}C NMR (100 MHz, DMSO-d_6) δ (ppm): 21.8 (Ar. CH_3), 72.7 (N-CH-C-Cl_2, azetidine ring), 97.8 (C-Cl_2 azetidine ring), 120.4-136.2 (aromatic carbons), 151.0 (CH=C-N pyridine ring), 160.3 (N-C=O,

azetidine ring), 163.7 (C-C=N-C, pyridine ring), 169.2 (HNCO-Ar).

6c) ***N,N'-bis[3,3-dichloro-2-oxo-4-(5-methoxypyridine-2-yl)-azetidin-1-yl]pyrazine-2,3-dicarboxamide*** IR (KBr) (υ, cm^{-1}): 3393-3172 (NH), 3010 (Ar. CH), 2998 (Ali. CH), 1712 (C=O, β-lactam), 1672 (C=O, sec. amide), 1648 (C=N), 1590 (C=C), 719 (C-Cl). ^{1}H NMR (400 MHz, DMSO-d_6) δ (ppm): 4.03 (s, 6H, Ar. OCH_3), 4. 90 (s, 2H, NC_3H, β-lactam), 7.25-8.90 (m, 6H, Ar. H, and 2H, NH), 9.02 (s, 2H, 2-pyrazine). ^{13}C NMR (100 MHz, DMSO-d_6) δ (ppm): 55.4 (Ar. OCH_3), 72.0 (N-CH-C-Cl_2, azetidine ring), 96.5 (C-Cl_2 azetidine ring), 119.8-137.8 (aromatic carbons), 151.4 (CH=C-N pyridine ring), 161.7 (N-C=O, azetidine ring), 162.8 (C-C=N-C, pyridine ring), 170.8 (HNCO-Ar).

6d) ***N,N'-bis[3,3-dichloro-2-oxo-4-(3-hydroxypyridine)-azetidin-1-yl] pyrazine-2,3-dicarboxamide*** IR (KBr) (υ, cm^{-1}): 3455 (OH), 3297-3185 (NH), 3010 (Ar. CH), 1721 (C=O, β-lactam), 1676 (C=O, sec. amide), 1648 (C=N), 1596 (C=C), 721 (C-Cl). ^{1}H NMR (400 MHz, DMSO-d_6) δ (ppm): 4.19 (s, 2H, Ar. OH), 5.48 (s, 2H, NC_3H, β-lactam), 7.02-7.70 (m, 6H, Ar. H, and 2H, NH), 8.92 (s, 2H, 2-pyrazine). ^{13}C NMR (100 MHz, DMSO-d_6) δ (ppm): 73.4 (N-CH-C-Cl_2, azetidine ring), 97.0 (C-Cl_2 azetidine ring), 120.8-136.0 (aromatic carbons), 151.8 (CH=C-N pyridine ring), 161.6 (N-C=O, azetidine ring), 163.5 (C-C=N-C, pyridine ring), 169.8 (HNCO-Ar).

6e) ***N,N'-bis[3,3-dichloro-2-oxo-4-(3-chloropyridine)-azetidin-1-yl] pyrazine-2,3-dicarboxamide*** IR (KBr) (υ, cm^{-1}): 3284-3180 (NH), 3080 (Ar. CH), 1706 (C=O, β-lactam), 1667 (C=O, sec. amide), 1642 (C=N), 1599 (C=C), 723 (C-Cl). ^{1}H NMR (400 MHz, DMSO-d_6) δ (ppm): 4.93 (s, 2H, NC_3H, β-lactam), 6.98-8.02 (m, 6H, Ar. H, and 2H, NH), 8.82 (s, 2H, 2-pyrazine). ^{13}C NMR (100 MHz, DMSO-d_6) δ (ppm): 74.2 (N-CH-C-Cl_2, azetidine ring), 98.3 (C-Cl_2 azetidine ring), 122.2-137.4 (aromatic carbons), 151.6 (CH=C-N pyridine ring), 161.5 (N-C=O, azetidine ring), 164.2 (C-C=N-C, pyridine ring), 169.8 (HNCO-Ar).

Table 3. Antibacterial and antifungal activities of newly synthesized compounds

	Zone of inhibition (mm) bacterial strains		fungal strains	
compd.	**Staph. Sciuri**	**Escherichia Coli**	**Aspergillus Flavus**	**Candida Albicans**
5a	14	14	17	21
5b	18	17	17	16
5c	13	11	21	21
5d	22	20	20	17
5e	16	18	18	18
6a	16	13	15	14
6b	19	16	19	16
6c	22	21	13	20
6d	17	20	19	19
6e	15	19	18	22
cefuroxime	18	22		
fluconazole			20	24

*concentration (100 µg/mL), diameter (mm); milliliter.

Variety derivatives of 2-azetidinone and related Schiff bases have been synthesized in good yields and cost-effective procedures. A coincidence for the proposed structures was achieved as deduced from their physiochemical and spectroscopic data. The newly 2-azetidinone compounds were screened for their antibacterial and antifungal properties. The results showed that most of these compounds have a good to excellent antimicrobial activities.

ACKNOWLEDGEMENT

Authors are thankful to the ministry of science and technology, as well as to the university of Al-Mustansiriayah, Bagdad-Iraq for operating most of this work.

REFERENCES

1. Fleming, A. On the Antibacterial Action of Cultures of Apenicillium, With Special Reference to Their Use in The Isolation of B. Influenza. *Br. J. Exp. Pathol.* **1929**, *10*, 226-236.

2. Knowles, J. R. Penicillin Resistance: The Chemistry of Beta-Lactamase Inhibition. *Acc. Chem. Res.* **1985**, *18*, 97-104.

3. Patel, N. B.; Patel, J. C. Synthesis and Antimicrobial Activity of Schiff Bases and 2-Azetidinones Derived from Quinazolin-4(3H)-One. *Arabian J. Chem.* **2011**, *4*, 403-411.

4. Gurupadayya, B. M.; Gopal, M.; Padmashaly, B.; Manohara, Y. Synthesis and Pharmacological Evaluation of Azetidin-2-ones and Thiazolidin-4-ones Encompassing Benzothiazole. *Indian J. Pharm. Sci.* **2008**, *70*, 572-577.

5. Ishwar, B. K.; Mubeen, M.; Kalluraya, B. Synthesis and Pharmacological Studies of Some Azetidinones bearing Ibuprofen Moiety. *Ind. J. Heterocycl. Chem.* **2003**, *13*, 183-184.

6. Gilani, S. J.; Alam, O.; Khan, S. A.; Siddiqui, N.; Kumar, H. Synthesis of Some Derived Thiazolidin-4-one, Azetidin-2-one and 1, 3, 4-Oxadiazole Ring System from Isonicotinic Acidhydrazide: A Novel Class of Potential Anticonvulsant Agent. *Der. Pharm. Lett.* **2009**, *1*, 1-8.

7. Mohan, J.; Kumar, A. Condensed Bridgehead Nitrogen Heterocyclic Systems: Synthesis, Bioactivity and Stereochemistry of Pyrazolo [3′,4′:4,5] Thiazolo[3,2-b]-s-Triazoles. *Ind. J. Heterocycl. Chem.* **2003**, *13*, 97–100.

8. Halve, A. K.; Bhadauria, D.; Dubey, R. N/C-4 Substituted Azetidin-2-ones: Synthesis and Preliminary Evaluation as New Class of Antimicrobial Agents. *Bioorg. Med. Chem. Lett.* **2007**, *17*, 341-345.

9. Jin, X.; Zheng, C. J.; Song, M. X.; Wu, Y.; Sun, L.; Piao, H. Synthesis and Antimicrobial Evaluation of L-Phenylalanine-Derived C5-Substituted Rhodanine and Chalcone Derivatives Containing Thiobarbituric Acid or 2-Thioxo-4-Thiazolidinone. *Eur. J. Med. Chem.* **2012**, *56*, 203-209.

10. Kishore, B.; Brahameshwari, G. Synthesis and Antimicrobial Activity of Benzimidazolyl Oxazolyl Thiazolidine-4-ones and Azetidine-2-ones. *Indian J. Chem. Sec. B.* **2018**, *57B*, 1042-1050.

11. Jaberi, H. R.; Fattahi, H.; Ahmannasrollahi, A.; Yarandpour, M.; Sedaghatizadeh, S. Synthesis of New 2-Azetidinone Derivatives and Related Schiff Bases from 3-Phenyl-2,3,6,7-tetrahydroimidazo [2,1-b] Thiazolo [5,4-d] Isoxazole. *Org. Chem. Res.* **2019**, *5*, 42-50.

12. Sankar, P. S.; Divya, K.; Dinneswara, R. G.; Padmavathi, V.; Grigory, V. Z. Synthesis, Characterization and Antimicrobial Activity of Azetidinone and Thiazolidinone Derivatives. *AIP Conf. Proc.* [Online] **2019**, *2063*, 040047-1.

13. Marri, S.; Kakkerla, R.; Krishna, M. P. S. Synthesis, QSRT Studies and Antibacterial Activity of 4-Aryl-3-chloro-1-(3,5-dimethyl isoxazol-4-yl)-azetidine-2-ones. *Indian J. Chem. Sec. B.* **2019**, *58B*, 381-386.

14. Nikpour, F.; Kazemi, S.; Sheikh, D. A Facile and Convenient Synthesis of 1H-Isoindole-1,3(2H)-diones. *Heterocycles.* **2006**, *68*, 1559-1568.

15. Brian, S. F.; Antony, J. H.; Peter, W. G. S.; Austin, R. T. *In Practical Organic Chemistry,* 5th ed.; Vogel's, Eds.; Longman Scientific Technical: New York, 1989; pp. 1077-1079.

16. Gupta, A.; Halve, A. K. Synthesis & Antifungal Screening of Novel Azetidin-2-ones. *Open Chemistry Journal.* **2015**, *2*, 1-6.

17. Arthington-Skaggs, B.; Motley, M.; Morrison, C. J. Comparative Evaluation of PASCO and National Committee for Clinical Laboratory Standards M-27-A Broth Microdilution Methods for Antifungal Drug Susceptibility Testing of Yeast. *J. Clin. Microbiol.* **2000**, *38*, 2254-2260.

REVIEW ARTICLES

Acta Pharm. Sci. Vol 57 No: 4. 2019
DOI: 10.23893/1307-2080.APS.05728

Role of Nutraceuticals in Neurodegenerative Diseases

Anitha Nandagopal[1*], Kulsum Siddiqui[1]

1 Department of Pharmacology, Sultan-ul-Uloom College of Pharmacy, Road No: 3, Banjara Hills, Hyderabad-500034, Telangana State, India.

ABSTRACT

Nutraceuticals are food-derived compounds considered beneficial for human health. It has been recently shown that nutraceuticals play an important role in the regulation of brain physiology and in the prevention of neurodegeneration and cognitive decline. Nutraceuticals differ structurally and therefore act at different biochemical and metabolic levels and have shown different types of neuroprotective properties which include mitochondrial dysfunction, intracellular calcium overload, oxidative stress and inflammation. Nutraceuticals have recently gained importance owing to their multifaceted effects. These food-based approaches are believed to target at multiple pathways in a slow but more physiological manner without causing severe adverse effects.

Keywords: Nutraceuticals, neurodegeneration, mitochondria, calcium, oxidative stress.

INTRODUCTION

Neurodegenerative disease indicates a range of conditions which primarily affect the neurons. Neurons are building blocks of the nervous system and don't reproduce or replace themselves. Neurodegenerative diseases are characterized by progressive degeneration or death of the neurons. Neurodegenerative diseases occur as a result of damage to the neurons. These diseases are associated with mutated genes, accumulation of abnormal proteins, increased reactive oxygen species or destruction of neurons in specific part of brain.

*Corresponding Author: Anitha Nandagopal, e-mail: anirajan_76@yahoo.co.in
Anitha Nandagopal ORCID Number: https://orcid.org/0000-0002-4294-9412
Kulsum Siddiqui ORCID Number: https://orcid.org/0000-0002-7332-7704
(Received 13 May 2019, accepted 12 August 2019)

TYPES OF NEURODEGENERATIVE DISEASES

There are four types of neurodegenerative diseases which are shown in Figure 1.

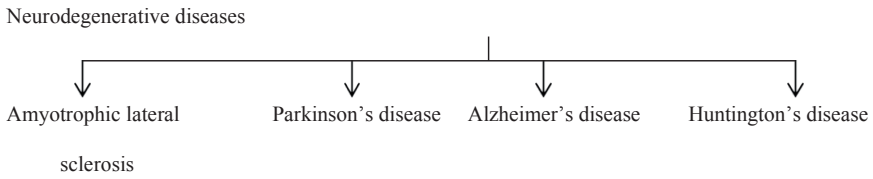

Figure. 1 Types of neurodegenerative diseases.

Amyotrophic lateral sclerosis (ALS)

ALS is a disease of motor neurons of the anterior horns of spinal cord and motor neurons in the cerebral cortex. It is a specific disease which causes the death of neurons controlling voluntary muscles. It is characterized by stiff muscles and muscles twitching. It begins with weakness in the arms or legs or with difficulty in speaking or swallowing[1]. Excitotoxicity mediated by glutamate and elevated calcium ion is considered to be a major mechanism of neuronal death in ALS[2].

Parkinson's disease (PD)

It is an extrapyramidal motor disorder characterized by rigidity, tremor and hypokinesia with secondary manifestations like defective posture and gait, mask like face and sialorrhoea[3].

It is characterized by,

- Degeneration of dopaminergic neurons that produces dopamine in basal ganglia.
- An imbalance between acetylcholine and dopamine in brain.
- Formation of lewy bodies.
- Loss of dopamine results in akinesia, rigidity and bradykinesia.
- Excess amount of acetyl choline result in tremor and sialorrhoea.

Alzheimer's disease (AD)

AD is a neurological brain disorder which is the most common form of dementia and it is a group of disorders which impairs mental functioning[4]. It is progressive and irreversible. Memory loss is the earliest symptoms, along with gradual decline of other intellectual and thinking abilities, called cognitive functions and changes in personality or behavior.

It is characterized by,

• Decrease in acetylcholine levels in cerebral cortex and hippocampus which results in progressive and significant loss of cognitive and behavioral function.

• Deposition of amyloid plaques and neurofibrillary tangles.

• Microglial and astroglial activation which finally leads to neuronal dysfunction and death.

Huntington's disease (HD)

HD is an inherited disease which results in death of the brain cells. As the disease advances, uncoordinated and jerky body moment become more apparent[5]. Physical abilities gradually worsen until coordinated movement become difficult and the person is unable to talk[6]. Mental abilities generally decline into dementia. The disease is caused by autosomal dominant mutation of a gene called huntingtin[7].

MECHANISM OF NEURONAL DAMAGE

There are several mechanisms recognized which leads to neurotoxicity as shown in Figure 2.

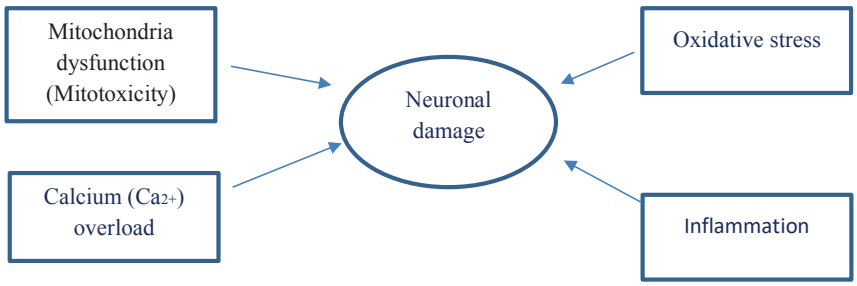

Figure. 2 Mechanism of neurotoxicity Mitotoxicity mediated neuronal damage

Mitotoxicity mediated neuronal damage

Pathophysiology of neurodegenerative diseases such as AD, ALS, PD and HD involves damage to mitochondria[8]. Mitochondrial function is under the control of two genomes i.e. nuclear DNA (nDNA) and mitochondrial DNA (mtDNA). Mutation in either of these genomes can result in mitotoxicity-mediated neurodegeneration[9].

The neurotoxicant, 1 methyl-4-phenylpyridium(MPP+), generated from the mono amine oxidase MAO)- catalyzed oxidation of 1-methyl-4-phenyl-1,2,3,6-

tetrahydropyridine (MPTP) within the brain which is concentrated inside the mitochondria of dopaminergic cells and inhibits complex I of the respiratory electron transport chain (ETC), which leads to the development of PD[10].

Mutant huntingtin, the gene which is responsible for the development of HD, directly impair mitochondrial functions[11]. Defective mitochondrial complex I, II, III and IV were found in the postmortem tissue of HD patients[12]. Mitochondrial abnormalities also result in the neuronal damage in AD and ALS.

Calcium overload-mediated neuronal damage

In general, calcium in extracellular space remains in milli molar range, while inside the cell it remains in micro molar range[13]. Maintenance of intracellular Ca^{2+} is very important for the survival of neuronal cells. If there is a sudden rise in intracellular Ca^{2+}, it triggers a cascade of neurotoxic events, including mitotoxicity and cessation of ATP synthesis, over activation of several Ca^{2+} dependent hydrolytic enzymes such as proteases, phospholipases, nucleases, nitric oxide synthase and phosphatases. These events lead to the onset of neurotoxicity, impaired neuronal functions and eventually death of the neuronal cells.

Accumulation of Ca^{2+} in neuronal cells occur through several routes such as activation of voltage-sensitive Ca^{2+} channel, receptor operated Ca^{2+} channel (N-Methyl-D-Aspartate (NMDA)), ATP-dependent Ca^{2+} channel, cyclic nucleotide-gated Ca^{2+} channel, Ca^{2+} channel coupled to G protein receptors. Plasma membrane, endoplasmic reticulum and mitochondria can only handle rise in intracellular Ca^{2+} up to a certain extent but if there is a persistent rise in intracellular Ca^{2+} it will lead to disturbances in endoplasmic reticulum and mitochondrial Ca^{2+} homeostasis which results in neurodegenerative diseases[14].

In AD, amyloid beta induced neuronal cell death is associated with deregulation of Ca^{2+} dependent pathways[15]. In PD deregulation of intracellular Ca^{2+} lead to the selective destruction of dopaminergic neurons[16]. In HD mutant huntingtin releases Ca^{2+} from endoplasmic reticulum which results in neuronal death[17].

Oxidative stress-mediated neuronal damage

Excessive production of reactive oxygen species (ROS) due to the imbalance of cellular biochemical process results in a condition known as oxidative stress[18]. ROS and reactive nitrogen species (RNS) mediated damage to cellular macromolecule is involved in the pathogenesis of neurodegenerative disease.

Neuronal degeneration and amyloid neurotoxicity in AD patients are associated with oxidative damage to DNA, RNA, proteins and lipids[19]. Oxidation of dopamine to a reactive 6-hydroxy dopamine results in the development of

PD[20]. Oxidative stress induced mutations in the gene encoding for ubiquitous Cu/Zn- superoxide dismutase (SOD-1) enzyme and damage to protein, lipid and DNA is associated with familial and sporadic forms of ALS[21]. Increased incidence of oxidative DNA strand breaks and exacerbated lipofucin, a pigment which is produced by the reaction of cellular amino compounds with aldehydic products of oxidative damage to the tissue macromolecule, is associated with HD[22].

Inflammation mediated neuronal damage

Macrophages are present in the brain near glia and microglia and plays a fundamental role in inflammation-mediated neurodegenerative diseases. In disease state, the activated microglia mediate neuronal injury through the production of pro-inflammatory factors such as cytokines and chemokine[23]. Production of the cytokines and chemokines lead to the trans-endothelial migration of immune cells across the blood brain barrier.

There are several mechanisms identified for the microglia-mediated phagocytic and cytotoxic action which is responsible for neuronal damage. One of the major mechanisms is phagocytic oxidase mediated oxidative stress- induced neurotoxicity[24]. Inflammatory activation of phagocytic oxidase results in activation of microglia[25] which in result in production of TNF-α, IL-Iβ and inducible NO synthase (iNOS). iNOS results in increased NO production leading to neuronal death.

CURRENT THERAPY FOR NEURODEGENERATIVE DISEASES

The drug treatment for neurodegenerative diseases is shown in the Table 1.

Though there are many pharmaceuticals available that improves the neuronal health, but the major disadvantage is that the chronic use of these pharmaceuticals is associated with multiple adverse effects as shown in Table 1. As a result nutraceutical are used over pharmaceuticals which are cost effective, beneficial and include lesser or no adverse effects. Hippocrates the father of medicine said that “let food be your medicine and medicine be your food”[26].

Table 1. Drugs used in various neurodegenerative disease along with their mechanism of actiond and adverse effects.

Neurodegenerative Disease	Drug	Mechanism of Action	Adverse Effect
Amyotrophic lateral sclerosis (ALS)	Endaravone (Radicava)	Decreases the effect of oxidative stress	Hypersensitivity reaction, respiratory failure, eczema
Parkinson's disease	Levodopa/ Carbidopa (Sinemet)	Levodopa-metabolic precursor of dopamine, a neurotransmitter depleted in PD, crosses BBB and get converted to dopamine by striatal enzymes Carbidopa-inhibit aromatic amino acid decarboxylase which in turn inhibit the peripheral breakdown of levodopa	Edema, anxiety, ataxia, dyskinesia, confusion
Alzheimer's disease	Rivastigmine (Exelon)	Reversible acetyl-cholinesterase inhibitor that cause increase in concentration of acetylcholine and enhances cholinergic neurotransmission	Tachycardia, seizure, allergic dermatitis, anorexia, headache, dizziness
Huntington's disease	Tetrabenazine (Xenazine)	Reversibly inhibit vesicular monoamine transporter type 2 resulting in decrease uptake of monoamine into synaptic vesicles and depletion of monoamine stores from nerve terminal	Sedation, fatigue, insomnia, depression, extrapyramidal events, anxiety, nausea

NUTRACEUTICALS

Nutraceuticals is a term coined in 1979 by Stephen De Fliece[27]. It is a term combining the word nutrition (a nourishing food or a food component) and pharmaceutical (a medical drug) as shown in Figure 3.

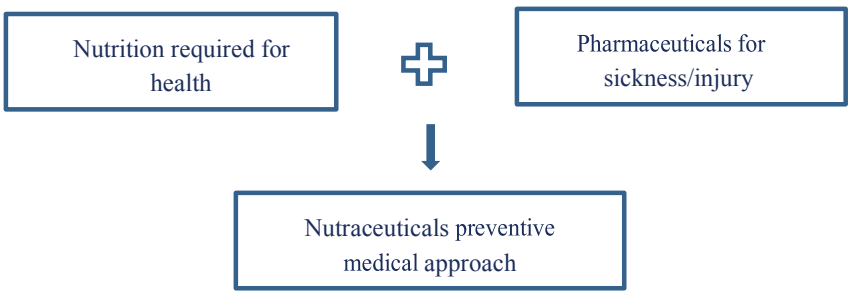

Figure 3. Concept of Nutraceuticals

Nutraceuticals is defined as a food or a part of food that provide medical or health benefit including the prevention and treatment of disease[28].

Food and nutrient play an important role in the normal functioning of body. They are helpful in maintaining the health and reducing the risk of various disease. They are medicinal foods that play a role in maintaining wellbeing, enhancing health, modulating immunity and thereby preventing as well as treating specific diseases. Thus, the field of nutraceuticals are emerging as one of the missing block in the health benefit of an individual and it has been scientifically proven that nutraceutical are efficacious to treat and prevent various disease condition.

BENEFITS OF NUTRACEUTICALS

The major benefits of nutraceuticals include lesser or no adverse effects.

- They help us to avoid taking medications.
- They are economically affordable, easily available and has multiple therapeutic effect.
- They increase the health value by improving medical condition of the individuals.
- They act on multiple pathways linked to the neuronal cell death.

CLASSIFICATION OF NUTRACEUTICALS

Nutraceuticals are classified on the basis of food source and chemical nature.

Nutraceuticals are classified into seven different types based on food source as shown in Figure 4.

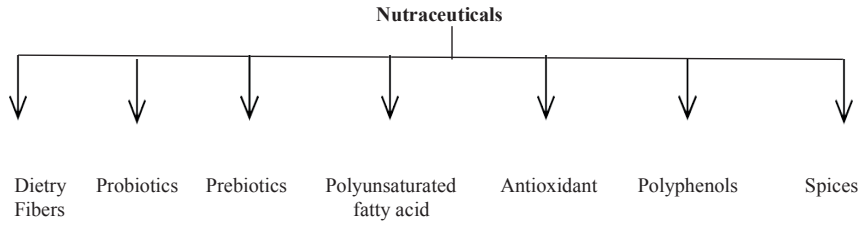

Figure 4. Classification of nutraceutical based on food source.

Dietary fibers

Plant origin substances present in food which are not digested and add bulk to the intestinal contents. Examples: Fruits, barley, oats, lignin, cellulose, pectin.

Probiotics

These are live microbial feed supplements which when administered in adequate dose, helps in improving the intestinal microbial balance of the host.

Examples: Lactobacilli, bifidobacilli, sacromyces cervicea.

Prebiotics

These are the dietry ingredients that benefit the host by selectively altering the composition or metabolism of gut microbial flora.

Examples: Chicory roots, banana, tomato and beans.

Polyunsaturated fatty acids

These may be,

Omega 3 fatty acids Examples: α-linolenic acid, eicosapentaenoic acid, docosahexaenoic acid.

Omega 6 fatty acid Examples: arachidonic acid found in sunflower, soyabean and corn.

Antioxidant

These include vitamin C, vitamin E and carotenoids. These vitamins are abun-

dant in many fruits and vegetables and possess singlet oxygen quenching and lipid peroxidation preventing properties.

Polyphenols

These phytochemicals are produced by plant for protection against photosynthetic stress and reactive oxygen species. Examples: Flavonoids, anthocyanins and phenolic acids.

Species

These are food adjuncts used to enhance sensory quality of foods. Most of the components of spices are terpenes and essential oils.

Classification of nutraceutical based on chemical nature

Table 2 shows the classification of nutraceuticals based on their chemical nature.

Table 2. Classification of nutraceuticals based on chemical nature

S. No	Class/component	Source
1	Fatty acids	Milk and meat
2	Omega-3 fatty acids (DHA, EPA)	Fish oils, maize, mustard and grape seed
3	Polyphenols -Anthocyanidine -Catechins -Flavonone -Flavones -Proanthocyanidine	Fruits Tea, mustard seed, grape seed Citrus fruits Fruits, vegetables, soyabean Cocoa, chocolate, tea, grap
4	Saponins	Soya bean, chick pea
5	Phytoestrogen -Diadzein, Zenistein -Lignans	Soya bean, flax, lentil seed, maize Flax, rye, vegetables
6	Carotenoids -ß-caroteine -Luteine -Zeoxanthine -Lycopene	Carrot, maize, oats Fruits, vegetables Eggs, citrus fruits, corn Tomatoes
7	Isothiocyanate -Sulforphane	Broccoli

ROLE OF NUTRACEUTICAL IN NEURODEGENERATIVE DISEASES

Docosahexaenoic acid

• It is an essential omega 3 polyunsaturated fatty acid that is found in marine fish. Mechanism of action:

• It produces anti-inflammatory effect by decreasing the production of pro inflammatory cytokines such as IL-1β, IL-6 and TNF-α and inhibits NF-kβ transcriptional activity.

• It decreases Aβ secretion from neuronal cells

• It is an important modulator for dopaminergic neuron in basal ganglion.

Resveratrol

• It is a polyphenolic phytoalexin, present in grapevines and legumes such as peanuts and tea. It exists in two geometric isomers, cis resveratol is unstable while trans resveratrol is biologically more active.

• It has a strong ability to remove free radicals due to the presence of OH group in position 3, 4 and 5 aromatic rings and a double bond in the molecule.

Mechanism of action:

• It reduces Aβ induced neuronal loss and memory impairment through reduction of iNOS expression.

• Acts as a free radical scavenger

• Increases 5-HT activity

Epigallocatechin gallate

• It is also known as epigallocatechin-3-gallate. It is the ester of epigallocatechin and gallic acid and is a type of catechin. It is mostly abundant in tea and also trace amount are fond in apple skin, plum, onion and hazel nut.

Mechanism of action:

• It has Iron chelation

• Act as free radical scavenger

• Modulates the ROS-NO pathway.

Curcumin

Curcumin is a diaryl hepatanoid polyphenol isolated from the rhizomes of Cur-

cuma longa. It has multiple activities and it is effective against wide variety of diseases due to its anticarcinogenic, hepatoprotective, cardioprotective and neuroprotective properties.

Mechanism of action:

• It is a potent antioxidant because of its capacity to scavenge free radicals due to the presence of its unique structure which can donate H atoms or transfer electron from the phenolic sites.

• It also has anti-inflammatory activity as it inhibits lipopolysaccharide induced morphological changes of microglia and decreases the production of pro inflammatory factors.

• Restores glutathione levels which protect neurons against protein oxidation and preserves mitochondrial complex-I activity.

Sulforphane

Sulforphane is a compound within the isothiocyanate group of organosulfur compounds. It is obtained from cruciferous vegetables such as broccoli and cabbages.

Mechanism of action:

• In AD it increases acetylcholine levels and decreases acetylcholinesterase activity and also increases acetylcholine transferase expression in hippocampus and frontal cortex.

• It decreases ROS and inhibit pro inflammatory signaling through NF-kβ.

Anthocyanin

• It is a polyphenol. Plants rich in anthocyanin include blueberry and raspberry. Mechanism of action:

• It negatively regulates pro inflammatory cytokines signaling pathway.

Apigenin

Apigenin is a flavonoid found in the flower of chamomile plants and also in celery, parsley and peppermint.

Mechanism of action:

It shows potent antioxidant antiapoptotic activity by protecting neuronal cells that are subjected to oxygen and glucose deprivation.

Coenzyme Q 10

It is also known as ubiquonone. It is a coenzyme that is ubiquitous in animals and most bacteria.

Mechanism of action:

Potent antioxidant that can reduce oxidized form of α-tocopherol to prevent lipid peroxidation.

Maintain proper transfer of the electrons in electron transport chain of mitochondria and ATP production.

α-lipoic acid

It is chemically synthesized, but also considered as a natural compound as it is a naturally occurring precursor of essential cofactors for mitochondrial enzymes including pyruvate dehydrogenase and α-ketoglutarate dehydrogenase. It is a low molecular weight compound which easily crosses blood brain barrier (BBB). After crossing BBB, it is absorbed into the cells and reduced to dihydrolipoate acting as a potent antioxidant.

Mechanism of action:

- It increases acetylcholine production in AD
- It inhibits the formation of hydroxyl radicals and ROS and increases the level of reduced glutathione.
- It can scavenge lipid peroxidation products.

Vitamin C

It is also known as ascorbic acid, is a water-soluble vitamin which is naturally present in some foods and also available as a dietary supplement. It is an important physiological antioxidant and has been shown to regenerate other antioxidants within the body.

Mechanism of action:

- Free radical scavenger in the cytosol[29].

Vitamin E

Vitamin E is a fat-soluble vitamin that plays a role as an antioxidant in the body

Mechanism of action:

- It prevents lipid peroxidation.

Ginsenoside

It is a phytoestrogen, which belongs to a class of molecules extracted from several species of ginseng

Mechanism of action:

• It maintains glutathione levels

• It prevents elevation of iron levels by regulating the expression of iron transport proteins.

Genistein

It is a phytoestrogen found mainly in soy and peanuts

Mechanism of action:

It increases the levels of malondialdehyde, superoxide dismutase and monoamine oxidase and exhibit antioxidant activity.

CONCLUSION

In recent years there is a growing interest in nutraceuticals which provide health benefits and are alternative to modern medicine. By using nutraceuticals, it may be possible to reduce or eliminate the need for conventional medications and reducing the chances of any adverse effects. Nutraceutical is demonstrated to have a physiological benefit and provide protection against neurodegenerative diseases.

CONFLICT OF INTEREST

There is no conflict of interest between the authors.

REFERENCES

1. Van, E. S. M. A.; Hardiman, O.; Chio, A.; AL-Chalabi, A.; Paterkamp, R. J.; Veldink, J. H.; Vnderberg, L. H. Amyotrophic lateral sclerosis. *Lancet*. **2017**, *390*, 2084-2098.

2. Hardiman, O.; AL-Chalabi, A.; Chio, A.; Corr, E. M.; Logoroscino, G.; Robberecht, W.; Shaw, P. J.; Simmon, S.; Van den berg, L. H. Amyotrophic lateral sclerosis. *Nat. Rev. Dis. Prim*. **2017**, *3*, 17071.

3. Tripathi, K. D. Antiparkinsonian Drugs. In *Essentials of Medical Pharmacology*. 7th ed. 2013, pp 425.

4. Wang, J.; Gu, B. J.; Masters, C. L.; Wang, Y. J. A systemic view of Alzheimer disease-insight from amyloid beta metabolism beyond the brain. *Nat Rev Neurol*. **2017**, *13*, 612-623.

5. Huntington disease information page: National institute of neurological disorder and stroke (NINDS) **2016**. Archived from the original on 27, July. Retrived 19 July 2016.

6. Dayalu, P.; Albin, R. L. Huntington disease: pathogenesis and treatment. *Neurol Clin*. **2015**, *33*, 101-114.

7. Raymond, A. C. Roos. Huntington disease: a clinical review. *Roos Orphanet J Rare Dis*. **2010**, *3*, 5-40.

8. Aliev, G.; Seyidova, D.; Neal, M. L.; Shi, J.; Lamb, B. T.; Siedlak, S. I.; Vinters, H. V.; Head, E.; Perry, G.; Lamanna, J. C.; Friedland, R. P.; Cotman C. W. Atherosclerotic lesions and mitochondria DNA deletions in brain micro vessels as a central target for the development of human AD and AD-like pathology in aged transgenic mice. *Ann. N. Y. Acad. Sci.* **2002**, *977*, 45-46.

9. Beal, M. F. Mitochondria take center stage in aging and neurodegeneration. *Ann. Neurol.* **2005,** *58*, 247-254.

10. Nicklas, W. J.; Vyas, I.; Heikkilia, R. E. Inhibition of NADH-linked oxidation in brain mitochondria by 1-methyl-4- phenyl-pyridine, a metabolite of the neurotoxin, 1-methyl-4-phenyl-1, 1, 5, 6-teterhydropyridine. *Life Sci.* **1985**, *36*, 2503-2508.

11. Tang, T. S.; Slow, E.; Lupu, V.; Stavrovskaya, I. G.; Sugimori, M.; Llinas, R.; Kristal, B. S.; Hayden, M. R.; Bezprozvanny, I. Disturbed Ca^{2+}signaling and apoptosis of medium spiny neurons in huntington's disease. *Proc. Natl. Acad. Sci. USA*. **2005**, *102*, 2602-2607.

12. Gu, M.; Gash, M. T.; Mann, V. M.; Javoy-Agid, F.; Copper, J. M.; Schapira, A. H. Mitochondrial defect in huntington's disease caudate nucleus. *Ann. Neurol.* **1996**, *39*, 385-389.

13. Schalaepfer, W. W.; Bunge, R. P. Effects of calcium ion concentration on the degeneration of amputated axons in tissue culture. *J. Cell. Biol.* **1973**, *59*, 456-470.

14. Celsi, F.; Pizzo, P.; Brini, M.; Leo, S.; Fotino, C.; Pinton, P.; Rizzuto, R. Mitochondria, calcium and cell death: a deadly triad in neurodegeneration. *Biochim. Biophys Acta*. **2009**, *1787*, 335–344.

15. Zündorf, G.; Reiser, G. Calcium dysregulation and homeostasis of neural calcium in the molecular mechanisms of neurodegenerative diseases provide multiple targets for neuroprotection. *Antioxid. Redox. Signal.* **2011**, *14*, 1275– 1288.

16. Chan, C. S.; Gertler, T. S.; Surmeier, D. J. Calcium homeostasis, selective vulnerability and Parkinson's disease. *Trends Neurosci.* **2009**, *32*, 249–256.

17. Lim, D.; Fedrizzi, L.; Tartari, M.; Zuccato, C.; Cattaneo, E.; Brini, M.; Carafoli, E. Calcium homeostasis and mitochondrial dysfunction in striatal neurons of Huntington disease. *J. Biol. Chem.* **2008**, *283*, 5780–5789.

18. Betteridge, D. J. What is oxidative stress? *Metabolism*. **2000**, *49*, Suppl. 1, 3–8.

19. Hensley, K.; Butterfield, D. A.; Hall, N.; Cole, P., Subramaniam, R.; Mark, R.; Mattson, M. P.; Markesbery, W. R.; Harris, M. E.; Aksenov, M. Reactive oxygen species as causal agents in the neurotoxicity of the Alzheimer's disease- associated amyloid beta peptide. *Ann. N. Y. Acad Sci*. **1996**, *786*, 120–134.

20. Napolitano, A.; Crescenzi, O.; Pezzella, A.; Prota, G. Generation of the neurotoxin 6-hydroxydopamine by peroxidase/H_2O_2 oxidation of dopamine. *J. Med. Chem*. **1995**, *38*, 917–922.

21. Pedersen, W. A.; Fu, W.; Keller, J. N.; Markesbery, W. R.; Appel, S.; Smith, R. G.; Kasarskis, E.; Mattson, M. P. Protein modification by the lipid peroxidation product 4-hydroxynonenal in the spinal cords of amyotrophic lateral sclerosis patients. *Ann. Neurol.* **1998**, *44*, 819–824.

22. Goebel, H. H.; Heipertz, R.; Scholz, W.; Iqbal, K.; Tellez-Nagel, I. Juvenile Huntington chorea: clinical, ultrastructural, and biochemical studies. *Neurol.* **1978**, *28*, 23–31.

23. Gendelman, H. E. Neural immunity: Friend or foe? *J. Neurovirol.* **2002**, *8*, 474–479.

24. Bal-Price, A.; Matthias, A.; Brown, G. C. Stimulation of the NADPH oxidase in activated rat microglia removes nitric oxide but induces peroxynitrite production. *J. Neurochem.* **2002**, *80*,

73–80.

25. Mander, P. K.; Jekabsone, A.; Brown, G. C. Microglia proliferation is regulated by hydrogen peroxide from NADPH oxidase. *J. Immunol.* **2006**, *176*, 1046–1052.

26. Biesalaki, H. K. Nutraceuticals: the link between nutrition and medicine. In: Kramer, K.; Hoppe, P. P.; Packer, L.; editors. Nutraceuticals in health and disease prevention. New York, Marcel Dekker Inc. **2001**, pp 1-26.

27. Defeliece, S. L. Nutrceuticals: Oppurtunities in Emerging Market. *Scrip Mag*. **1992**, 9.

28. Defelice, S. L. The Nutraceutical Revolution – Its Impact on Food Industry R&D. *Trends Food Sci. Tech.* **1995**, *6*, 59-61.

29. Garima, V.; Manoj, K. M. A review on nutraceuticals: classification and its role in various diseases. *Inter J. Pharm. Thera.* **2016**, *7*, 152-160.